

WATER WALLS ARCHITECTURE: MASSIVELY REDUNDANT AND HIGHLY RELIABLE LIFE SUPPORT FOR LONG DURATION EXPLORATION MISSIONS

Michael T. Flynn, Principal Investigator, NASA Ames Research Center

Co-Investigator Team

Dr. Marc M. Cohen, Arch.D, Astrotecture™,

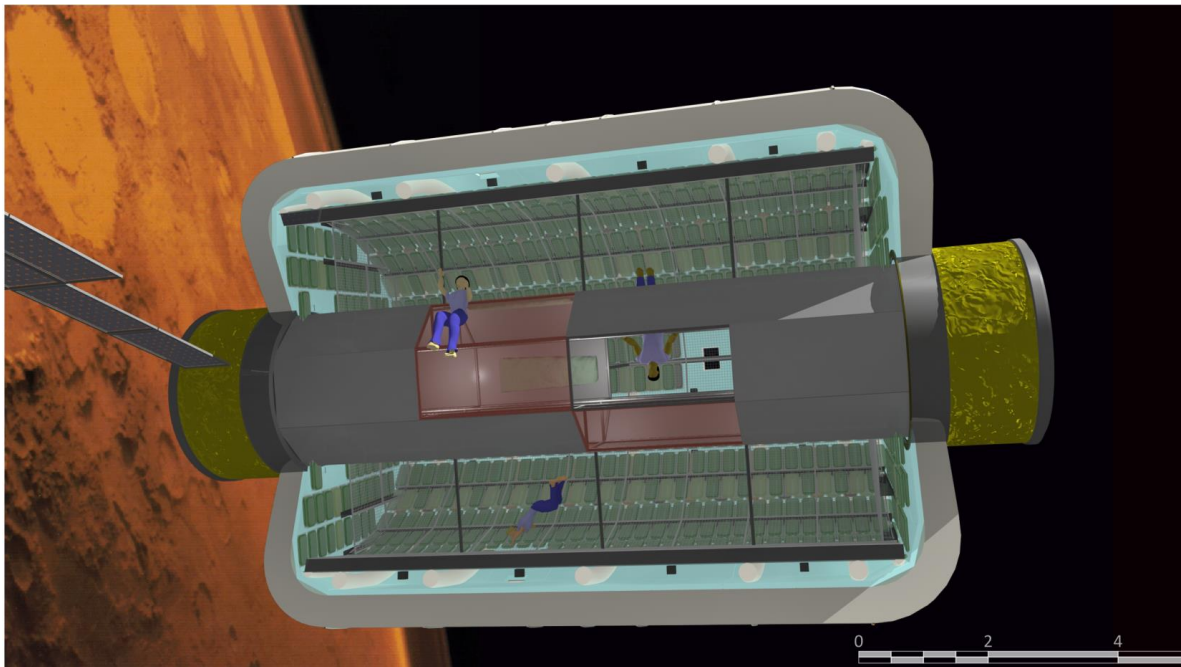
Renée L. Matossian, Space Architect, Astrotecture™,

Dr. Sherwin Gormly, PhD, Desert Toad LLC,

Dr. Rocco Mancinelli, PhD, Bay Area Environmental Research Institute

Dr. Jack Miller, PhD, Consultant

Jurek Parodi and Elyse Grossi, Universities Space Research Association



1. Abstract	4
2. Introduction	4
2.1 Long Duration Life Support	5
2.1.1 A New Approach	5
2.1.2 Limitations of the Current Approaches	5
2.1.3 Key to Success: Incrementally Consuming the System – Not Driving it to Failure	6
2.2 Background	6
2.3 Water Walls and Spacecraft Architecture	9
3. System-Integration Challenge for the Water Walls Project	14
4. Water Walls System Level Functional Flow Architecture	14
4.1 System Concept and the Long-Term Goal	15
4.2 Functional Flow Architecture and the Short-Term Goal	15
4.3 System Sizing and the Functional Flow Architecture	15
5. 5. The Process Block Level	16
5.1 The Climate Control Block 1	16
5.2 The Contaminant Control Block 2	19
5.3 Air Revitalization Process Block 3	19
5.4 Power and Waste Process Block 4	19
6. Subsystem Level	20
6.1 Humidity Control: Latent heat - Dehumidification	20
6.2 Thermal Control – Sensible Heat	23
6.3 Semi-Volatile Contaminant Control and Removal	23
6.4 Volatiles Destruction and Removal	24
6.1.1 Visible Spectrum Photo-catalyts.....	25
6.5 Algae Growth	25
6.6 Urine and Graywater Processing	29
6.1.2 The HTI XPack™	29
6.7 Blackwater and Solids Processing	32
6.8 Bioelectrochemical System (BES)	33
6.9 Radiation Protection	36
6.10 Summary Specifications for a Water Walls Application	38
6.11 Technology Readiness Levels	39
7. Component Level: Membranes, Process Cells, and FO Bags	39
7.1 Algae Growth Units as Components in a Life Support System	40
7.1.1 Light Reaction and Mass/Area Balance for CO ₂	40
7.1.2 Nitrogen Mass Balance and Other Factors	43
7.1.3 Carbon Dioxide Sequestration (CO ₂ /O ₂) initial (Phase I, NIAC) Testing	43
7.1.4 Materials and Methods	44
7.1.5 Resulting Mass, Volume, and Reactor Area Analysis	44
7.1.6 Trace Containment Control.....	46
7.1.7 Algae Metabolism Utilization Calculations.....	46
7.1.8 Solid Waste Digester Gas Emissions Scrubbing (Servicing the Water/Solids Vent Gas Odors and toxics).....	47
7.1.9 Micro-Filtration (MF) Element Fouling and Trapping Rate, the Ultimate Drivers and Values For Algae Reactor Sizing.....	51
7.1.10 Algae-cyanobacteria/Air Revitalization Element Summary	52
7.2 Wastewater Processing Bags as Components	53
7.2.1 FO Rejection of Urine Salts	56
7.2.2 NH ₄ and Urea Rejection at the Membrane.....	56
7.2.3 Total Organic Carbon (TOC) Rejection.....	57
7.2.4 Initial GAC Treatment for TOC.....	58
7.2.5 Initial GAC and FO Membrane Treatment for TOC	59

7.2.6	Biological Testing	59
7.2.7	Total Mass Per Liter Processing Rate	59
7.2.8	Concept Development Consideration	59
7.2.9	Considering Necessary Product TOC Levels.....	61
7.2.10	Water Process Theory Summary	61
7.2.11	Baseline Theoretic on Sizing Constraints Provided by the WW from Water Processing Bag elements.....	62
7.3	Solid Waste Processing Units as Components	64
7.3.1	Initial FO Sizing for Post Dewatering Solids/Residuals Processing in Membrane Walls.....	64
7.3.2	Composted Biosolids for Hydrocarbon Wall Shielding Area and Volume Calculation	65
7.3.3	Converting Biomass to Stable Humus	Error! Bookmark not defined.
7.3.4	Composted Biosolids for Hydrocarbon Wall Shielding Metabolic Mass Balance Calculation	66
7.3.5	Aerobic Digestion	67
7.3.6	Anaerobic Denitrification	69
7.3.7	Experimental Testing to Determine Life Cycle Flux Decline and Related Design Area Expansion.....	70
7.3.8	Water Processing Summary	70
7.4	Microbial Fuel Cells as Life Support Components	72
7.4.1	Extracellular Electron Transport.....	74
7.4.2	The Biology of MFCs.....	75
7.4.3	Anode and Cathode Configuration	76
7.4.4	Membranes and membrane-less systems	76
7.5	Radiation Protection.....	77
7.5.1	Current NASA permissible exposure limits	80
7.5.1	Evaluating career limits	81
7.5.2	Evaluation of cumulative radiation risks	83
7.5.3	Radiation attenuation strategies	84
7.5.4	Radiation shielding approach	84
7.5.5	Shielding of SPE radiation	84
7.5.6	Shielding of GCR in deep space.....	90
8.	Conclusion	107
8.1.2	Specific Aim 1 -- Module Assembly	107
8.1.3	Specific Aim 2 -- Functional Flow Architecture.....	108
8.1.4	Specific Aim 3 -- Sizing	108
8.1.5	Specific Aim 4 -- Organic Fuel PEM Cell.....	108
8.1.6	Specific Aim 5 -- Spacecraft Architecture	109
9.	Appendix A – Hazardous Waste Handling.....	110
	Appendix B –Nitrogen Loop Balances	114
10.	References.....	115

1. Abstract

The Water Wall concept proposes a system for structural elements that provide, thermal, radiation, water, solids and air treatment functions which are placed at the periphery of inflatable or rigid habitats. It also provides novel and potentially game changing mass reduction and reuse options for radiation protection. The approach would allow water recycling, air treatment, thermal control, and solids residuals treatment and recycling to be removed from the usable habitat volume, and placed in the walls by way of a radiation shielding water wall. It would also provide a mechanism to recover and reuse water treatment (solids) residuals to strengthen the habitat shell and a method of deriving radiation shielding from wastes generated on orbit. Water wall treatment elements would be a much-enlarged version of the commercially available hydration bags. Some water bags may have pervaporation membranes facing outward, which would provide the ability to remove H₂O, CO₂ and trace organics from the atmosphere and some would have hydrophobic internal membranes which would provide water, and waste recycling and some power generation.

2. Introduction

The lungs of our planet – the forests, grasslands, marshes, and oceans – revitalize our atmosphere, clean our water, process our wastes, and grow our food by mechanically PASSIVE methods. Nature uses no compressors, evaporators, lithium hydroxide canisters, oxygen candles, or urine processors. For very long-term operation -- as in an interplanetary spacecraft, space station, or lunar/planetary base -- these active electro-mechanical systems tend to be failure-prone because the continuous duty cycles make maintenance difficult and redundant systems to allow downtime bulky, expensive, and heavy. In comparison, Nature's passive systems operate using biological and chemical processes that do not depend upon machines and provide sufficient, redundant cells that the failure of one or a few is not a problem.

WATER WALLS (WW) takes an analogous approach to providing a life support system that is biologically and chemically passive, using mechanical systems only for plumbing to pump fluids such as gray water from the source to the point of processing or for final polishing prior to human consumption. WW provides six principal functions:

1. Gray and urine water processing for potable water.
2. Black water processing for solid waste.
3. Air processing for CO₂ removal and O₂ revitalization.
4. Air processing for volatile organic removal.
5. Thermal and humidity control.
6. Radiation protection.

Although chemically and biologically different, these cells are physically similar in size and shape, so they can be physically integrated into the WW system. With this cellular and modular approach, the WW system is designed to be highly reliable by being massively redundant. As part of the spacecraft design, the replaceable cells, and modules are installed in the structural matrix. Before departure of a staging point in LEO, they are

primed with water and starter ion solutions. As one cell for each function is used up, it is turned off; opening valves to admit the appropriate fluids turns on the next one. As the standard operating procedure, the crew replaces exhausted WW cells with new units. In this concept, WW can replace much of the conventional mechanically driven life support that is so failure-prone with a reliable system that also affords “non-parasitic” radiation shielding.

2.1 Long Duration Life Support

The *romance of the machine* hits its limits in designing, building, and operating mechanically- driven life support systems for long duration space missions such as a human asteroid exploration or a mission to Mars. The repeated failures and crises on Mir and ISS demonstrate the difficulty of operating a mechanical life support system smoothly and successfully over a period of years. It is not possible to launch all the necessary spare parts with the technicians and repair shop to keep these systems operating efficiently and reliably. Instead, NASA must look in another direction, a far simpler and more reliable system, that functions passively as the oceans and forests that are the air revitalization “lungs” of the planet Earth.

2.1.1 A New Approach

Water Walls (WW) presents a new approach to long duration life support. Instead of providing one or two heavy, excessively complex and, sensitive, expensive, and failure-prone pieces of mechanical equipment, the WW approach provides a large number of simple units based on forward osmosis (FO) to handle the same functions as conventional systems – and more. Instead of continuously active mechanical systems, WW is mostly passive, with only valves and small pumps as active elements – no compressors, evaporators, sublimators, distillers, adsorbers, or desorbers. Instead of the failure-prone mechanical ECLSS equipment, WW modules are designed to have their capacity consumed gradually throughout the mission. As one unit is used up, the next in line takes over.

An interplanetary spacecraft would launch with its WW modules dry, then in LEO or at an Earth-Moon Lagrange Point, they would be primed with water to “fuel” the life support. WW offers the promise of an inexpensive, modular, simple, low maintenance, highly reliable, and massively redundant system to outfit human interplanetary spacecraft, lunar, and Mars bases. Between interplanetary missions or for scheduled maintenance at a lunar/planetary base, crewmembers refurbish the Water Walls systems simply by replacing the disposable bags or membranes. The WW approach also provides a way to acquire radiation protection resources from ISS water recycling system waste brines.

2.1.2 Limitations of the Current Approaches

Life support systems in human spacecraft today are entirely electro-mechanical. They are high duty-cycle mechanical systems subject to maintenance, repair, and replacement costs. They are highly failure-prone as demonstrated time and again by the life support systems on Mir and ISS. Because Water Walls are passive like the natural systems on Earth, they are not vulnerable in the same way to single-point mechanical failure.

2.1.3 Key to Success: Incrementally Consuming the System – Not Driving it to Failure

Instead of wearing out and failing at unpredictable intervals like electro-mechanical systems, the Water Walls bags or tanks are consumables. They process a time period's increment of effluent and so use up the capacity of one set of bags. Then, the Water Walls operating system switches the processing to the second set, then the third set, and so on.

Preparing the Water Walls system for use involves charging most of the bags with water. It is not necessary to launch the vehicle with the water; the idea is to launch the water separately and then pump it into the spacecraft for the Water Walls system. In that way, the radiation shielding is in place from the outset. It also reduces the initial launch mass to LEO for the deep space vehicle launched on a Space Launch System (SLS) or other heavy lift launcher; the water can be launched on a much less expensive EELV or equivalent.

2.2 Background

Over the last 10 years much research has gone into the development of the WW technology. NASA has developed 3 major water-recycling systems based on variations of technology. They are:

1. The Direct Osmotic Concentration System (DOC), which was delivered from NASA Ames to JSC in 2009.:
2. The Osmotic Distillation (OD) system, completed in 2011, and
3. The Forward Osmosis Secondary Treatment (FOST) system delivered to JSC in 2013. FOST is funded by the Space Technology Mission Directorate (STMD) Next Generation Life Support (NGLS) system.



Figure 1. Forward Osmosis Bag (FOB) flight test, STS 135.

FO has also been developed commercially by the NASA PI as a green building water recycling system, sized for a 240-person office building at Ames Research Center. In addition, a company called Hydration Technology Innovations (HTI) sells a line of personal and passive FO water treatment systems that are used by military and civilian disaster relief applications. The most known of these commercial products is the XPack™. NASA uses this product extensively to test WW functional elements. NASA has a patent on a modification of the XPack™ to treat urine, no. 7,655,145 B1. NASA also has a patent on the use of algae in a WW type bag to sequester CO₂ and produce useful byproducts such as fuels and oxygen, 8,409,845. NASA also has a patent application covering the entire WW concept as described in this report, 61/502,222

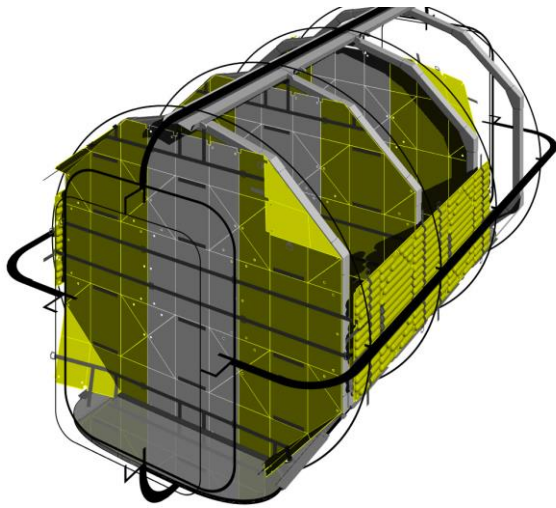


Figure 2. Artist rendering of an ISS-style habitat, outfitted with Forward Osmosis Cargo Transfer Bags (FO-CTBs).

NASA is also developing a passive water-recycling product for use on ISS called the forward osmosis Cargo Transfer Bag (FO-CTB). The FO-CTB provides the field-and flight-test basis for the WW water recycling element. The FO-CTB is designed to be a modification to a standard ISS cargo transfer bag that allows an inner bladder to be filled with water. Once filled, they can be used for radiation protection or to recycle water. Typically, the crew discards cargo transfer bags after one use. This modification enables them to become reusable. Figure 2 shows an artist view of how these CTB bags could be placed in a habitat structure to provide radiation protection.

A NASA team comprised of staff from Ames, JPL, and JSC tested a prototype of the FO-CTB element during the 2011 and 2012 Desert Research and Technology Studies (D-RATS) simulation as part of the Habitation Demonstration Unit (HDU), also known as the Deep Space Habitat (DSH). The 2011 exercise tested the water-recycling element to treat a simulated hygiene wastewater feed. The objective was to demonstrate the function of the water-recycling element integrated with the HDU. The 2012 test was similar to the 2011 test except that real HDU crew hygiene water was used as the feed, product water production was measured and a laboratory analysis of the feed and product was completed. Figure 3 shows the FO-CTB water-

A flight test of an XPack™ derivative was completed as a sortie payload Shuttle Mission, STS-135 in early July 2011. This mission tested a flight-qualified version of the system called the Forward Osmosis Bag (FOB), see Figure 1. The main goal of this flight was to investigate the function of the forward osmosis membrane in space microgravity tests. Results demonstrated that FO functions in microgravity. The tests also showed a measurable reduction in membrane flux, which was expected. A second flight is being planned to re-run the experiment in order to quantify the reduction in flux.



Figure 3. 2011 FO-CTB FY D-RATS Test.

recycling element being tested in the HDU in 2011 and Figure 4 shows the functional testing in FY 12.

Both of these HDU tests were conducted using the first generation WW water-recycling element. In 2013 we initiated the development of the second-generation water-recycling element. This system will not use the XPack™ but will use a specially developed bladder that will run the entire length of the CTB. The NASA AES Logistics to Living program currently funds this work.

Development of the second generation FO-CTB is being conducted as an informal collaboration between Thales-Alenia Space and NASA. This collaboration is directed at fabricating a flight qualified FO-CTB and conducting microgravity verification testing. Thales-Alenia is a supplier of CTBs for the European Space Agency and can solicit ESA for flight opportunities.

The Inspiration Mars (IM) Foundation has been evaluating elements of the WW concept for inclusion into their privately funded 500+day Mars Fly by mission, currently scheduled for the free-return launch window in 2018. We are currently preparing a proposal for IMF/NASA collaboration. For details see

<http://www.newscientist.com/article/dn23230-mars-trip-to-use-astronaut-poo-as-radiation-shield.html>

New Scientist – 26 FEB 2013 - Taber McCallum told *New Scientist* that solid and liquid human waste products would get put into bags and used as a radiation shield...”which is an idea already under consideration by the agency's Innovative Advanced Concepts program, ... called Water Walls, which combines life-support and waste-processing systems with radiation shielding.”

http://spaceviewtimes.com/index.php?option=com_content&view=article&id=13892%3A%3Amars-mission-to-use-astronaut-feces-as-radiation-shield&catid=99%3A%3Ascience-technology&Itemid=155

The Water Walls team received the AIAA Space Architecture Technical Committee Best Paper of 2012 award for presenting a paper at the 41st IAIAA International Conference on Environmental Systems. This paper describes the advanced CTB technologies and how they are implemented into a system as describes in the NIAC grant. The award was presented at the 2012 International Conference on Environmental Systems. [Flynn, 2011]



Figure 4. 2012 FO-CTB DRATS Test.

2.3 Water Walls and Spacecraft Architecture

The Water Wall Life Support System is an integrated, modular, flexible and predominantly passive system, designed to adapt to any habitat setting for long duration missions. The Water Wall system main kit-of-parts consists of various specialized-membrane-based polyethylene bags filled with water and other requisite life support elements and components. Each bag is, in itself, a self-contained system that can be linked to other bags and system components, providing a complete and balanced closed life-support system for the habitat. By varying both the number and ratio of specialized bags, the WW system can be scaled to support the requirements of different crew sizes. It addresses the life support functions of climate control, contaminant control (both volatile organic compounds (VOC's) and semi-volatile organic compounds (SVOC's)), air revitalization, and waste processing, and generates some power.

Water Wall bags provide non-parasitic radiation protection, meaning that they provide the dual-purpose functions of both life-support and radiation shielding without incurring separate mass penalties for each function. The two main components of the WW bags, water and polyethylene, both provide substantial shielding capabilities due to their high hydrogen content. For missions where it is not the intention to distribute radiation shielding around the entire habitat, the WW bag installation can be concentrated around only the crew quarters to provide a protected safe haven during solar particle events. The WW bags are individual, relocatable, replaceable, reusable units, but they can be arrayed into a panel formation for ease of installation, accessibility and maintenance.

While WW can be installed in any type of space habitat, this paper portrays the system installed in an inflatable habitat module, with WW radiation shielding mass distributed around the entire cabin perimeter, see Figure 5. The given habitat consists of a multi-layered, inflatable composite shell, and an axial, central core with structural members spanning from one end of the cylindrical habitat to the other. To support the WW system at the periphery of the habitat, three additional types of structural elements are used. First, supportive beams that are attached to the core during stowage, and lie flat against it, are pivoted outward from their base to extend toward the inflated shell. Second, collapsed large inflatable hoops are filled with rigidizing foam. The outer diameter of these hoops extends nearly to the inflatable shell, and the hoops are fixed onto the ends of the radial arm beams extending from the core. Finally, a parallel series of T-shaped beams links the rigidized hoops together, establishing a fixed supportive grid formation on which to install the arrayed WW bags.

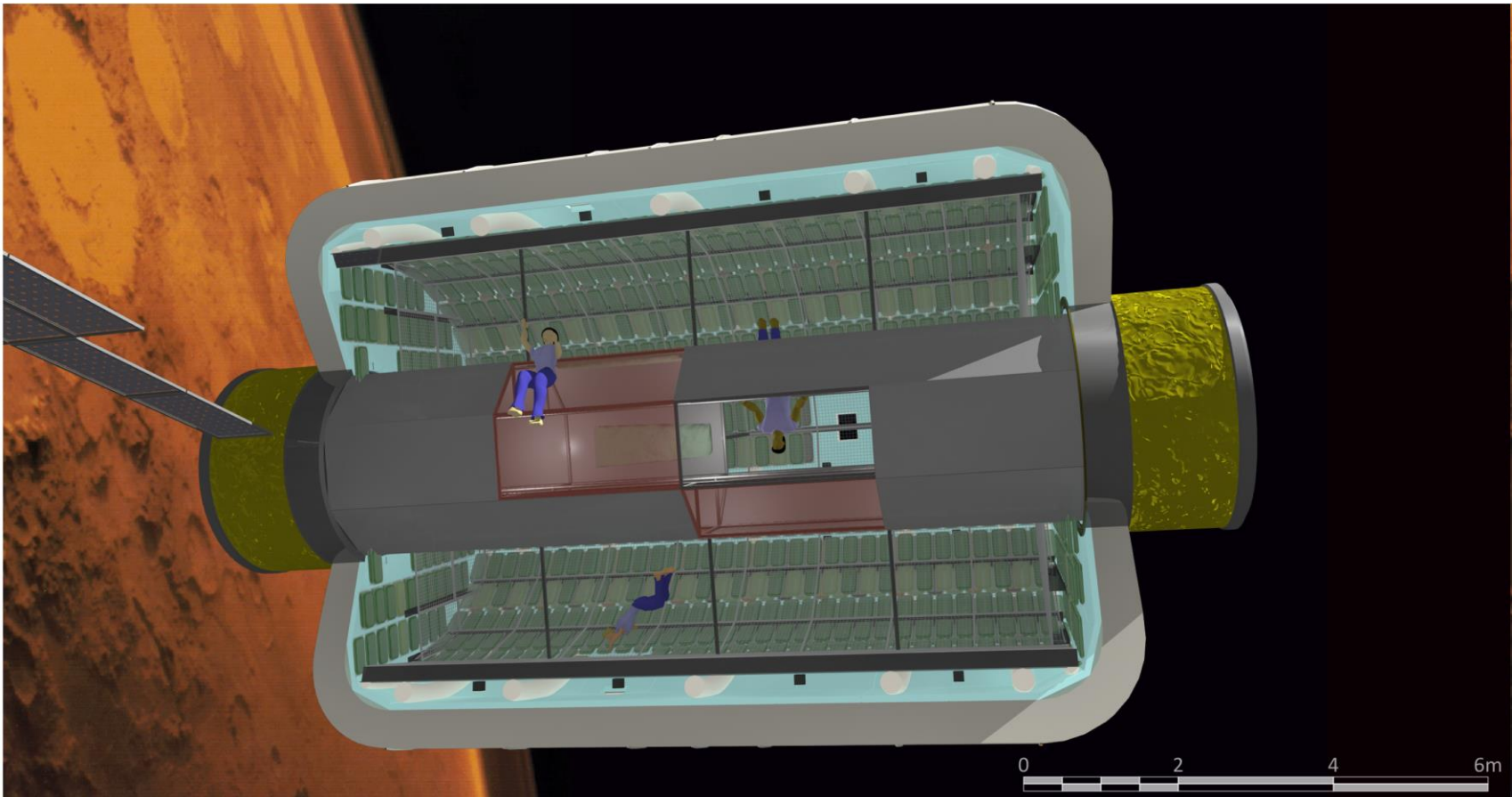


Figure 5. Cross-section of WW system installed in inflatable structure similar to the Bigelow Aerospace BA 330. It is 14 meters long and 6.7 meter in diameter and creates 330 m³ of habitable volume. Individual bags are shown and pockets attached to an internal frame that is supported by a central truss. A protective screen is provided to cover the front of the bags to both hold them in place and protect them from damage. (Credit: François Levy).

A pocketed open-weave mesh panel restrains each WW bag in a separate pouch, arranging them into a large array. The open-weave mesh of the panel and pockets allows for light and air to reach both faces of the WW bags. Space between each row of WW bags allows for distribution of tubing, and the mesh pockets have openings at each corner, enabling tubes to reach the individual bag ports. The panels of WW bags are installed between adjacent sets of T-beams at the perimeter of the structure.

The arrangement in Figure 5 and Figure 6 shows two layers of WW panels installed throughout the cabin, with the layers offset such that the bags of one layer overlap with the bag seams of the other layer. Figure 5 shows a rendering of a prospective WW application to a space habitat model, configured to resemble the Bigelow Aerospace 330 inflatable prototype. The 330 is 14 meters long and 6.7 meter in diameter. Individual bags are shown and pockets attached to an internal frame that is supported by a central truss. A protective screen is provided to cover the front of the bags to both hold them in place and protect them from damage,

The arrangement shown in Figure 5 and Figure 6 shows two layers of WW panels installed throughout the cabin, with the layers offset such that the bags of one layer overlap with the bag seams of the other layer. These bag layers are then protected by a rigid open-grid panel, mounted at the cabin-facing side of the panel assembly. The protective grid and WW panel layers are each hinged at the same side, see Figure 6. This enables the protective panel to be swung open, and for each WW panel to be lifted and turned like a book page, enabling easy access to and behind the panels as necessary. Tubes reaching the WW bags will also be distributed from the hinge-side of the panel, enabling panels/bags/tubing to be lifted and turned as a single unit.

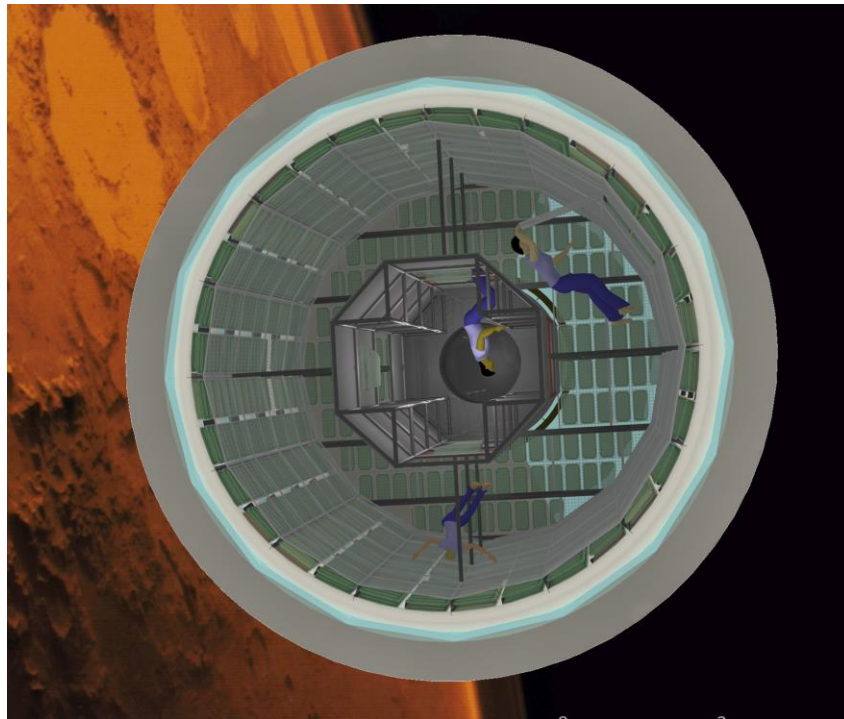


Figure 6. Section of WW concept showing two layers of WW bags, cross section of structure and central truss, and interface with inflatable (Credit: François Levy).

WW bags can be manufactured to be just about any shape or size, but the modular bag unit shown here is a standard rectangular bag, which works well with the mesh WW panel installation system. Depending on the crew requirements, the number, ratio and distribution of different types of WW bags will vary. However, each WW panel will consist of a selection of the following types of bags:

1. Wastewater Bags, which will use F.O. membranes and saline solution to remove water from the waste, and allow the residual matter to decompose into a non-biologically-active state. Reverse Osmosis (R.O.) pumps and an ultraviolet (UV) filter will desalinate and purify the water for habitat re-use, while a vacuum pump will be used to fully dry the waste matter into a stable, residual mass. The bags of dried mass can then be placed (out-of-site) at the cabin periphery to provide additional radiation shielding.
2. Algae Bags, with gas-permeable outer membranes which will sequester CO₂ and produce O₂ via photosynthesis, and also capture SVOC's).
3. Humidity-Control Bags, which will use water-vapor-permeable membranes, forward osmosis (F.O.) membranes, and a concentrated salt brine solution to wick moisture out of the air.

All WW bags will have built-in vent ports to allow for the release of any built-up pressure, and to prevent the possibility of bags rupturing and releasing contents into the cabin environment.

For optimal functioning, algae/cyanobacteria bags (which require light & air circulation) and humidity-control bags (also requiring air circulation) will be distributed throughout the habitat periphery, especially at the front (cabin-facing) WW layer. Unsightly wastewater bags, however, will be placed out-of-view at the rear WW layer. Small MFC units (which will use human waste, microbes and proton-exchange membranes to provide the minimal power necessary to run the WW bag valves, pumps and sensors) will be placed evenly at the edge of each WW panel. A single MFC unit will supply power to the WW bags within that panel zone.

Figure 7 shows the Water Wall FO bags installation truss, frame, connectors, plumbing, and protective screen. Also shown, the blue dotted line outlining bags, is the off set of two layers of bags so that a water filled portion of a bag is lying across the seam of the bag in front. This provides more uniform radiation protection as layers increase.

There will be an illuminated airspace between the front and rear WW panel layers, such that algae/cyanobacteria bags and humidity-control bags can also be installed at the rear panel layer. Algae/cyanobacteria bags and humidity-control bags will also contain an internal fluid-filled cooling coil. The contents of the coil will not affect the bag contents, other than to regulate the bag temperature and carry excess heat to the spacecraft radiator.

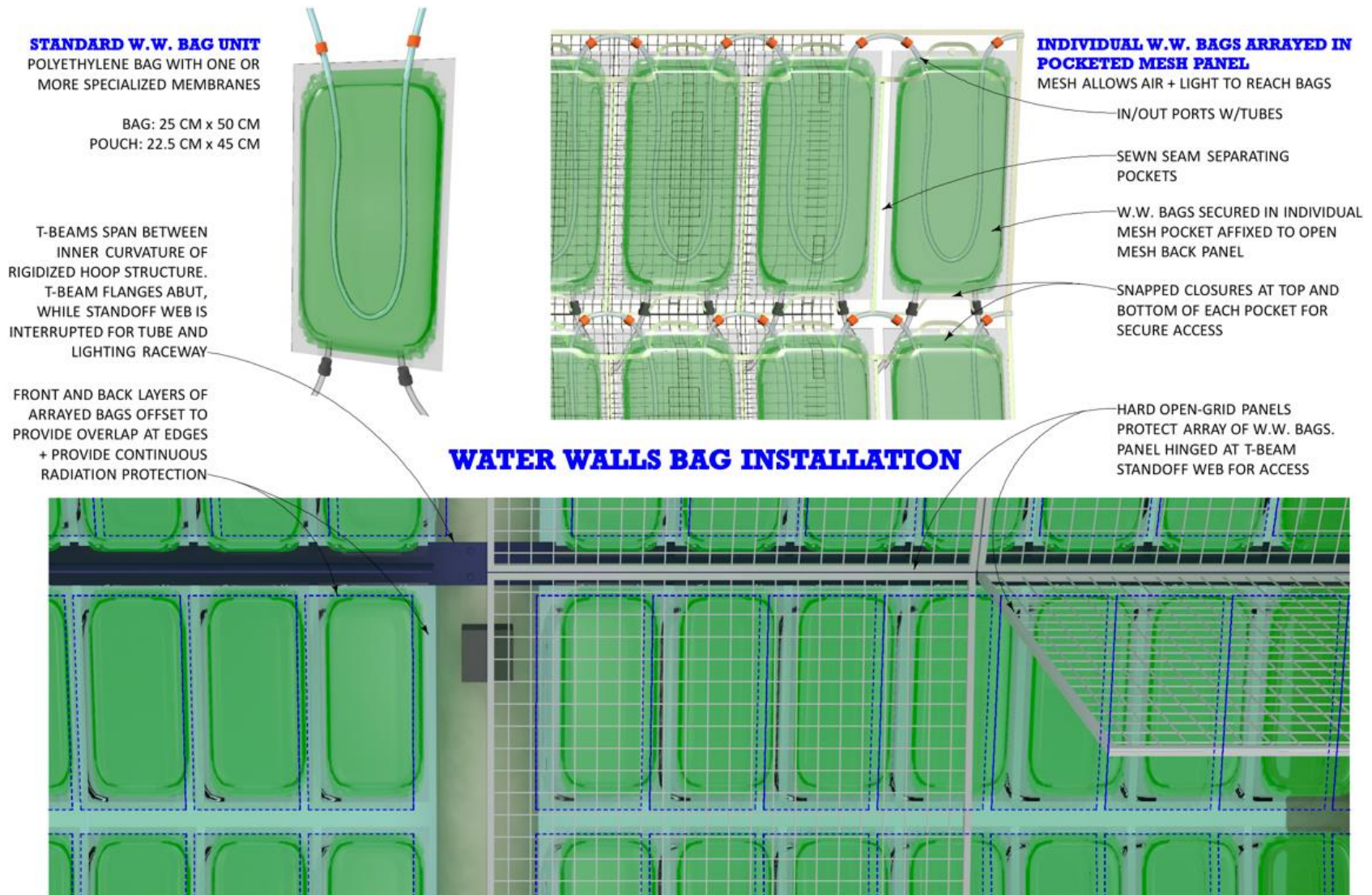


Figure 7. Detail of a Water Walls bag array assembly.

A non-bag element of the Water Walls system is responsible for controlling Volatile Organic Compounds (VOC's) in the cabin environment. For this part of the system, cabin surface elements (such as the open-grid panels protecting the WW bags) are painted with, or embedded with, volatile-oxidizing nanoparticles, which use UV light or ambient light as a catalyst for volatile destruction. The option is also provided for a thermal catalytic polishing system.

3. System-Integration Challenge for the Water Walls Project

The Water Walls Project faces the challenge of integrating a variety of scientific and technical inputs, from multiple sources, including the NIAC funded Phase-1, the Ames Director's Matching Fund grant, the Synthetic Biology Program's funding for a new generation of microbial fuel cells, the NASA AES and STMD membrane development projects. In order to integrate all these efforts into a coordinated overarching construct this proposal combines them into self-sustaining

system. To show how all these elements integrate together – how they must integrate for the WW to work at a system level instead of as a piecemeal collection of fragmentary parts.

As the Water Walls team pursued the research and development for NIAC Phase 1, they soon realized that an operational system must incorporate both a hierarchical, vertical integration plus a horizontal integration within each level. This dual-axis integration scheme took the form of a pyramid. Figure 8 shows this pyramid, with the four levels from the top down stated as the System Level, the Process Block Level, the Subsystem Level, and the Component/Membrane and Forward Osmosis Bag Level.

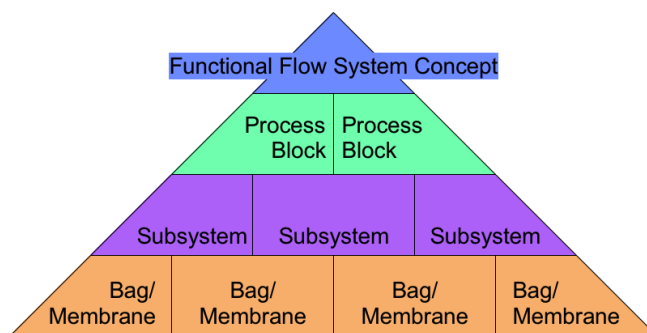


Figure 8. Water Walls System Integration Pyramid.

4. Water Walls System Level Functional Flow Architecture

The WW Functional Flow System Concept (Figure 9) stands at the top level of the WW Design Integration pyramid. It reflects the way the WW team envisions the project at the highest level. It portrays Water Walls as a largely passive ecosystem. This top System level representation of the Functional Flow Architecture derives from several vital precepts, including the stated long- and short-term goals for this NIAC project, and the Specific Aim 3–Sizing. These three precepts work together to establish

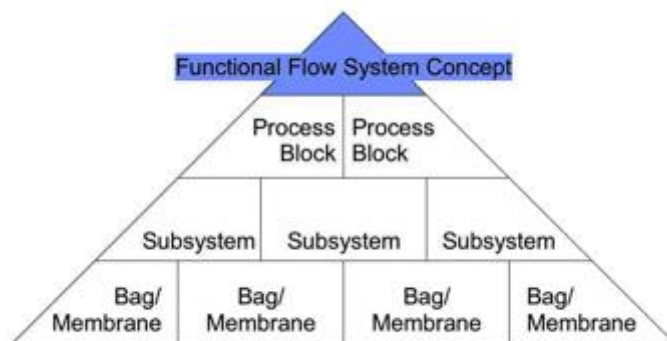


Figure 9. The Top Level Water Walls System Concept for the Functional Flow Architecture

the WW top System Level.

4.1 System Concept and the Long-Term Goal

The Long Term Goals of the System Concept are to reduce the cost of human spaceflight and improve system reliability. The cost of human space exploration has become prohibitive, it is the major impediment to the frequency and duration of current and future missions. What is needed is a radical departure from the status quo, one that would allow the cost of human spaceflight to be reduced by an order of magnitude.

The lessons learned from the development of the ISS life support system demonstrate that mechanically complex systems are unreliable for long duration missions [NRC, 2012.]

Long-term, a new generation of simpler more reliable life support technologies is required to enable long duration space flight. To do this will require a new approach to sustaining humans in space. This paper describes such an approach where life support, thermal, structural, and radiation protection functions are integrated into the walls of the spacecraft. This consumable approach is inherently more reliable than the existing mechanically complex life support systems. It achieves a mass savings by combining the function of radiation protection, thermal control, and life support functions within the mass of a radiation protection water shield.

The integrated, yet modular Water Walls Life Support System allows for a comprehensive and flexible system, with near-unlimited redundancy, so critical to long-duration missions. The membrane-based technology, combined with other mainly passive systems, provides maximum sustainability of the habitat and crew using the minimal amount of natural resources. As the Water Walls Life Support System develops, it will enable a sustainable human presence beyond Earth.

The Long-Term effect will lead to redefining and reshaping the whole approach to understanding cost-effectiveness for life support for spaceflight and terrestrial applications. Ultimately, it will lead to mitigating Equivalent System Mass as the sole criteria for evaluation within the Life Support System Engineering religion. Water Walls will help to introduce instead the criteria of quality of life, reliability, and sustainability for missions measured in years, decades, or human lifetimes.

4.2 Functional Flow Architecture and the Short-Term Goal

The Short Term goal is to size a WW system to fit in an existing spacecraft envelope and to develop functional and physical architecture that provides an integrated framework for the chemical, electrical, mechanical, plumbing, and structural subsystems. This information was used to generate the parameters for sizing the subsystems, most particularly each of the five FO life support capabilities plus the radiation shielding.

4.3 System Sizing and the Functional Flow Architecture

The primary objective of this proposal focused on sizing the Water Walls elements, both in terms of physical size and number of units. The proposal called for designing “a physical assembly for the water walls system that provides the life support and radiation shielding capabilities.” Figure 9 presents a representation of the Functional Flow Architecture.

Within this functional architecture matrix, the team found and began to implement a major restructuring and transformation of the Water Walls gestalt. This transformation emerged first as the Level 2 Process Blocks because the team recognized that it was not sufficient to think

primarily in terms of functional flows between units: it was equally important to understand the processes within those units, the Process Blocks. Within each process block reside two or more subsystems. A major revelation for the team was to realize the importance of the nitrogen cycles within the Process Blocks and between them as an aspect of the Functional Flow Architecture. Table 1 shows a mapping of how individual function are completed by multiple process blocks. It shows the nitrogen economy cuts across nearly all of the process blocks.

5. 5. The Process Block Level

The Second Level of the System Integration Pyramid is the Process Block Level. It provides support for integrating the Functional Flow Architecture vertically, and it is also the first level at which the elements can integrate horizontally, within the same level. Figure 8s 10 and 11, as well as Table 1 present the Process Block level of the Water Walls Architecture. At this level, the architecture consists of four process blocks:

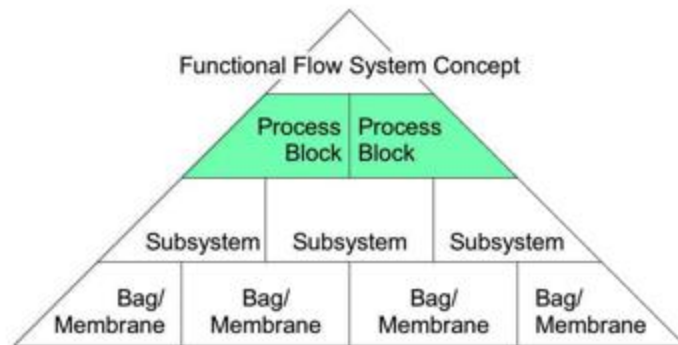


Figure 10. The Process Block Level of the Water Walls System Integration Concept.

Block 1. Climate Control

Block 2. Contaminant Control

Block 3. Air Revitalization

Block 4. Power and Waste

5.1 The Climate Control Block 1

The Climate Control block combines two subsystems, Thermal Control and Humidity Control. Among the features that these two subsystems have in common are that they both receive their inputs from air circulation over the FO membrane. Both subsystems consume salts and brine and both produce condensate that becomes an input to the Power and Waste Process Block. They both interact with heat balance of the cabin atmosphere. The Thermal Control subsystem handles the sensible heat. The Humidity Control subsystem handles the latent heat or humidity in the cabin atmosphere. Both subsystems remove heat from the air and both must reject it to the exterior of the spacecraft.

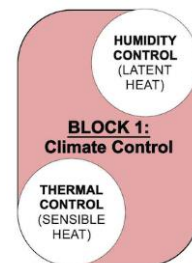


TABLE 1. Matrix of Water Walls Subsystems and The Processes They Perform

Process Blocks	Climate Control Process Block 1.		Air Process Block 2.	Power and Waste Process Block 4.		
	Humidity Control Subsystem	Thermal Control Subsystem	Algae Growth Subsystem	Blackwater/Solids Subsystem	Fuel Cell Subsystem	Urine Process Subsystem
WW Primary Functions: Inputs and Outputs						
O ₂ Revitalization			Photosynthesis			
CO ₂ Removal			Photosynthesis			
Denitrification/ Liberation of N ₂			N-Uptake	Produce NH ₃	Liberate N ₂	
Clean Water Production	Produce H ₂ O Condensate	Thermal Capacitance				Produce Clean H ₂ O
Produce Nitrates			Consume Nitrates	Produce Nitrates		
Ammonification: Produce NH ₃				Ammonification Produces NH ₃		Ammonification Produce NH ₃
Produce Brine NH ₄ Cl						Produce Amm. Brine NH ₄ Cl
Semi-Volatile Removal	Physical/Chemical Treatment		Microbial Treatment			
Produce CaCO ₃						Produce CaCO ₃
Produce CaSO ₄						Produce CaSO ₄
Nutritional Supplement Production			Produced by different algae than for Air.			
Electrical Power Production					Release CH ₄	

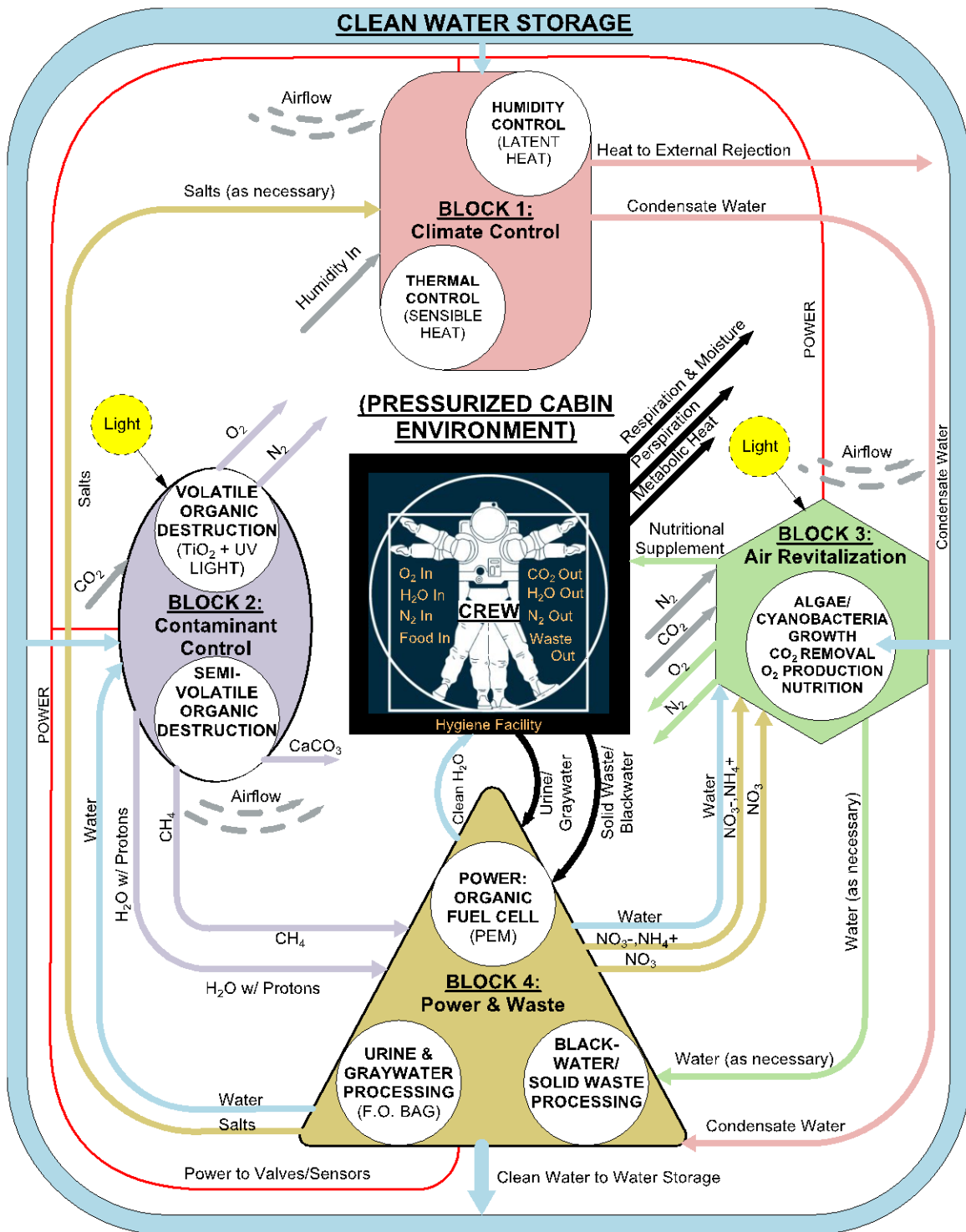
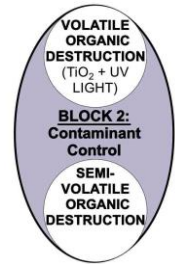


Figure 11. Water Walls Level 2 Process Block Diagram

5.2 The Contaminant Control Block 2

The three main classes of contaminants of concern are particulates, semi-volatile organics, and volatile organic hydrocarbons. Control of Semi-volatiles and Volatile organics in the cabin environment is very important to maintaining a safe and healthy cabin atmosphere that conforms to the Spacecraft Minimal Acceptable Concentration (SMAC) level standards [Marshburn,1999].

The system design utilizes the solubility of semi-volatiles in water and the biological decomposition of these organics. This occurs in the Climate Control block and the Air revitalization block. The primary means of breaking down VOCs is to expose them to light while in contact with a catalyst such as TiO₂. Ultraviolet light can be much more effective in terms of surface area of catalyst required, but ambient cabin lighting also works, albeit not as quickly.



5.3 Air Revitalization Process Block 3

The Air Revitalization uses Algae and Cyanobacteria Growth Subsystems to sequester CO₂ and produce O₂. This block with its unitary subsystem performs the greatest range of services of any of the Process Blocks. It removes CO₂ from the cabin atmosphere and sequesters the carbon in the tissue of the algae/cyanobacteria (also called blue-green algae), where it can do no harm. Having broken the C from the CO₂, the algae release the O₂, which can return to the breathable cabin atmosphere. In addition to these primordial functions, the algae and cyanobacteria can produce nutrition, or at least what is called in polite company “nutritional supplement.”

For photosynthesis to operate, the unique input is the light itself. In Process Block 3 light is provided by cabin illumination. The additional essential inputs for Process Block 3 include N₂, P, S, CO₂, and H₂O. An additional input may provide fertilizer from Process Block 4 the PB3 in the form of NO₃⁻, NH₄⁺, and NO₃. Outputs from Process Block 3 include O₂, N₂, and H₂O as necessary to regulate the mass balance in the bags.



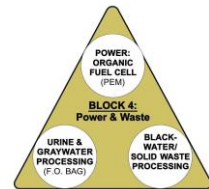
5.4 Power and Waste Process Block 4

The Power and Waste Process Block 4 combines three subsystems:

- The Urine and Graywater Processing Subsystem
- The Blackwater and Solid Waste Processing Subsystem
- The Microbial Fuel Cell

The subsystems within Process Block 4 are the most tightly bound together in terms of functional flows between them. Most tellingly, the Blackwater and Solid Waste unit produces partially treated waste that flows to the Microbial Fuel Cell to be consumed as fuel. In a similar way, the Urine and Graywater Bag passes ammonium byproduct from the decomposition of urea. The Urine Graywater bag also provides potable H₂O and a fortified drink that can be engineered to meet space flight requirements.

The inputs to Block 4 include condensate, urine, graywater, and blackwater/solids. The outputs include clean drinking water, N₂, gypsum (CaSO₄), calcium carbonate (CaCO₃), nitrate fertilizer, and methane CH₄.



6. Subsystem Level

This Subsystems Chapter goes through most of the Water Walls subsystems in deeper scientific and technical detail. The subsystems it covers are:

Process Block 1 Climate Control:

Humidity Control
Thermal Control

Process Block 2 Contaminant

Control:

Semi-Volatiles
Volatiles

Process Block 3:

Algae Growth

Process Block 4:

Urine and Graywater Processing
Blackwater and Solids Processing
Microbial Fuel Cell

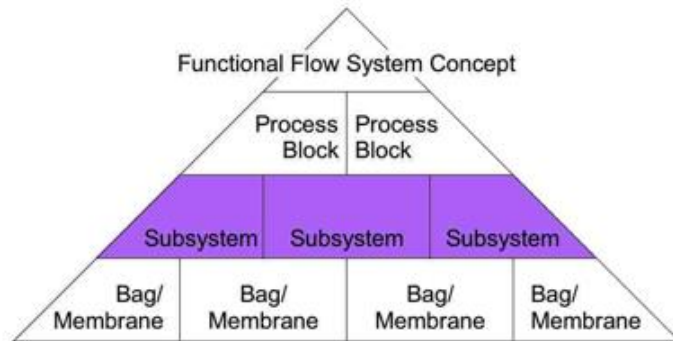


Figure 12. Subsystem Level in the Water Walls System Integration Pyramid

6.1 Humidity Control: Latent heat - Dehumidification

The WW system will use an Osmotic Membrane Dehumidifier (OMD). The use of an OMD provides a dehumidifier that operates at cabin temperature. The OMD is a membrane-based system that uses osmotic potential gradients to remove water vapor from cabin atmosphere. It is essentially the same as the forward osmosis process used in the Water Section except that it operates with higher salt concentrations and uses a gas diffusion membrane as an atmospheric contactor. An OMD uses a flexible, semi-permeable membrane to facilitate capillary condensation of water vapor and the transport of condensed water through the membrane into a salt solution by osmosis. Here a humid gas stream is brought into contact with a semi-permeable membrane, which separates the gas stream from an osmotic (e.g., salt) solution. Some of the pores of the membrane are small enough to permit capillary condensation. Liquid formed within these pores connects with liquid formed in adjacent pores, collectively forming continuous paths of liquid. These ‘liquid bridges’ extend across the thickness of the semi-permeable membrane and provide paths by which water can travel across the membrane.

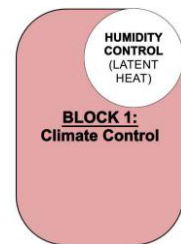


Figure 13 explains the functioning of the humidity control subsystem within the WW architecture. This figure shows the use of a highly saline solution with osmotic and gas permeable membranes to isothermally remove water from the cabin atmosphere. The subsystem uses a reverse osmosis (RO) pump to remove water from the saline solution resulting in a reconstituted saline solution. Individual bag cooling will remove the latent heat of condensation to the spacecraft thermal control system.

HUMIDITY-CONTROL BAG CYCLE

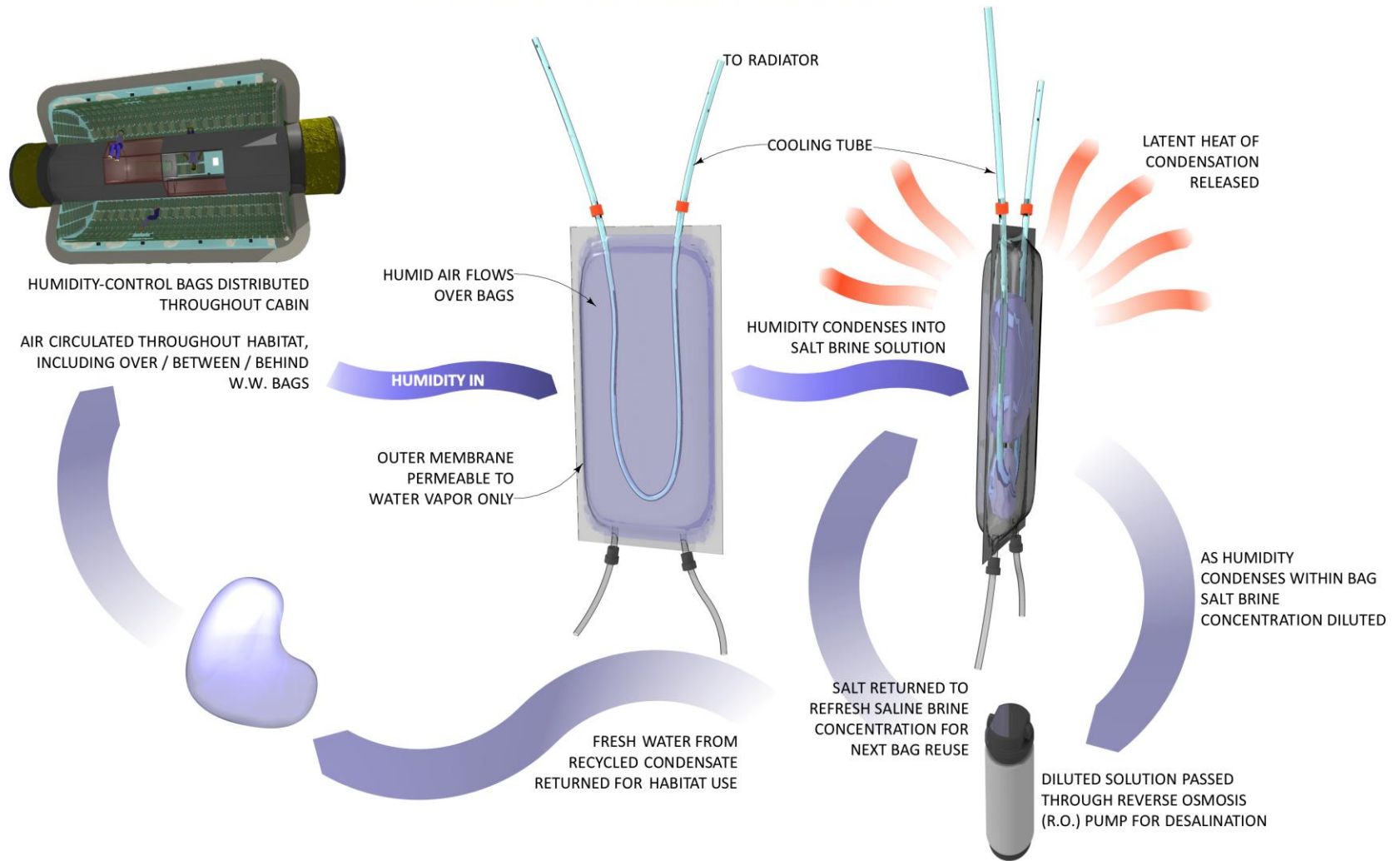


Figure 13. Humidity and Latent Heat Control Bag Diagram

The feasibility of using commercially available membranes for capillary condensation and subsequent transport of condensate into a salt solution has been demonstrated at a small scale. Membranes tested were commercially available polymer membranes. Salt solutions tested were sodium chloride, lithium chloride and magnesium chloride. Results suggest that 1 square meter of the membranes can remove about 0.7 liters/hr of water vapor at relative humidity levels between 80 and 90%.

This testing used an apparatus in which shallow trays were filled with a salt solution and each covered with a membrane. Trays were arranged in a cafeteria style with narrow spaces between the trays for airflow over the membranes. Air was blown over the membranes and then through an exhaust manifold. An anemometer was used to measure airflow and humidistats were placed upstream and downstream of the trays to measure temperature and humidity. A circulating pump was used to move the salt solution through the trays from inlet to outlet manifolds.

Tests were performed on arrays of trays and on single trays with various spacing and airflow. A single tray, for example, covered with a membrane of 0.13 square meters reduced relative humidity of an air stream flowing at 15 cfm (0.4 cubic meters per minute) by 7%. At 20 cfm, the relative humidity was reduced by 5%. An array of 12 of these trays (occupying a volume of less than 0.02 cubic meters) would remove about 0.5 liters/hr of water from a humid air stream. Reducing volumetric flow rates results in increased relative humidity reduction. However, current membranes are limited by pore size and relative humidity is generally not reduced below 65-70%. Based on these tests a design number of 0.32 L/m² hr is proposed for sizing. Based on predicted loading of 1.9L per crewmember day respiration [Duffield 2008] about 0.25 m² of membrane will be required per crewmember.

One of the problems with this technology is that it results in a damp outer layer of water on the condensing membrane surface. An alternative approach called Osmotic Distillation has been evaluated that maintains a dry outer membrane surface. In this case the driving force for mass transfer to occur is the difference in vapor pressure between water vapor in the cabin and the osmotic agent solution (NaCl in deionized water). Based on the design of the membrane (surface tension, contact angle, capillary pressure, and pore radius), the liquid phase has a high enough surface tension so that a meniscus forms across the pore inlet and outlet. Only volatile feed components, as vapor, are able to pass through the membrane pores.

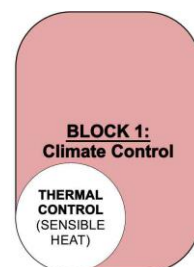
Although OD has the benefit of potentially maintaining a dry layer on the external surface of the membrane it has significantly lower flux rates than osmotic dehumidification. Typical rates of 20-mL/hr m² were measured with a 100% liquid feed. This correlates into a requirement of 115 m² of membrane area per person. The osmotic dehumidification approach requires only 3.3 m² per person.

In either case, as water vapor condenses into the distillate, latent heat is released resulting in a temperature increase of the osmotic agent. The subsequent temperature differential caused by this energy transfer counteracts the driving force for mass transfer to occur. Cooling is required to insure that the membrane bag remains at a constant temperature. This cooling is provided by heat transfer tubes integrated into the bags and connected to the spacecraft cool water bus which radiates this energy to space. About 650 W-hr/L of condensate will be generated.

6.2 Thermal Control – Sensible Heat

Sensible heat control will be accomplished by controlling the internal temperature of the water contained in all the WW bladders. The dehumidification and CO₂ bladders will be cooled using a cool water buss and this heat will be radiated to space. The WW system provides a thermal environment that is highly buffered and largely determined by the temperature of the water contained in the water bags.

The working assumption is that the surface area of the algae and humidity control bags would be enough to control the cabin temperature. If it is not additional bags can be installed as dedicated thermal control bags could be added. Detailed calculations have not been completed yet because experimental work to measure the heat transfer of the bags in the cabin environment in has not been completed. Ultimately measurements in microgravity are going to be required to accurately determine thermodynamics.



6.3 Semi-Volatile Contaminant Control and Removal

Semi-volatile removal is completed by air stripping the spacecraft cabin using gas permeable membrane water bags. These bags are either dedicated semi-volatile bags or Algae bags or both. These bags allow semi-volatile organics to condense in equilibrium with the gas phase. Henry's Law predicts this equilibrium. Henry's Law is a measure of the extent that a chemical separates between water and air. The functional form of Henry's Law is:

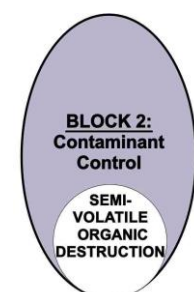
$$y_i/x_i = H_i/P$$

Where, y_i and x_i are the component vapor and liquid phase concentrations respectively, H_i is the component Henry's Law constant (in units of pressure), and P is the pressure of the system.

As the Henry's Law constant increases, the more likely a substance will volatilize rather than remain in water. Compounds with Henry's law contents less than 50 will appreciably solubilize in water across a gas permeable membrane. Compounds with higher constants are less well removed. Chemicals with excessively high Henry's Law constants volatilize out of water quite readily and cannot be removed using a bag. They will need to be removed in a separate volatile contaminate removal system.

Data and estimates of the performance of this system are based on the operation of the International Space Station (ISS) humidity control system. Water condensed in this system provides an indication of what the removal rates for a WW system would be. Data from 2009 Columbus condensate water is shown in Table 2 [Grizzaffi, 2010]

If we assume that during the condensation of cabin humidity, Henry's law equilibriums are met then we can conclude that the TOC equilibrium of the Columbus atmosphere is 122 mg of carbon/Liter of condensed water and the ammonia, as ammonium, equilibrium is 29 mg/Liter of water. Both the ammonia and organics can be removed from the water once they are removed from the cabin atmosphere using biological or physical chemical approaches.



Biological techniques are composed of dedicated bags containing seed organisms or opportunistic organisms living in the Algae bags. Physical chemical techniques are primarily wet oxidation techniques such as used in the Volatile Removal assembly on ISS. Regardless of which treatment is used the individual solubility's of each compound will be the rate-limiting step.

Sizing of this subsystem has not yet been completed because generation rates of volatile organics in the WW system have not yet been defined. However based on ISS data about 122 ppm of TOC can be removed for every L of water that comes in contact with the space craft cabin.

Table 1- Volatile removal using heat exchanger in ISS Columbus module	
Compound	Columbus Crew Latent Condensate (mg/)
Ammonium	
Total Inorganic Carbon	
Total Organic Carbon	1
Total Carbon	2
Parameter	
Conductivity [μ S]	
PH	7.
Turbidity [NTU]	

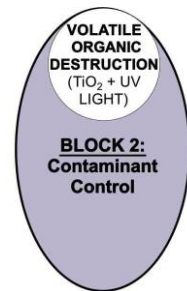
6.4 Volatiles Destruction and Removal

Volatile removal in the WW system will be performed using primarily visible spectrum, photo-catalytic oxidation (PCO). PCO shown to effectively remove air pollutants [Zaho, 2003 & Carp, 2004]. Its ability to oxidize organics to carbon dioxide, and water makes PCO especially attractive for treating spacecraft cabin pollutants. A great deal of research has already focused on this technique and many advances have occurred [Tomaszewski, 2007 & Chen, 2003].

TiO₂ is the most popular photocatalyst employed in PCO due to the hydrophilic properties of TiO₂ and its ability to degrade a wide range of inorganic and organic compounds under irradiation of UV or near UV-light. The most important step of a photoreaction using TiO₂ is the formation of hole-electron pairs that need energy to overcome the band gap between the valence band (VB) and conduction band (CB). When the photon energy is equal to or exceeded the band gap energy E_g, the electron-hole pairs are created in the semiconductor, dissociating into free photoelectrons in the conduction band and photoholes in the valence band, respectively.

Simultaneously, the photo-oxidation and reduction reactions occur in the presence of air. During the reactions, the hydroxyl radical (OH), coming from the oxidation of adsorbed water or OH⁻, is highly reactive. In addition, the reducing power of the electrons can induce the reduction of molecular oxygen (O) to superoxide O⁻. The highly reactive species OH and O₂ show strong ability to degrade microorganisms [Kikuchi, 1997 & Agrios, 2005] as well as organic [Agrios, 2005 & Demeestere, 2007] and inorganic pollutants.

In this reaction, the photonic excitation of the catalyst appears as the initial step of the whole catalytic system, the produced h⁺ and e⁻ are powerful oxidizing and reducing agents, respectively.



The PCO photoefficiency can be reduced by electron-hole recombination, which corresponds to decreased electron and hole density as well as separation. The presence of oxygen can prevent the recombination of hole-electron pairs.

In short, the overall photocatalytic reactions can be decomposed into several steps, such as mass transfer of reactants from a gas to the photo-catalyst surface, production of electron-hole, separation of the photo generated electrons and holes, redox reactions between the trapped electrons and holes and adsorbed reactants, as well as desorption products and re- construction of the surface.

6.1.1 Visible Spectrum Photo-catalysts

The commonly used TiO₂ is an effective catalyst in photocatalytic oxidation. However, this type of catalysts only exhibits high catalytic activity in UV-light. Few TiO₂ catalysts exhibit high activity for VOCs in visible-light. In order to extend the applicable wave- length range and widen the practical applications, recent efforts have been focused on the doping of TiO₂ by metal ions like iron and tungsten and non-metal species like carbon, nitrogen and sulphur in order to reduce the band gap energy [Bloß, 2007].

Anpo and Takeuchi [Anpo, 2003] reported that the metal ion implanted catalysts were able to absorb the light in the visible wavelength of 400 - 600 nm. Wu and Chen [Wu, 2004] have also reported that vanadium doping provided a promising strategy to improve the photocatalytic activity of TiO₂ under visible light.

Fuerte *et al.* [Fuerte, 2002] reported the preparation and application of titanium-tungsten mixed oxides in the photocatalytic degradation of toluene using sunlight-type excitation. The photocatalytic activity of Ti-W mixed oxides increased with W content and is much better than TiO₂ itself and TiO₂ P25. However, Chapuis *et al.* [56] found that doping of TiO₂ by metal oxides such as Ag₂O, CuO, NiO, CaO, and Cr₂O₃ gave much lower catalytic conversion. Nanosized doping TiO₂ photocatalysts were more effective in the degradation of toluene than TiO₂ itself and P25 TiO₂

Sizing of this subsystem has not yet been completed because generation rates of volatile organics in the WW system have not yet been defined and the performance of the semi-volatile organic removal system has not yet been defined. Future work will define the requirements of this system. The ISS TCCS is fully developed and thus sizing data at this time is limited to the specification of the TCCS.

6.5 Algae Growth

Carbon Dioxide removal and oxygen generation in the WW system architectures is a function of flexible bioreactor algae bags. These algae bags will be sized to treat all of the CO₂ generated by the crew and other biological or chemical generation sources. The bags will also, through the process of photosynthesis, generate the O₂ that the crew needs. Interior cabin lighting will provide light for the growth of algae in the bags. These Algae bags will also remove semi-volatile organics through symbiotic growth with aerobic bacteria.



Bags will be recycled until performance drops off. The primary foulant that will effect the algae bags is dead cell mass. This mass can be filtered out to extend the life of the bags or simply accumulated until the bag is filled dead cells. Figure 14 shows an example of a living algae bag. Figure 15 shows a representation of the cycle of the Algae bags during operation.

Bags use ambient cabin light to convert CO₂ to O₂. As dead algae and bacteria build up in the bag the solids can be filtered out and the bags reused or the bags can be replaced with solids retained in them.

Dead cellular wastes generated in the algae bag are further processed in solid waste bags to generated dried radiation protection and structural materials. Nutrients are provided as a byproduct of wastewater and solid waste treatment and from stored supplies. Nitrogen is particularly important in this system and is provided from urea decomposition and from stored supplies.

For air revitalization the primary mass input is carbon from CO₂ originating from crew respiration, not biomolecule/biomass carbon (CH₂O) from solids in the urine, or other human wastes or hygiene wastes in water. Thus, the solids mass balance coupling between air and water/solids treatment occurs at the micronutrient level, as well as at the nitrogen transfer level. This allows for some optimal control of the algae/cyanobacteria system independent of the primary mass associated with water processing and recovery, wastewater solids capture and sequestration, and shielding. As a result the growth of Algae in bags has been extensively researched and NASA has a patent on the growth of algae in bags for alternative fuel production (8,409,845).

The CO₂ removal and O₂ generation WW elements are flexible plastic bag based reactors about 5 cm thick. They have basically the same geometry as the FO water and solid waste elements but they have gas permeable membranes on the exterior of the bag. Based on the governing initial marine cyanobacteria growth and carbon uptake rates determined using BG-11 secondary wastewater simulant 3.5 m²/crewmember is required, and is semi-continuous. These will be serviced by microfiltration elements for the concentration and removal of excess algae biomass accumulation. The area ratio of microfiltration to active algae reactor is as high as 1 to 100, making the microfiltration area background noise level input to the algae reactor area design values for continuous operation.

Retirement rate of the algae-cyanobacteria reactors must still be determined in future work. Only theoretical mass accumulation rates for algae are available at this time, and retirement of algae reactor volume will likely need long term empirical testing to determined. Theoretical mass production rate for the marine algae used is 182mg/L hr. If it is assumed that microfiltration is capable of up to 3% solids (dry) on wastewater algae rejection that is 3,000 mg/L or 94% dewatering. Table 3 gives the mass balance for algal reactor operations. Table 2



Figure 14. Experimental Green Algae Growth FO Bag.

gives area progression/permanent stable shielding area accumulation rates for the algae reactor/MF filter trap system.

At this point the only limit on algae-cyanobacteria reactors is bio-fouling of membranes, which should be manageable over many month to years, and advanced algae biomass use. The primary task in Phase II is to integrate algae-cyanobacteria biomass production with its various uses, as well as determine mass balances of algae biomass and solids digester overcapacity through actual algae growth and biosolids digestion testing. However, based on the values in Tables 5 and 6 given later as well as those showing FO bag consumption area rate in the water/solids analysis, the primary sizing of the WW system is more or less complete.

Table : lgae/Ai i li i lance/flow			
Algae/Air Revitalization Mass Balance (all in per crewmember – day			
Driving Inputs		Output Algae solid	
Water Flux from FO	CO ₂	Dry Mass Algae	Same as 10% Solids
16.95L	1 kg	31.85 grams	0.3185

Algae will be rejected as a wet sludge and digester to a stable hydrated solid with 10% to 20% solids content in its permanently stabilized and/or sequestered form in the WW shield.

Table . i lgae reactors and MF algae bi .			
Area Program (per crewmember			
Continuous Operation Area		Consumable Area/Progression in Shield Growth Rate	
Algae Reactor	MF	CO ₂ /Biomass Accumulation Area	90 Fouling Are
3.5m ²	0.035m ²	6.3 X 1 ⁻ /day	3.9 X 1 ⁻ /da

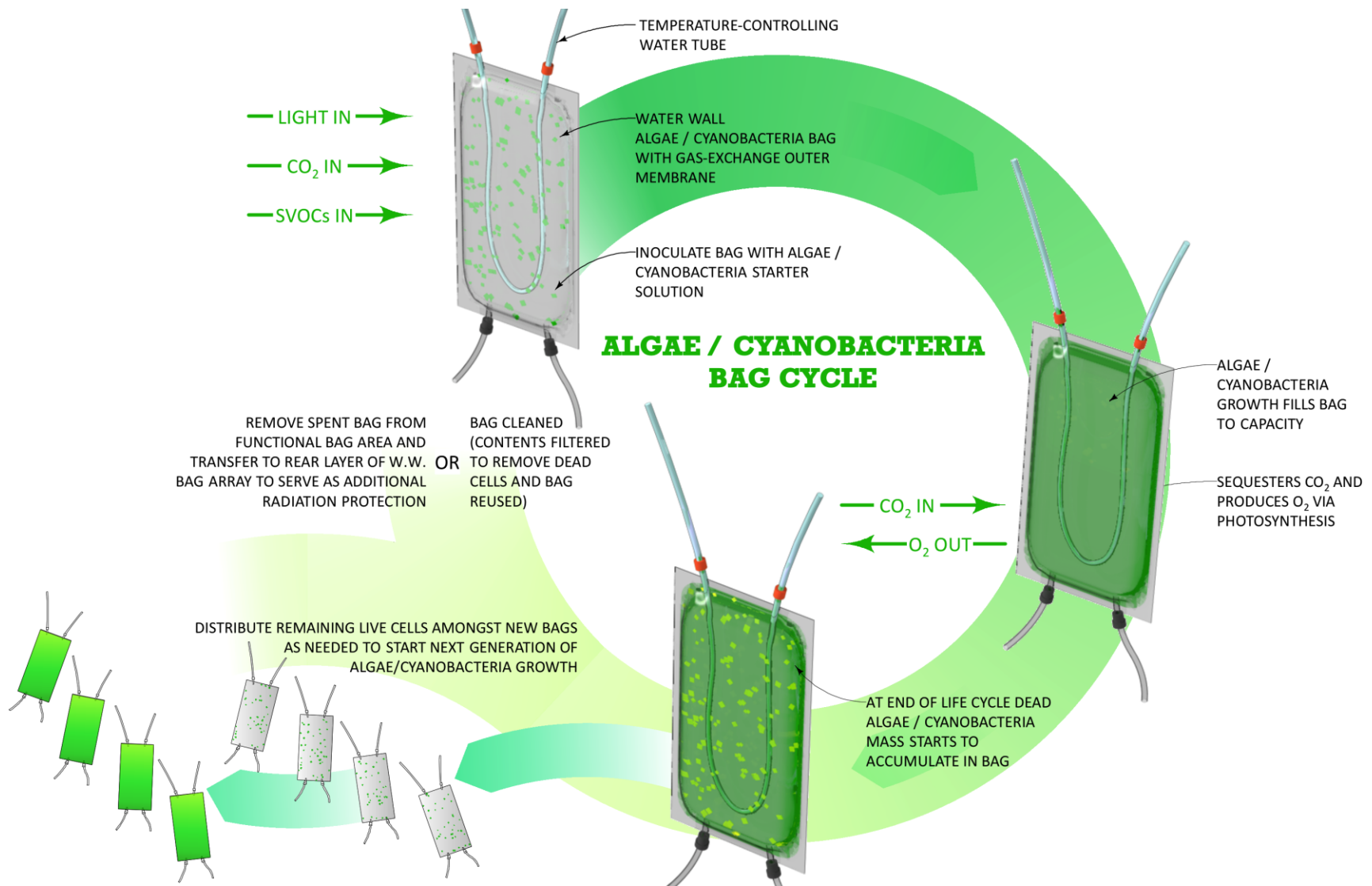
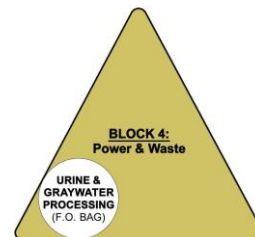


Figure 12. Operational life cycle of algae bags.

6.6 Urine and Graywater Processing

Water recycling in the WW system is accomplished using forward osmosis. Forward Osmosis (FO) is a process where the osmotic potential between two fluids of differing concentrations equalizes by the movement of water from the less concentrated solution to the more concentrated solution. Typically this is accomplished through the use of a semi-permeable membrane that separates the two solutions and allows the water, but not the contaminants, to pass through it. This flux of water across the membrane continues until the osmotic potential across the membrane is equalized and the concentrations on both sides of the membranes are in equilibrium. In wastewater treatment applications the semi permeable membrane is designed to maximize the flux of water and the rejection of contaminants. In such a system the feed, or wastewater, is passed on one side of the membrane and an osmotic agent, such as salt water, is passed on the other. The osmotic agent (OA) can use any solute with an osmotic pressure higher than that of the feed. The OA should also not permeate through the membrane. Typically sodium chloride or sugar are commonly used as OAs. The operational progression of the water recycling bag is provided in Figure 16.



6.1.2 The HTI XPack™

The WW system uses FO in a format similar to that of the commercially available HTI XPack™. In this system wastewater is placed on one side of a bag that is separated in two by a semi permeable hydrophobic membrane. On the other side a high osmotic agent (OA) potential draw solution such as NaCl or sugar is placed. The OA then draws the water across the membrane but contaminants that are rejected by the membrane do not pass. The water treatment capability of an individual bag is utilized until the membrane becomes fouled and production starts to decrease. When this happens the bag is transitioned into a solid waste function where concentrated byproduct brines, feces, and trash are placed in the bag and dewatered. The bags then become solid waste treatment systems.

Water recycling in the WW system is accomplished using a technology that is very similar to the commercially available Hydration Technology Innovations (HTI) X-Pack™ water treatment bag. The X-Pack™ is a forward osmosis (FO) water treatment bag that can be used to create a fortified drink from wastewater. The X-Pack™ is currently marketed for this application and is sold worldwide for commercial/recreational use, disaster relief, and military use. The X-pack™ is shown in Figure 17.

The procedure to use the X-Pack first requires opening the red port through which the bag is filled with wastewater. Once the bag is filled with wastewater, the red cap is resealed. Next, the green product cap is removed and the osmotic agent (OA) is poured into the inner membrane bag. The OA is composed of concentrated fructose/glucose and other food product components that make the OA a balanced and palatable fortified drink. The OA can be either a solid powder or a concentrated liquid (syrup). Once the OA is added the green cap is resealed.

When the bag has been loaded with wastewater and OA, it is allowed to process the wastewater for 6 to 8 hours. The service life of the bag is limited by the potential for biological contamination on the product side of the membrane that enters through the green port.

WASTEWATER BAG CYCLE

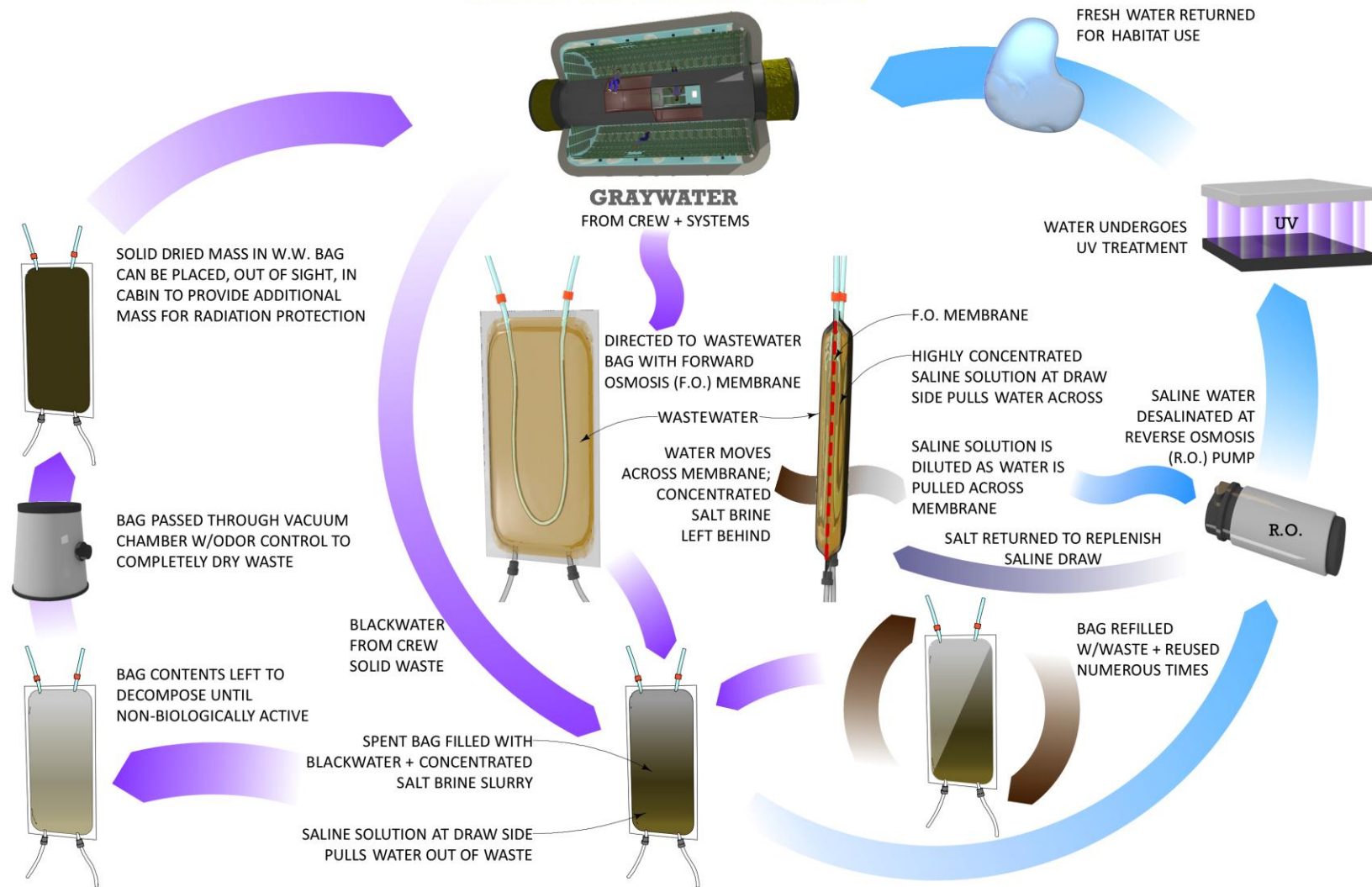


Figure 16. Wastewater Recycling Diagram

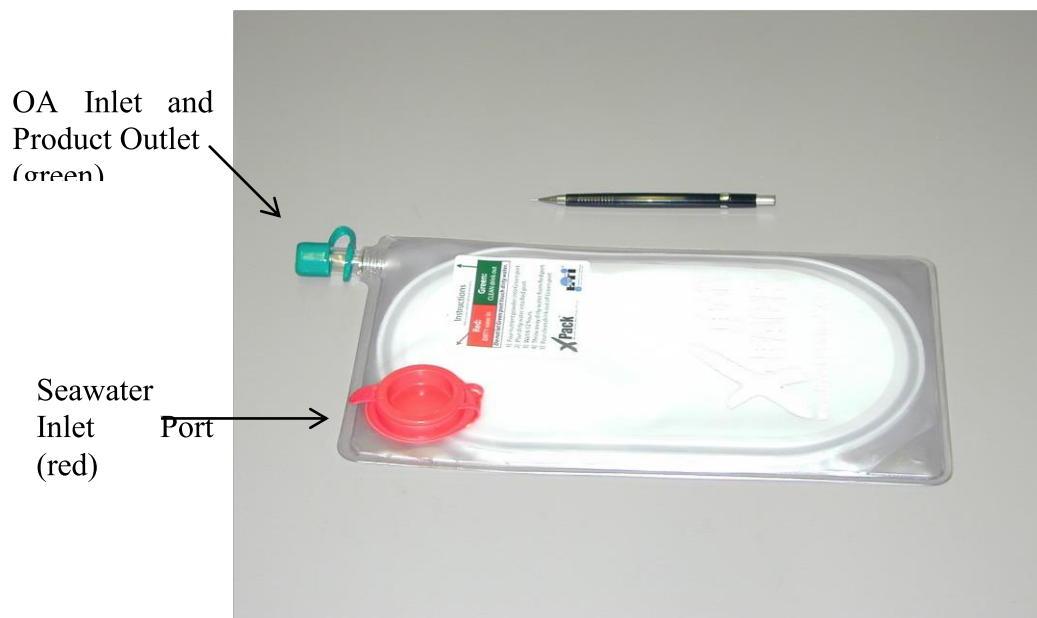


Figure 17: Hydration Technologies Inc. X-Pack™ Desalination Bag

The X-Pack™ produces 1 L of purified drink from seawater and should require about 250 g of process mass to function for the first use. This represents a 75% reduction in stored water mass. After first use, the X-Pack™ requires 200 g of OA replacement per reuse, less if it is supplied as a dry powder. The OA can also be optimized to provide a liquid diet containing all the fluids, calories, and minerals a crew member requires on an ongoing basis thus eliminating the need for stored food supplies in an emergency. The X-Pack™ is a passive device with no moving parts or electrical components. It is a simple and reliable device that is easy to use and requires little or no training to operate.

One of the advantages of FO is its inherent resistance to fouling. Conventional membrane based systems, such as reverse osmosis (RO), are not well suited for high water recovery ratio applications where solids precipitation occurs. FO systems are ideal for high solids feeds because they do not require high hydraulic pressure to operate and thus are resistant to fouling. Unlike RO, which utilizes a hydraulic pressure difference, FO utilizes an osmotic potential difference to provide the driving force for water diffusion across the membrane. As long as the ionic potential of water on the permeate side of the membrane is higher than that on the feed side, water will diffuse from the feed side through the semi-permeable membrane and into the OA. The feed stream flows are maintained at a very low hydraulic pressure and a high cross flow velocity so that contaminants are not forced into the membrane pore spaces and the membranes are not fouled.

The equipment used in FO is relatively inexpensive because it operates at low pressures. The membranes used in FO are a type of RO membrane adapted for use in the FO process. These membranes are designed to maximize the flux of water and ensure that most contaminants are rejected. Only water and some smaller, non-polar molecules permeate to the OA side.

In house testing of the X-Pack™ demonstrated the ability to treat simulated ersatz wastewater in a bag with a water recover ratio of up to 90%. The testing also measured flux rate. Flux rates are the rate at which water crosses the FO membrane and is equal to the

production rate. It is important as it defines the amount of membrane required to treat the wastewater on a given mission. The maximum flux of water in the X-Pack™ is 3.5 L/m²hr when treating wastewater. Flux rates decrease as a function of time. This effect occurs because during a run, the feed is concentrating and the OA is becoming diluted. As a result, the osmotic potential difference across the membrane decreases during the run. A run is complete when the osmotic potential equalizes and water no longer flows across the membrane.

Area values for a conservative baseline design based on our testing program appear in Table 5. The experimental results and calculation used to generate this table are presented in section 7 and are given here for a 5 cm deep bag based on initial FO bag research. Radiation protection work has modified this to 3.5 cm for radiation protection.

Table 5. Area values for FO bags in design in m ² of membrane area/crewmember day.	
Water Process; Start-up (i.e. urine and condensate based)	Water Process; Based on a Mature Habitat (i.e. hygiene water based)
0.072	0.24

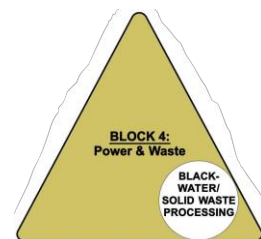
Using the values presented in Table 5 and the conservative assumption that each bag can be reused 10 times one can calculate that for a 500 day mission 3.6 m² of membrane area would be required for the start up case per person and 12 m² of membrane per person would be required for the mature habitat case.

As noted, the testing also evaluated the reduction in flux that occurs as the bag is reused. Each bag was reused 10 times during this experiment. During each run, solids were formed and some of these solids stayed on the membrane surface. The membranes were rinsed between uses but not cleaned, and no mixing during a run occurred. As the runs proceeded, these solids inhibited the flux of water across the membrane. During these tests the flux rate decreased by about 25% after 10 reuses of the bag.

The results of this experimental testing demonstrate that the concept of a membrane based FO water treatment system integrated into the walls of a water wall is feasible. The system will treat wastewater and achieve a high water recovery ratio. The FO membranes are reusable but their life will be limited as the flux rate decreases with every reuse. Product water purity has been analyzed and is available in Gormly et al [Gormly, 2007]

6.7 Blackwater and Solids Processing

Solid waste treatment is the processing and dewatering of solid wastes to produce structural elements that aid in radiation protection. It is completed in several steps. The first step is the collection of the concentrated brines that are produced as a result of the water treatment function. These brines are then combined with feces and wet trash and placed in a FO bag, Figure 18 a. A concentrated salt solution is then used to dewater these solids. Once the solids are partially dewatered biological composting is allowed to take place. Composting is used to reduce the potential of pathogenic organisms growing in the solid waste and rendering the waste biologically inactive. This solid is then fully dried by venting to the vacuum of space or through a vacuum pump. At the end of this process the solids waste are dried to a biologically inactive dense tar like substance contained in a bag. Figure 18 b shows the solids at the end of this process with the bag cut open to expose the solids inside. A picture of the final dried product removed from the bag is shown in Figure 18 c.



All of these steps are completed in an FO bag much like an enlarged XPack™. The urine brine and feces are directly placed in the FO bag and dried in place. The result is a structural material that is composed of human waste and is used for radiation and structural purposes. In fact, in this approach the inflatable structure eventually becomes a rigid structure as more and more of these bags become filled with solid waste and processed. Figure 19 shows the conceptual progression of this conversion.

The progression of this approach to process in solid waste and the integration of the solids waste and liquid waste processing step using the bags are presented in Figure 16. This figure shows how bags are first used for liquid waste treatment and then transitioned into solid waste treatment and then ultimately converted into solid waste tile structures that are affixed to the inside or outside of the spacecraft to provide radiation protection

The results of this testing and previous investigations [Flynn, 2011] can predict the amount of active membrane area that would be required to treat the solid waste, urine brine and feces. Table 6 provided our prediction for membrane use requirements.

Table 6. Modified area values for FO bags in design in m ² /crewmember day.	
Solids; Start-up Habitat (i.e. urine and condensate based)	Solids; Mature Habitat (i.e. hygiene water based)
0.019	0.22

Using the values presented in Table 6, a 500-day mission would require 9.5 m² of solid waste membrane treatment capacity per person. For a mature habitat, one with hygiene water, 110 m² of membrane area would be required.

The WW approach converts what is traditionally a problem, for conventional systems into a benefit. For example, on ISS the Urine Processing Assembly (UPR) has failed do to precipitation of calcium based solids. As a result in 2009 ISS had to replace this unit on orbit and then operate it at a lower water recovery ratio. As a result ISS is currently running on a negative water balance and will require resupply of water. This mode of failure does not exist in the WW system. WW ultimately recycles 100% of solids so everything is taken to a dried solid. The calcium that caused the UPA to fail on ISS is the glue that holds the structural solids of the WW system together, and it turns a negative into a positive.

6.8 Bioelectrochemical System (BES)

Energy from waste systems are being developed to provide localized low power sources for the WW system to eliminate the need for complicated wiring harnesses to provide power to sensors, valves, and even small pumps. This approach provides localizes power generation adjacent to the power consumer. So, for instance a low power valve or sensor could be powered by solid waste in an adjacent bag. A sensor could be continuously powered. A higher powered intermit operation actuator, such as a valve, would be powered by a battery that was then recharged. In either case, a bioelectrochemical system can provide this power. The Water Walls project has baselined a Microbial Fuel Cell (MFC) to provide this utility. Running the MFC on human waste would provide the power source.

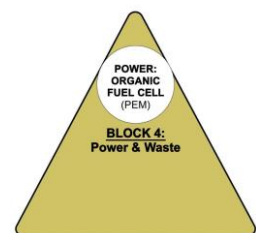




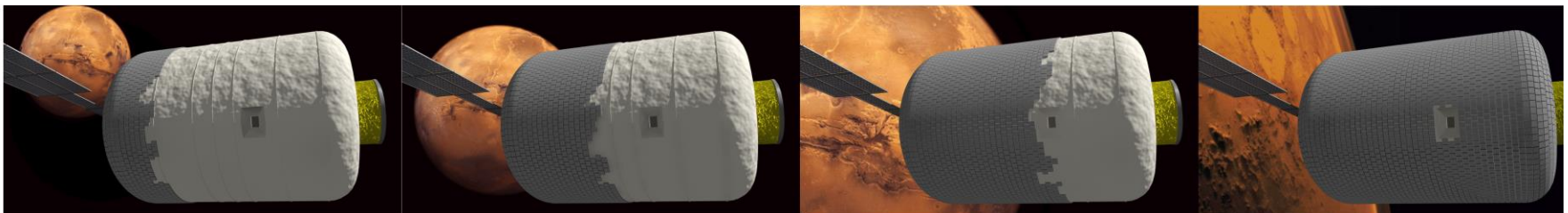
Figure 18 a. XPack filled with fecal simulant and urine brine at start of experiment.



Figure 18 b. XPack cut open to show solids material at the end of the experiment



Figure 18 c. Solid material removed from the XPack to show that it is a dense tar like solid.



Time 1

Time 2

Time 3

Time 4

Figure 19. Architectural Rendering: Conversion of inflatable structure with time to rigid structure due to accumulation of human metabolic byproduct solids in WW bags.

Microbial fuel cells utilize microbial functions to produce an electrical current, or to catalyze a reaction with the addition of an electrical current [Rabaey, 2004, Logan, 2006, Ghangrekar, 2006, & Ishii, 2012]. While there are many configurations for the functionality of MFCs, the classic design, as illustrated in Figure 17, involves two electrode chambers, an anode and a cathode, that are separated by a proton exchange membrane (PEM). The design and components of each electrode chamber are dependent on the desired result or product of the overall system, and can involve microbial cultures or communities, electrolytes, electrochemical reactions, and water.

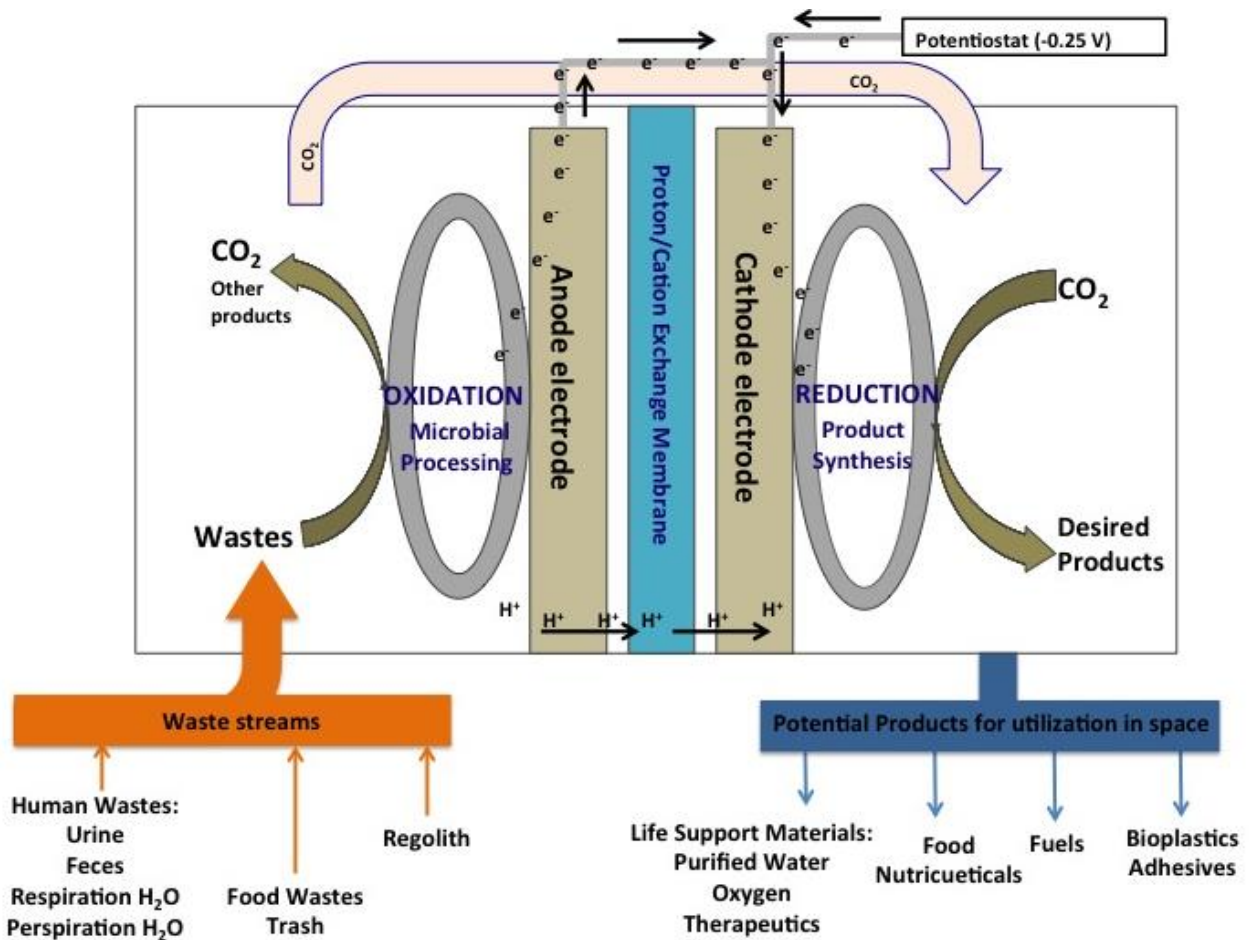


Figure 20. Schematic of potential MFC application for space exploration.

Figure 20 illustrates the potential inputs and products that are targeted for MFC use during space exploration. The synthesized product is dependent on the waste stream used as an input, and the species or community of organisms used within the system.

The microbial functions that are commonly exploited within MFCs are oxidation and reduction reactions, or “redox reactions” [Rabaey, 2004, & Logan, 2006]. Oxidative reactions occur when a molecule or compound loses electrons, acting as an electron donor, which results in the molecule or compound having a more positive charge. Reduction reactions occur when a molecule or compound gains electrons, acting as an electron acceptor, resulting in a negative charge. In MFCs, reduction reactions always take place at the cathode, and oxidation reactions

always take place at the anode [Renslow, 2011]. Electrons are conserved in MFCs, maintaining no net change in charge within the system.

The movement of electrons from one molecule or compound to another provides an exchange of energy that is used to fuel metabolic processes within the system. Conductive electrodes permit electric currents to be added to the system, typically to the cathode chamber, and electric potentials to be measured from the anode chamber. The energy flow within MFCs is defined by the configuration of the system, in either a forward or reverse fashion.

Forward MFCs utilize microbial metabolism, such as the metabolism of organic substrates, to generate electrical power. The measurements of generated current are dependent on the species of microbes used, the medium and electrolyte solutions utilized, the size of the system, and the materials used for electrode construction. Our testing activated sewage sludge feed in a 100 gal MFC demonstrated power densities on the order of 1 W/m² of electrode area. Prediction of where this power density could go in the future run as high as 4 W/m² of electrode. Conversely, reverse MFCs use an additional electrical current to catalyze microbial metabolism, which often results in the synthesis of products.

The reverse MFC configuration (microbial electrosynthesis) is ideal for the recycling of resources and the synthesis of products in space environments, while forward MFC configurations are used for the modest generation of electric current from existing waste streams. Additionally, the energy produced at the anode can be exploited to drive cathode reactions, thereby reducing overall system power requirements.

6.9 Radiation Protection

Radiation protection is arguably one of the biggest obstacles to long duration human space flight. Without adequate protection it can be deadly. The ionizing radiation affecting humans during spaceflights comes from three different sources and consist of every known particle including energetic ions formed from stripping the electrons from all of the natural elements. The three sources of radiations are associated with their different origins identified as:

- Particles of galactic origin, Galactic Cosmic Rays (GCR)
 1. Particles produced by the acceleration of the solar plasma by strong electromotive forces in the solar surface and propagating through coronal mass ejection, Solar Energetic Particles (SEP)
 2. Particles trapped within the confines of the geomagnetic field (Van Allen Belts).

Occupational radiation exposure from the known space environment is sufficiently severe that it may increase cancer morbidity or the mortality risk in astronauts. A long-term human mission to Moon or Mars will not be feasible unless adequate shielding and counter measures are developed. Many believe that the major obstacle to human space exploration at this time is the limitation imposed by the adverse effects of long-term radiation exposure in the space environment and the cost of providing adequate protection.

The effects of radiation can be mitigated by providing radiation shielding. There are two primary approaches to providing radiation shielding. They are the use of a polyethylene liner and the use of a water wall surrounding the habitat volume of the spacecraft. These materials are preferred do to their high hydrogen densities. In either case protection can be provided by tens of centimeters of these materials for SPE and meters for GCR. The resulting impact on mission mass is substantial. For a 240 day mission with a 150 mSv career dose limit and an ISS derived

cylindrical habitat, 130,000 kg water or polyethylene would be required. For the same mission where solar radiation protection is all that is required, a 20 cm thick water wall would require 25,000 kg.

A life support system for a 6 person Mars transit mission would require 16,642 Kg of equivalent system mass, based on ISS derived hardware [Duffield, 2008]. If a surface stay is part of the mission this mass rises to 52,996 Kg. By using the mass of the radiation water wall to offset the mass of life support significant mass savings can be potentially realized.

The approach also allows the base radiation protection water mass to be derived sources already on orbit. Water to fill the water wall can be provided by contaminated wastewater such as the concentrated brines that are being generated on orbit by the ISS water recycling system (WRS). This byproduct of operation of the WRS is currently considered a waste and returned to Earth for disposal. A 6 person crew producing 15 L/person-day of wastewater with an 80% recovery ratio will produce 6500 Kg/year of concentrated wastewater byproducts. It would require 4 years of operation at this rate to accumulate enough water to provide a SEP water wall for a single ISS element. If there were 24 people living in orbit, it would produce enough waste brine to provide GRC protection in an ISS module after 5 years.

For radiation protection the WW system will use layers of 3.5 cm deep water bladders to provide a continuous layer of protection, see Figure 5, 6, and 7. In combination with other elements in the inflatable habitat wall, 7 to 9 layers could provide protection that reduces the unshielded GCR dose to between 39% and 36% of the unshielded GCR dose, and almost complete protection against SPE. Table 7 provides an analysis of the radiation protection potential of the WW bladders for both SPE and GCR. The bases for these calculations are provided in Section &.

Table 7: The radiation shielding effects of mature multi layer WW.				
Profile of layers, 3.5 cm each in depth, no Al, deep space	$\delta D/\text{layer}$	Daily SPE dose	$\delta D/\text{layer}$	Daily GCR dose
Unshielded	0.000	19.178	0.000	3.288
1 st layer H ₂ O 3.5 cm	83.711	3.124	0.160	2.760
2 nd layer	45.698	1.650	0.145	2.335
3 rd layer	31.359	1.136	0.131	1.995
4 th layer	23.902	0.842	0.118	1.730
5 th layer	19.318	0.654	0.107	1.528
6 th layer	16.228	0.505	0.096	1.379
7 th layer	14.009	0.371	0.087	1.276
8 th layer	12.345	0.237	0.079	1.209
9 th layer	11.056	0.096	0.071	1.174

Considering the career dose limit of 520 *mSv* for a 25 *years* old male astronaut, a 10 *layer* (35 *g/cm²*) WW would guarantee a safe deep space mission for more than 440 *days*

for GCR. For a 30 years old male astronaut subject to a career dosed limit of 620 mSv, an 8 layer WW would guarantee enough protection for a 500 days mission to Mars. With such a protection, the most acute dose-rate of $500 \frac{mSv}{hour}$ calculated for the King SPE will be almost neglected, dropping this value to about $6 \frac{mSv}{hour}$. Considering a total SPE exposure dosage of 1200 mSv in the unshielded case corresponding to year 1972, during which occurred the King SPE, and assuming a constant distribution over the year, a 2 layer WW will drop this value to about 103 mSv, which is about one fifth of the career dose limit mentioned above. A 6 layer WW, which corresponds to about 20 g/cm² of water, would increase the astronaut's protection by dropping this value to less than 32 mSv/year. A 2 layer WW will not be enough to shield humans in deep space from neither GCR nor SPE, but it will definitely guarantee to not exceed the current dose limits in LEO when severe solar events happen, moreover if used in combination with the conventional shielding mass of the ISS's walls.

6.10 Summary Specifications for a Water Walls Application

Table 8 provides a summary of the specifications for the WW system based on sizing data for the subsystem level definition. Data used to complete it is taken from the proceeding sections and the section to follow. This data is modified for a 500 day 6 crew member mission. The radiation protection is sized for SPE protection only assuming use of a BA 330. This assumes the use of a 2 layer deep array of bags to provide SPE protection. The BA 330 inflatable has approximately 270 m² of internal surface area.

Table 8. WW system design parameters for a 500 day 6 person transit mission in a BA 330 providing only SPE protection.				
	Area m ²	Volume m ³	Mass Kg	Power W
1. Climate Control				
Humidity Control - Latent Heat	56	2	2000	tbd
Thermal Control - Sensible Heat	tbd	tbd	tbd	tbd
2. Contaminant Control				
Semi-Volatile Removal	tbd	tbd	tbd	tbd
Volatile removal	tbd	tbd	tbd	tbd
3. Air Revitalization				
CO ₂ Removal & O ₂ Production	29	1.0	740	tbd
4. Power and Waste				
Water recycling	216	8	8000	tbd
Solid waste Treatment	57	2	2000	tbd
Energy from Waste	12	0.04	40	+48
5. Radiation Protection				
Water Wall	270	19	19,000	tbd
Shelter in place	< 270	tbd	tbd	tbd

tbd = to be determined in phase II

The BA 330 has an interior volume of 330 cubic meters (12,000 cu ft). It is 9.5 meters (31.2 ft) long by 6.7 meters (22 ft) in diameter. It weighs weighing between 20,000 kilograms (45,000 lb) and 23,000 kilograms (50,000 lb). For this study we have assumed that it contains an internal surface area 270 m². Based on the sizing completed through this proposal, the WW system will require 370 m² of membrane area which can be correlated to the internal surface area. This sizing value assumes that semi-volatile removal function of the Contaminate Control functions are integrated into Air Revitalization and Climate Control subsystems. This functionality is called out in Table 1. Therefore, if we assume that the BA will have a minimum of 2 layers of bags to provide for SPE protection then the WW functionality will completely cover the first layer of bags and about 35% of the second layer, resulting in a factor of safety in our sizing of 32%, meaning that the sizing could be off by 32% and still fit within the tow bag layer constraint of the BA 330. This configuration is shown in Figures 5, 6, and 7.

In addition, the total mass of the WW would be 19,000 kg, which is equal to the mass of the radiation protection water wall alone. This would displace about 16,642 (from 240 day Mars Transit Mission) of life support ESM using traditional ISS derived system. Thus the 19,000 kg WW system would displace a 36,000 conventional system with radiation protection and life support functions included (46% reduction in system mass). Note that these calculation are based on preliminary design data. In addition, it is possible to generate this 19,000 kg from waste residual brines generated on orbit by ISS crew or commercial crewed missions. The WW system is uniquely capable of treated these high solids wastes.

6.11 Technology Readiness Levels

The WW Subsystems are composed of a variety of component level technologies that exist at differing levels of technology readiness. Some of the elements such as water and waste treatment are developed to a higher level and sizing is based on our experimental program and others such as trace contaminate and thermal control are less developed and design parameter are based on literature values. The corresponding technology readiness levels (TRL) of each Subsystem and the components that make up each subsystem are summarized in Table 9.

1. Component Level: Membranes, Process Cells, and FO Bags

This section takes an in depth look at a few of the subsystems from the perspective of the components that make up their functionality (Figure 21). These components include the higher TRL algae growth units, the wastewater treatment units, the solid waste treatment units, and the microbial fuel cells. The discussions in this chapter present the laboratory research which is relevant to determining production rates for each of these components so they can be sized to fit the WW concept. The Air Revitalization algae experiments exemplify new lab research conducted with funding from this proposal. The results

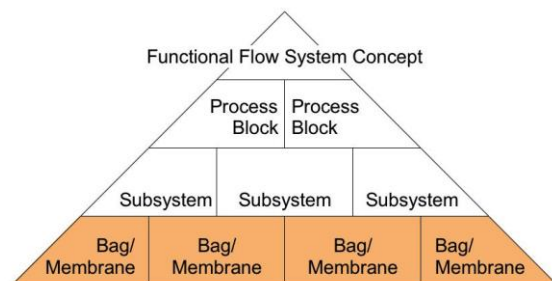


Figure 21. Water Walls System Concept Level Component Level Bags and Membranes.

The results

for Block 4, Power and Waste were at least partially funded through other sources, specifically the water, MFC, and part of the solids waste. Some solid waste work was funded through this proposal.

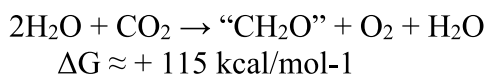
Table 9. Technology Readiness Level (TRL) of the WW Elements		
Process Block & Subsystem	TRL	Discussion
PB 1. Climate Control		
Latent heat - Dehumidification	2	Analysis
Sensible heat Thermal Control	2	Analysis
PB 2. Contaminant Control		
Semi-volatile Removal	2	Analysis
Volatile removal	2	Analysis
PB 3. Air Revitalization		
CO ₂ Removal & O ₂ Generation Algae Growth Nutritional Supplement	2-3	In house experimentation and analysis for biofuels research
PB 4. Power and Waste		
Water recycling	6	Flight test on STS 135
Solid waste Treatment	4	Experimental testing using fecal simulant
Energy from Waste	3	Currently constructing first functional prototype
Radiation Protection		
Water Wall	4-5	Beam testing, analysis, and field tests
Shelter in place	4-5	Beam testing and analysis

7.1 Algae Growth Units as Components in a Life Support System

This chapter presents Carbon Dioxide Removal and Oxygen Production accomplished through the use of algae growth units.

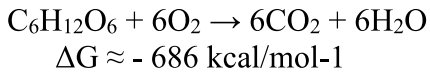
7.1.1 Light Reaction and Mass/Area Balance for CO₂

The basic light and mass balance reactions are well understood for algae. Photosynthesis is given as follows:



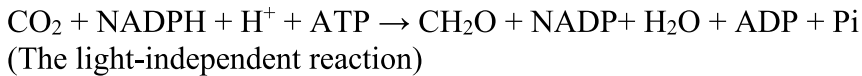
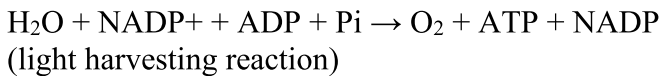
“CH₂O” is an environmental engineering short hand for more complex and varied carbohydrates, and represents all the carbohydrate associated with biomass production. The reverse of this reaction is aerobic respiration:





The second equation is normally written for simple sugars and has an energy equivalent of slightly less than 6 times the above formation reaction based on carbon balance, and the realities of the second law of thermodynamics as it applies to chemical physics ($115 \times 6 = 690$, and 686 results from the a small inefficiency in the reverse reaction).

Functionally this simple equation drives a two-step energy capture and conversion process given by [Graham, 2009].



With unlimited nitrogen and other trace nutrients one can expect algae biomass to utilize up to 50% of the CO_2 available and likely return 10% + by weight as biomass production based on lab empirical experience these flexible bag like reactors, as demonstrated in previous Ames Research Center biofuels research using a similar flexible bioreactor [Wiley, 2013].

Sizing and utility for air algae/cyanobacteria reactors for CO_2 will be decoupled from the area sizing of the water and solids system by the careful manipulation of nitrogen species, and other low weight micronutrient additions within the osmotic agent for FO, which will function as the growth medium for the algae in a mature system. In this way the air revitalization algae reactor bag area function calculation can be based solely on the CO_2 to O_2 conversion area requirements, and treated as a 5 cm depth flat sheet light reactor, with the balancing interface between the water/solid bags and the algae/air bags being control by small scale manipulation in the connecting water loop (the Osmotic agent (OA)/algae/cyanobacteria growth medium common loop). The initial water/solids “start-up” system low operation on the water/solids only area calculation given in the previous section can be seen in Figure 22. Figure 23 adds the components necessary to incorporate initial algae/air scrubbing.

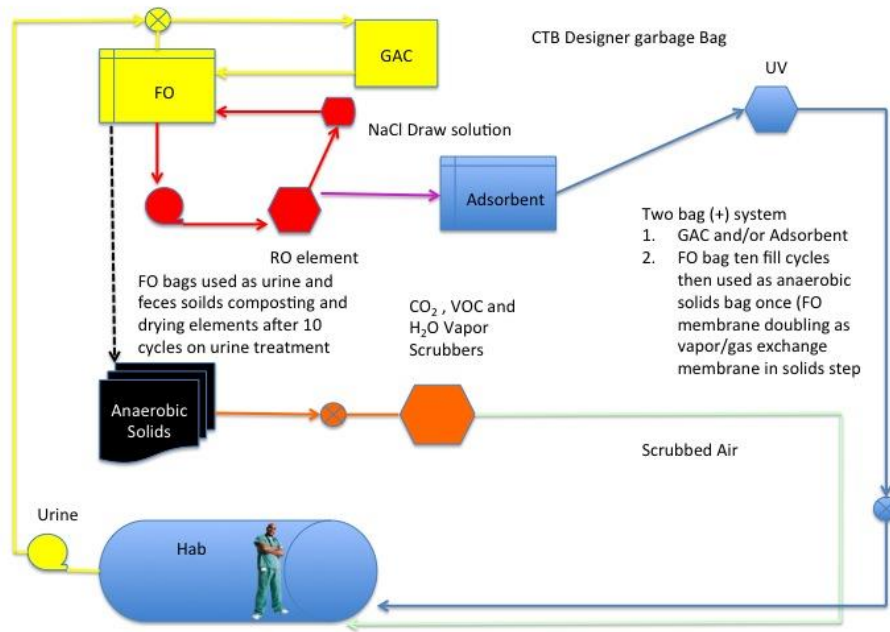


Figure 22. The water/solids “start-up” system baseline flow schematic.

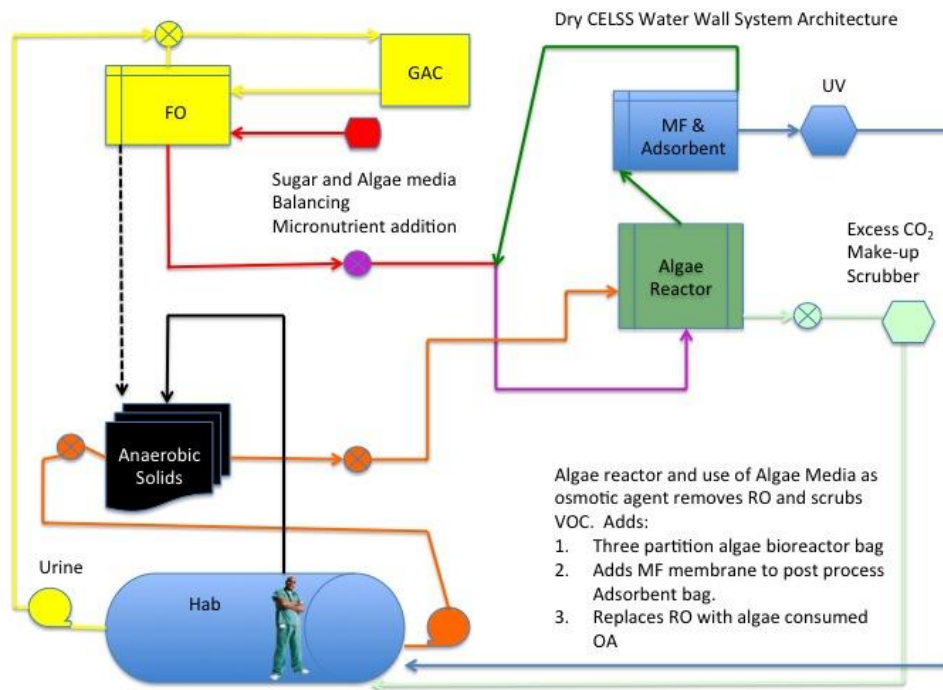


Figure 23. The initial air scrubbing system schematic.

1.1.2 Nitrogen Mass Balance and Other Factors

Ammonia nitrogen is a more challenging proposition to control than the CO₂ and H₂O. Urine in transit mission waste and the concentrated ammonia nitrogen loading of all habitat wastewater streams indicates that vapors containing large amounts of ammonia are a particular concern. The limiting nutrient in most growth scenarios for algae is bioavailable nitrogen [Graham, 2009] but not for cyanobacteria due to their nitrogen fixing capability. Nitrogen in the form of ammonia is bioavailable for algae. The C:P:N ratio for algae biomass is roughly 105:1:15 [Tchobaoglous 1991] when operations in secondary effluent biomass design. This indicates that stable algae biomass can uptake a substantial amount of nitrogen and fix it for later thermal stabilization. At the same time small to mid-sized trace organic contaminants (SVOCs/VOCs and/or toxic trace organics) would be dissolved in water and then absorbed by the biomass, where they are also sequestered for thermal processing.

Note: The distinction between Semi-Volatile Organic Carbon (SVOC) and Volatile Organic Carbon (VOCs) is an important one for the physical/chemical process research engineer in life support recycle systems, but is more or less wholly absent from distinctions of biological unit process engineering in wastewater. This difference can generate a language barrier between life support researches and mainstream environmental process engineering. So for the purpose of clarification, the wording in the WW mass balance discussion and referencing we will use VOC to describe more or less all organic carbon that is not part of colloidal or gross particulate matter, in this particular discussion.

7.1.3 Carbon Dioxide Sequestration (CO₂/O₂) initial (Phase I, NIAC) Testing

In the reactors, the total organic carbon is directly related to the amount of CO₂ fixed, because all of the organic carbon is derived from carbon in CO₂. Studies have suggested that the biofixation of CO₂ by cyanobacteria in photobioreactor systems is a sustainable strategy, since carbon dioxide can be incorporated into the molecular structure of cells in the form of proteins, carbohydrates and lipids by way of photosynthetic reactions. The advantages of these processes are related to the greater photosynthetic efficiency of cyanobacteria compared to eukaryotic algae and higher plants, as well as the resistance of these microorganisms to high carbon dioxide concentrations, and the possibility of better controlling the culture growth conditions.

In addition, the biomass produced by the bioconversion of carbon dioxide allows one to obtain products of high added value, such as, fuel or food. According to Lee et al. [Lee, 2006] and Jacob-Lopes et al. [Jacob-Lopes, 2007], only part of the carbon dioxide injected into the photobioreactors is incorporated into internal cellular biomass, the remainder goes into the formation of extracellular biopolymers (extracellular biomass as defined in environmental process engineering), as well as inorganic precipitates such as carbonates and bicarbonates and volatile organic compounds (VOCs). Note that in the analyses done for this proposal the extracellular biopolymers were taken into account but the carbonates were not because their decomposition temperature is above the temperature used for combustion in our tests.

Initial testing utilized BG-11 algae growth medium. BG-11 is traditionally used as a secondary effluent feed simulant, which is to say it has a nutrient balance that simulates the water encountered in the secondary clarifier of a wastewater treatment plant, after primary settling has occurred. This provides us a rough, though admittedly imperfect initial approximation of the feed contaminant environment of the osmotic agent (salt water draw solution) loop of the FO bag element-based system. Thus it is used to initially size an algae/cyanobacteria reactor running on the FO product brine, prior to the production of large quantities of FO brine from actual human waste.

7.1.4 Materials and Methods

Pure cultures of the freshwater *Anabaena* (PCC 7120) were obtained from the ProvoSolli-Guillard culture collection and the marine *Synechococcus* (BG04351) was obtained from the Hawaii culture collection. *Anabaena* cultures were maintained and grown on BG-11 medium (Sigma-Aldrich) and *Synechococcus* cultures were maintained on BG-11, to which 30 g/L of commercial sea salts (Sigma-Aldrich) were added.

This 30 g/L corresponds to the baseline osmotic agent reference concentration for FO flux/performance testing and FO membrane operational assumptions used in water/solids sizing (and the data from previous FO bag testing and development. It is effectively seawater strength salt water/brine and function as the baseline flux assumption for most FO membrane test rating/published performance specifications to date. And thus function as a convenient benchmark for assessing competing FO membranes and their derived elements.

Ten mL of mid log-phase cultures of *Anabaena* and the marine *Synechococcus* were used to inoculate 500 mL Erlenmeyer flasks containing 100 mL of either BG-11 medium (*Anabaena*) or BG-11 to which 30 g/L of commercial sea salts (Sigma-Aldrich) were added (*Synechococcus*). In addition one mL of mid-log-phase cultures were used to inoculate 9 mL of medium contained Opticell membrane systems. The flasks and Opticell systems were incubated at room temperature (22 °C) under ambient room fluorescent lights (16 hrs on 8 hrs off) for 7 to 14 days. After incubation the total organic carbon content of each culture was determined by combustion compatible with Standard Methods for the Examination of Water and Wastewater, 2012, Total Organic Carbon, High-Temperature Combustion Method 5310 B. Briefly, Samples for combustion were dried overnight at 80 °C. The dried samples were weighed then heated for three hours at 600 °C and re-weighed.

1.1.5 Resulting Mass, Volume, and Reactor Area Analysis

The overall rate of CO₂ fixed by *Anabaena* was 5.36×10^{-5} g CO₂ fixed cm⁻² hr⁻¹. This equals 53.6 mg CO₂ fixed L⁻¹ hr⁻¹, very close to the published value of 55 mg fixed L⁻¹ hr⁻¹ under similar conditions. The overall rate of CO₂ fixed by the marine *Synechococcus* was greater, equaling 25×10^{-5} g CO₂ fixed cm⁻² hr⁻¹, equaling 250 mg CO₂ fixed L⁻¹ hr⁻¹. The reasons for the difference in results between the freshwater and marine cyanobacteria are under investigation. Ongoing tests include conducting similar experiments using species of the green alga *Chlorella*, and the edible cyanobacteria *Spirulina*. The next major step is to examine CO₂ fixation rates in the WaterWalls candidate bags.

Sizing parameters from CO₂ sequestration results for freshwater *Anabaena* (PCC 7120) cultures:

CO₂ When scrubbing = 53.6 mg CO₂ fixed/L/hr. or 5.36×10^{-5} kg CO₂ fixed/L/hr.

5.36×10^{-5} kg/L/hr. x (24) hrs. = 1.286×10^{-3} kg/L/day

1 kg CO₂ produced per crewmember/day

$\frac{1 \text{ kg/day CO}_2 \text{ exhaled}}{1.286 \times 10^{-3} \text{ kg/L/day}} = 777.3 \text{ L } Anabaena \text{ required per crewmember per day for CO}_2$

Since 1000 L of water = 1m³ of water (visualize as a 1m x 1m x 1m water column)

1m = 100 cm, therefore $\cong 800\text{L}$ *Anabaena*/water solution (777.3 rounded up for significant figures) = 0.80m^3 (1m x 1m x 80cm water column)

(5cm = max. depth of *Anabaena* bags if illuminated on both sides)

80 cm = (22) m^2 *Anabaena* bag surface area @ 5 cm thickness per crewmember
5 cm at any given time. (5 cm = max. thickness of cyanobacteria bags if illumination on two sides)

For CO₂ sequestration results for marine (i.e. salt water/OA compatible) *Synechococcus* (BG 04351) cultures:

CO₂ When scrubbing ambe = 250 mg CO₂ fixed/L/hr. or 2.50×10^{-4} kg CO₂ fixed/L/hr.

2.50×10^{-4} kg/L/hr. x (24) hrs. = 6.0×10^{-3} kg/L/day

1 kg CO₂ produced per crewmember/day
= 1 kg/day CO₂ exhaled
= 166.7 L *Synechococcus* required per crewmember per day for CO₂
 6.00×10^{-3} kg/L/day

Since 1000 L of water = 1m^3 of water (visualize as a 1m x 1m x 17cm water column)
1m = 100 cm, therefore $\cong 170\text{L}$ (166.7 rounded up for significant figures)
Synechococcus/water solution = $.17\text{m}^3$ (1m x 1m x 17cm water column)

(5cm = max. depth of *Synechococcus* bags if illuminated on both sides)

17 cm = (4.8) m^2 (round to 3.5m^2) *Synechococcus* bag surface area (@ 5 cm thickness)
5 cm per crewmember at any given time).
(5 cm = max. thickness of cyanobacteria bags if illumination on two sides)

Note: the light penetration depth required is 2.5 cm, and responds poorly to any modification in any tested bioreactor (i.e. mixing and water column light penetration devices like optical fibers have repeatedly showed little effect when compared to flat sheet reactors, based on volumetric biomass efficiency).

Experience in fuel reactors indicates that the lower bound of nitrogen is in the range of 40 mg/L for wastewater processed when achieving maximum productivity on native wastewater algae. At 16.95 L/crewmember day that is a balancing nitrogen requirement of 678 mg of bioavailable nitrogen per crew member day for an annual requirement of 247 grams (1/4 kg) of nitrogen fertilizer (dry weight as NH₃ and NO₂⁻ equivalent) addition to the OA draw loop supplying the algae reactor bags from the water/solids bags per crewmember year. This is well within an incidental control chemistry allotment for the habitat start-up. It is likely that the nitrogen bleed through the membranes will supply most of this nitrogen, but this addition rate is well below the amount that would be consider a major resupply if it was all provided externally.

Iron and other micronutrients could be added in at rates that would bring the potential algae maintenance dry chemistry requirements up to the point that a BG-11 like medium would safely

result when accepting FO product water at seawater level salt concentration, without exceeding a maintenance supply chemistry requirement of greater than ½ kg/crewmember year. The bleed rate of ammonia nitrogen across the FO membrane into the OA/growth media will offset the need for most if not all of this nitrogen addition, but is unpredictable based on the variable properties of human waste and treatment timing, so 100% backup on nitrogen fertilizer for algae is a safe starting position until optimized in advanced development.

Thus, CO₂/O₂ conversion can be run on FO produced salt water media with a low level of nitrogen and micronutrient addition, effectively decoupling the air/algae-cyanobacteria reactor area/volume requirement from the water/solids area/volume requirement calculation given earlier. Power and humidity control are still in advanced development and are not sizeable at this time. However, these are secondary benefit enhancements, with air/water/solid waste cycle closure and rationally sized possible at this time.

The other major role the algae/cyanobacteria reactors can prove is trace air contaminant control. Industrial high rate bio-air scrubbing is a mature air emissions control technology used throughout the food processing and wastewater management industries. This requires far less volume to produce effective results than CO₂/O₂, and will not affect sizing of the algae/cyanobacteria reactor area or volume. However, it will be examined here as a primary beneficial function that will likely be available before carbon sequestration and oxygen recovery benefits of the algae/cyanobacteria reactors come fully on line.

1.1.6 Trace Containment Control

Initially, algae air processing achieves a more immediate payback potentially for odor control and trace gas management, than CO₂ to O₂ recovery as is often assumed. Small volumes and areas of algae-cyanobacteria reactors can have profound effects on trace contaminants. This is not a small or secondary function, but rather an important primary air processing function.

Bio-air scrubbing has been used in industrial air pollution control and most particularly odor control for some time [Devinsky, 1999]. Models for trace contaminant control can be projected based on these industrial air pollution control systems. The technology of gas exchange membranes is also well developed. These membranes are based on hydrophobic (liquid water rejecting) gas permeable membrane elements. These membranes will pass CO₂, CH₄, NH₃, and O₂, and other semi-volatile organics, but will not allow liquid water to pass through them.

These membranes have been employed as internal diffusers for CO₂ in algae bioreactors which resemble flexible clear plastic bags with internal gas exchange membranes (Figure 24) and could be used to provide NH₃, CO₂, trace toxics and odor related VOC removal from the cabin and process gases.

1.1.7 Algae Metabolism Utilization Calculations

One point of clarification on the biology selected. In most cases VOC and odor scrubbers use microbial culture referred to as “bacteria” not “algae”, but most “micro-algae” used in wastewater treatment are cyanobacteria, so we are really selecting for a microbial community that is both an odor control “bacterial turf scrubber” while also having a photosynthetic gas exchange metabolism dominant in the culture. By using conditions that select for cyanobacteria of specific types we get a way to control the bioreactor and use only phototrophic high O₂ algal “bacteria” that we can multi-task. In this way a beneficial community is maintained in the VOC scrubber while potentially developing the future CO₂ scrubber over time. Once said it should be

pointed out that the near term use of the algae for VOCs also minimizes the production of algae biomass which would also be a draw back of biological CO₂ scrubbing at a larger scale.

An algal metabolism is usually presented based on CO₂, but in fact is more often limited by nitrogen availability (unless the community has nitrogen fixing cyanobacteria among its members), light limitations, and CO₂ bioavailability due to speciation in water (i.e. CO₂/CO₃⁻ balance). These factors are more important and relevant to the function of the algae metabolism, and thus the design of an algal reactor based air scrubbing water wall element.

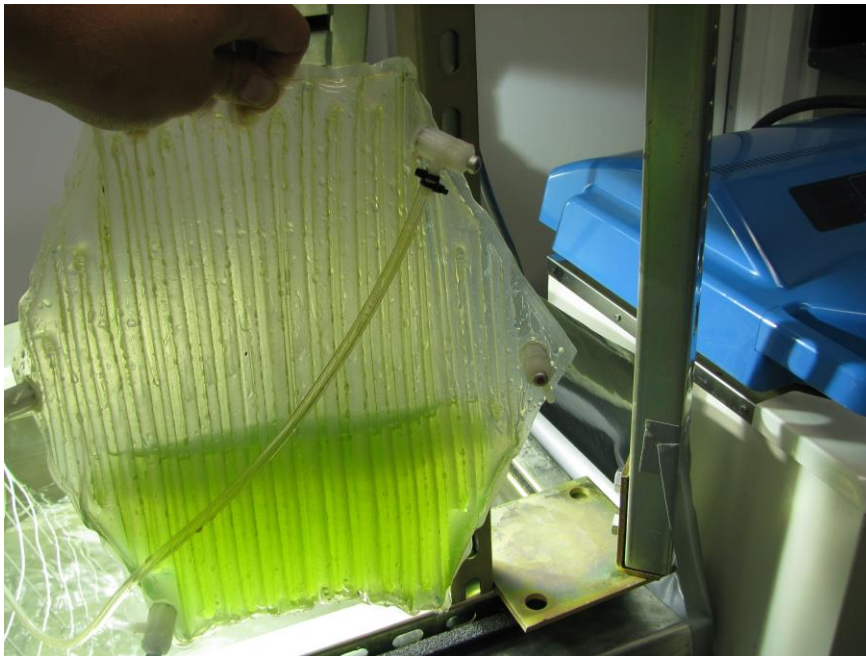


Figure 24: Algae membrane bioreactor developed at NASA Ames for algae bio-fuels research. Note the CO₂ gas exchange membrane labyrinth, visible as a clear liner pattern in the bag.

1.1.8 Solid Waste Digester Gas Emissions Scrubbing (Servicing the Water/Solids Vent Gas Odors and toxics)

A system where a solids digester is required to accept all wastewater and garbage in the habitat it would most likely produce an emission gas stream similar to landfill gas. Landfill gas varies over time based on the percentage of available oxygen in the solid wastes (which is rapidly used up in freshly covered waste), but tends to rapidly approach anaerobic equilibrium. Landfill gas at equilibrium, and thus that assumed for a steady state anaerobic digester processing a similar, garbage dominated, solid waste stream, is 55% CH₄, 40% CO₂, and 5% N₂ [Davis, 2000]. Digesters that are in a transition phase of aerobic digestion prior to going anaerobic will have elevated NH₃ and CO₂. Transition to anaerobic digestion is characterized by low to nonexistent CH₄ production, slightly higher CO₂ production and a transient spike in H₂ production. Then the gas emissions from operating a mixed waste digestion process will follow the 55%-40%-5% brake-down, with process inefficiencies possibly driving the CO₂ to CH₄ ratio closer to equal, and possibly allowing trace H₂ and NH₃ emissions to come through.

This provides little nitrogen support to mixed community algae air scrubber. In this case, the cabin CO₂ and ammonia gas from a urine tank degasser might be used as the primary feed gas

streams to grow stable algae/cyanobacterial cultures, with the cabin air being scrubbed by cultures on a cyclical basis. Noting that this is a less crucial application from an algae type than the high rate oxygen regeneration application and it could operate with less selective culturing (thus the tern algae turf scrubber used from wastewater processing) In this mode the algae/cyanobacterial bioreactor would run on light and cabin air for most of the time funding, as a cabin air algae/cyanobacteria turf scrubber for VOC and trace toxic organic cabin air pollutants most of the time, but periodically being transitioned to ammonia nitrogen rich waste gasses for a period of time to boost biomass.

This shows that better nitrogen balance can be perused, but as with CO_2/O_2 less than $\frac{1}{4}$ kg of targeted nitrogen fertilizer per crewmember year is required to make the entire discussion irrelevant from a mass balance perspective. More than likely this amount of nitrogen will be present as part of startup, and be accessed as balancing feed at very low levels throughout the life of the system. These levels of resupply being several orders of magnitude below current ISS levels.

As shown by the aerobic output gas stage calculation in the solids handling section below, the CO_2 to NH_3 production ratio is 80:6 by weight. This gives a C to N ratio of 22:5 or about 4.5:1. Optimal C:N is 105:15 or about 7:1 for algae [Tchobaoglous 1991]. This indicates that full utilization of NH_3 would be archived, but only if additional CO_2 was provided by the air revitalization system. However, it is likely that a substantial amount of this ammonia would be nitrified (converted to NO_3^-) and retained by the solids and eventually reduced by anaerobic digestion to N_2 . If this percentage is near half (as it generally is noted to be in wastewater effluent testing) then the off gassing CO_2 would be in near perfect balance with the nitrogen uptake needs of the algae/cyanobacteria and both should be nearly fully utilized (theoretically at least).

Urine Solids Dominated Metabolic Mass Balance for Early “Transit” Wastewater Dominated (i.e. Start Up Operations Scrubbing, urine dominated vent gas and bleed trough ammonia nitrogen). Paradoxically the transit mission (our start up assumption) water treatment residuals only digestion, with its ultra-high ammonia nitrogen content from urea, actually may be optimal for algae reactors as a feed gas. This indicates that urine tank off gas (with or without the water wall urine treatment) would also benefit from an algal ammonia nitrogen and VOC treatment provided by the algal gas treatment elements (thus having potentially immediate utility for ISS sustainability).

This gas would follow the pattern for initial aerobic degradation of urea given previously. This model requires that every 120 mg/L of urea converted consumes 544 mg/L O_2 , and this in turn results in 68 mg/L NH_3 and 616 mg/L CO_2 . Urea content for urine is modeled at approximately 2.5 g/L [Verostko, 2004], and is by far the single most dominant organic component. This would indicate 2500 mg/L urea, which is a bit high based on laboratory observations (during LWC-WRS testing) but can work as a worst case benchmark. If we assume about a 50/50 dilution rate with humidity condensate transit water, this gives urea content on the order of 1,250 mg/L in the waste stream. This is roughly 10 times the normal treatment concentrations in wastewater treatment, but if properly metabolically balanced should follow a similar mass balance. This gives a demand of 5,440 mg/L O_2 and produces 680 mg/L NH_3 and 6,160 mg/L CO_2 .

This indicates that (again regardless for whether the water wall bags are used to concentrate the urine brine) the urine dominated transit wastewater brines/solids will be stabilized by driving off ammonia and carbon dioxide at about a 10:1 ratio in cabin (aerobic) air. The long-term goal

is stable and sustainable deep space habitat design. However, current mission experience is likely to dominate in early mission (start up) operations even for long-term habitats. So it makes sense to examine this waste profile more deeply.

A transit mission and/or early “startup” long term habitat will likely continue to be highly constrained in terms of hygiene and other non-drinking water uses. The type of wastewater that is generated in this situation (whether truly an interplanetary transit mission or from a permanent free space habitat) is currently referred to as a transit mission wastewater [Verostko, 2004]. This is a wastewater that consists of source separated urine and cabin air humidity control system condensate water, with few if any other inputs. In this scenario, the habitat crew uses sponge baths for hygiene, and feces are not mixed with water and are sealed (and in some cases dried) and disposed of as solid waste. In this model, solid waste other than water treatment residuals from humidity condensate and urine are handled in an entirely separate process. Urine salts and urea/ammonia nitrogen therefore dominate the resulting transit wastewater with the volatile organic carbon from humidity condensate being a minor constituent by mass, but potentially important from a toxicity perspective.

Urine simulant or ersatz used in testing has high levels of urea (5.2 g/L), ammonium citrate (1.2g/L), sodium chloride (2.3 g/L), potassium sulfate (0.7 g/L), and a number of other salts including magnesium, calcium and carbonate containing simple salts. Digestion in these transit mission bags will require a simple sugar feed to balance the carbon to nitrogen ratio followed by nitrification and denitrification digestion steps. Nitrification is aerobic and will convert all urea and ammonia nitrogen to nitrate nitrogen. Denitrification is strictly anaerobic and will convert nitrate nitrogen to N₂ gas. Operating the bags as two stage batch denitrification reactors should convert the majority of the urea and organics to N₂ and CO₂ with very little residual organic matter. The N₂ and CO₂ produced will be processed by the atmospheric control system and utilized as makeup gas. The remaining wastewater will be primarily dilute brine.

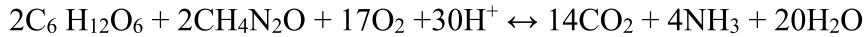
However, the FO is a poor rejecter of ammonia nitrogen and the “bleed rate” of nitrogen into the algae reactor/OA draw solution loop could be large. It is likely that enough nitrogen would be lost to provide a substantial portion of the algae nitrogen need prior to the reject being moved on to the assumed solids digester covered above in solids handling. As before, any remaining deficiency of nitrogen in the OA/algae-cyanobacteria medium loop could be mitigated and an extremely small mass penalty.

The Total Dissolved Solids (TDS) used to model the theoretical discussion of urine solids is derived from the accepted ersatz for transit wastewater and is taken from Verostokos et al., [Verostko, 2004]. This is recognized as a convenient, and in some ways less than fully representative model that must be verified in process research with actual urine testing in all cases; however, it does allow for basic process chemistry. Mass balance should be less rigorously applied using grams of particular product per liter of wastewater treated than can be done for the planetary wastewater case due to the large variability in urine TDS per volume, but for consistency a similar analysis is presented.

The mass balance for transit brine based residuals will be dominated by NaCl, NH₄⁺ (from urea), and CaCO₃²⁻ with some SO₄²⁻, and miscellaneous additional solids representing less than 10% of the initial TDS value. The other salts and complex organics, while important from a treatment requirement and biological processing perspective, are minor components from an accumulative mass balance perspective.

From a processing perspective, this is a urine dominated wastewater stream that is significantly carbon limited [Morse, 2004].

Initial stabilization of urine-based organics is modeled as microbial mediated urea hydrolysis to ammonia due to its relative abundance in comparison to all other organics:



This metabolism will result in little biomass production in comparison to the inorganic precipitates present and thus biomass is neglected at this point. For every 120 mg/L of urea converted this requires the consumption of 544mg/L O₂ and gives 68 mg/L NH₃ and 616 mg/L CO₂. Because of the variability of urine this mass balance is not used in favor of the empirically derived wastewater engineering values to follow.

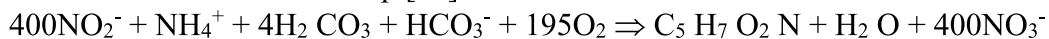
What results at this point is high salt, high ammonium, but low organic carbon concentration wastewater. The ammonium not used by the algae (a small fraction of it likely) must then be converted to nitrate nitrogen (NO₃⁻) and then reduced to N₂. Nitrification (NH₄⁺ to NO₃⁻) is a two-step biological process:

Nitrosomonas mediated step [12]:



Note: $\Rightarrow C_5H_7O_2N$ being the general expression for microbial biomass produced

The Nitrobacter mediated step [11]:



In conventional wastewater treatment plant operations 4.3 mg of O₂ are required to convert 1 mg of NH₄⁺ to N₂. No determination is made regarding how much of that is urea or ammonium as it enters the wastewater treatment plant. 8.64 mg of HCO₃⁻ (from CaCO₃) are consumed in the process resulting in Ca(OH)₂ precipitate under correct pH conditions. This reaction will coprecipitate with CaMg(CO₃)₂, where natural deposits go by the name dolomite, and CaSO₄, which goes by the natural deposit name of gypsum (Note: gypsum is more accurately presented in the hydrated form Ca(SO₄)•2H₂O and should be recognized for water weight mass balances, but is presented in the anhydrite form for stoichiometric purposes here). These recognizable natural mineral (rock) like predicates will deposit in a matrix of NaCl (halite or rock salt) to form a gypsum wallboard like solid. The dissolution source solid (natural rock) and precipitation solids produced by these four materials, both as mineral interaction with natural waters [Morel, 1993] and as part of industrial water treatment “sweep floc” chemistry [Benefield, 1982] is extremely well understood and commonly used in the field of environment process engineering. This urine salt derived wallboard filling would be dried in place or removed, sealed within the bag to be dried in forms probably still never being removed from the FO bag.

However, this last set of conversions only occur if the ammonia nitrogen is in excess of the amount that the algae in the reactor can use to build biomass. This is likely zero, and thus nitrification and denitrification will likely not occur or be required in the algae reactors (it will likely occur on the solids waste residual side digestion).

1.1.9 Micro-Filtration (MF) Element Fouling and Trapping Rate, the Ultimate Drivers and Values For Algae Reactor Sizing

The flexible algae bioreactors are effectively a steady state device that can be sized to the 3.5m²/crewmember specification in initial habitat design, and that would correspond to their maximum capacity role in CO₂/O₂ conversion. This would leave them in over capacity for the role of cabin and vent gases scrubbing, and at a size appropriate for use once the biomass associated with O₂ is demanded by advanced utilization (fuel cell and food). Alternately O₂ could begin immediately if nitrogen and micronutrient control was instituted, and a small number of MF algae biomass capture bags where dedicated to a role similar to the spent FO bags in water/solids treatment.

The element on the algae/air revitalization side that is most relevant to sizing is the MF post filter bag associated with the algae reactor in Figure 24, rather than the algae reactor itself. This MF filter is a simple bag element with the same dimensions and shape as the water/solids element, and the algae bag element. The membrane in this element will flux at a rate of 20 L/m² hr based on applied transfer pump pressure only (less than 2/3 atm or 10 psi), and based on common off the shelf MF membranes designed for high solids applications. These MF membranes will give a 3% dry mass solids without fouling of long operational periods. Thus, one MF element would service a 1-crewmember day/m² water throughput in under an hour.

Calculating for area:

$(16.95\text{L}/\text{crewmember day})/(20\text{ L}/\text{m}^2\text{ hr})(24\text{ hr}/\text{day}) = 0.035\text{ m}^2/\text{crewmember continuous operation.}$

This result means that 3.5 m²/crewmember of algal/cyanobacterial reactor coupled with and 0.035 m²/crewmember of MF tap unit area is required to service the crew's air revitalization needs through CO₂/O₂ scale up and sustainable operations. So if this full capacity is developed for trace continent scrubbing the question will not be expanding the area of the algae system but finding a use for increasing amounts of biomass, if O₂.

The only other parameter potentially driving progression (area per day use) from an algae reactor and/or filter unit perspective (the integration of the two seem reasonable considering the 1/100 reactor/MF membrane area required) is fouling based deterioration and abandonment of the elements. Algae/cyanobacteria reactors with internal LED lighting would likely be made accessible and maintained for months to years, and never be abandoned. Simple MF filter elements may be less valuable and treated as more consumable (like the FO bags).

MF elements, even without back flushing and/or cleaning, will likely last over 90 day before more aggressive biofilms render them inoperative. Also, it may be desirable to simply dispose of some of the excess algae biomass rather than moving it on to fuel and food production requiring more and advanced architectures. Thus, MF abandonment and/or algae/cyanobacterial biomass accumulation rate are the drivers for airside area rate values. Using the maximum theoretical rate of 182 mg/L hr productivity for salt water cyanobacteria (algae) in ambient air:

$3.5\text{ m}^2 \times 0.05\text{ m} = 0.175\text{ m}^3$ or 175 L converting 1 kg/day CO₂ to 31.85 grams of biomass.

If dewatering is taken only to 10% dry mass solids (i.e. 100 g/L), this gives 0.3185 L/crewmember day of wet solids volume.

A 1 m² at 5 cm depth is 50 L, so if MF bags were used to dead head these solids, digest them anaerobically, and stabilize them as 10% solids. This gives an algae solids bag retirement rate of 6.3×10^{-3} m²/crewmember day or roughly 1 m² every 157 days per crew member. This may be acceptable as is, but will be further lowered by advanced developments in fuel cell elements designed to consume waste algae biomass, and/or use of waste algae biomass to provide nutrient input for food production.

Another possible governing factor would be fouling of the algae/cyanobacteria reactors by surface biofilm and thus light blockage, or fouling of the MF membrane by biofilm growth. As stated earlier these reactors can be accessed and cleaned to maintain them as assets, but the MF filters would probably be allowed to decline and take on a similar role to spent FO bags. This process could be conservatively set to 3 months for any active units operating in a completely passive mode (i.e. no backflushing and using only transfer pump residual and bag seem compatible driving pressure of less than 10 psi (2/3 atm)).

A 3 month MF bag progression would give:

$(0.035 \text{ m}^2/\text{crewmember})/90 \text{ day} = 3.9 \times 10^{-4} \text{ m}^2/\text{crewmember day}$ or 2,571 days per m² per crewmember, thus approaching the service life of most habitat mission likely.

1.1.10 Algae-cyanobacteria/Air Revitalization Element Summary

In summary, the air regeneration (CO₂ removal and CO₂) and trace contaminate control WW elements are flexible plastic bag based reactors similar in size and shape (3.5 cm thick fluid elements) to the FO water and solid waste elements, and contaminant gas exchange membranes. They are largely decoupled from direct sizing based on the water/solids element area by manipulation of the nitrogen and other micronutrients in the connecting osmotic agent loop, which also functions as the algae growth media.

Based on the governing initial freshwater and marine cyanobacteria growth and carbon uptake rates determined using BG-11 secondary wastewater simulant 3.5 m²/crewmember is required, and is semi-continuous. These will be serviced by microfiltration elements for the concentration and removal of excess algae biomass accumulation. The area ratio of microfiltration to active algae reactor is as high as 1 to 100, making the microfiltration area background noise level input to the algae reactor area design values for continuous operation.

Retirement rate of the algae-cyanobacteria reactors must still be determined in Phase II. Only theoretical mass accumulation rates for algae are available at this time, and retirement of algae reactor volume will likely need long term empirical testing to be determined. Theoretical mass production rate for the marine algae used is 182 mg/L hr. If it is assumed that microfiltration is capable of up to 3% solids (dry) on wastewater algae rejection that is 3,000 mg/L or 94% dewatering. Table 1 gives the mass balance for algal reactor operations. Table 2 gives area progression/permanent stable shielding area accumulation rates for the algae reactor/MF filter trap system.

*Algae will be rejected as a wet sludge and digester to a stable hydrated solid with 10% to 20% solids content in its permanently stabilized and/or sequestered form in the WW shield.

At this point the only limit on algae-cyanobacteria reactors is bio-fouling of membranes, which should be manageable over many months to years, and advanced algae biomass use. The

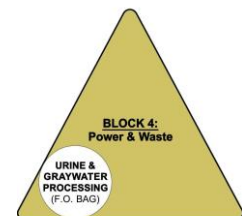
primary task in Phase II is to integrate algae-cyanobacteria biomass production with its various uses, as well as determine mass balances of algae biomass and solids digester overcapacity through actual algae growth and biosolids digestion testing. However, based on the values in Tables 10 and 11, as well as those showing FO bag consumption area rate in the water/solids analysis, the primary sizing of the WW system is more or less complete. Advanced development of fuel cell, food production and thermal/humidity control, while valuable in their own right operationally, will have negligible effects on sizing, and arguably the primary mass savings payback for WW system development. Thus, these two sections (water/solids and algae/air revitalization) provide the primary sizing design criteria now and in the future, with the advanced development area providing future auxiliary benefit, but little change to the fundamental mass balances.

Table 10. Algae/Air revitalization mass balance/flow Algae/Air Revitalization Mass Balance (all in per crewmember – day)			
Driving Inputs		Output Algae solids	
Water Flux from FO	CO ₂	Dry Mass Algae	Same as 10% Solids*
16.95L	1 kg	31.85 grams	0.3185L

Table 11: Area progression rate for algae reactors and MF algae biomass traps Area Program (per crewmember)			
Continuous Operation Area		Consumable Area/Progression in Shield Growth Rates	
Algae Reactor	MF	CO ₂ /Biomass Accumulation Area	90 Fouling Area
3.5m ²	0.035m ²	6.3 X 10 ⁻³ m ² /day	3.9 X 10 ⁻⁴ m ² /day

1.2 Wastewater Processing Bags as Components

Water recycling in the WW system is accomplished using a technology that is very similar to the commercially available Hydration Technology Innovations (HTI) X-Pack[®] water treatment bag. The X-Pack[®] is a forward osmosis (FO) water treatment bag that can be used to create a fortified drink from wastewater. The X-Pack[®] is currently marketed for this application and is sold worldwide for commercial/recreational use, disaster relief, and military use. The X-pack[®] is shown in Figure 25.



The procedure to use the X-Pack first requires opening the red port through which the bag is filled with wastewater. Once the bag is filled with wastewater, the red cap is resealed. Next, the green product cap is removed and the osmotic agent (OA) is poured into the inner membrane bag. The OA is composed of concentrated fructose/glucose and other food product components that make the OA a balanced and palatable fortified drink. The OA can be either a solid powder or a concentrated liquid (syrup). Once the OA is added the green cap is resealed.

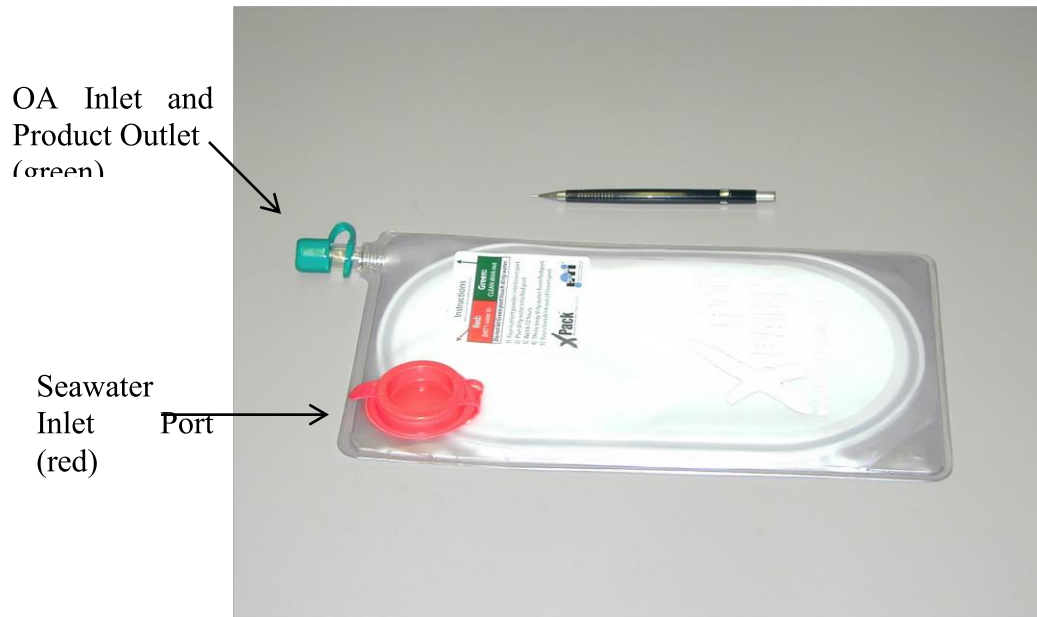


Figure 25: Hydration Technologies Inc. Seapack[®] Desalination Bag

When the bag has been loaded with wastewater and OA, it is allowed to process the wastewater for 6 to 8 hours. The service life of the bag is limited by the potential for biological contamination on the product side of the membrane that enters through the green port.

The X-Pack produces 1 L of purified drink from seawater and should require about 250 g of process mass to function for the first use. This represents a 75% reduction in stored water mass. After first use, the X-Pack requires 200 g of OA replacement per reuse, less if it is supplied as a dry powder.

The percentage of water recovery from the membrane treatment step will vary with urine concentrations (primarily as NaCl) and OA composition. The draw solution (OA) will be a flavored electrolyte solution such as Powerade[®]. This is a liquid food product that is roughly similar to the intended urine recovery product for the system. Its primary dissolved solid (thus primary OA) is 62.5 g/l sugar, primarily high fructose corn syrup with some glucose fortification. By comparison the Coca-Cola Classic[®] soft drink and comparable soft drink formulas have approximately 120 g/l sugar (assumed to be a mix of fructose and sucrose).

The flux testing urine ersatz was a simplified solution of NaCl in DI Water. NaCl concentration was set at 5.2 g/l. Fructose, glucose, and sucrose OA draw solutions were tested. Glucose and fructose results were indistinguishable, with sucrose being substantially less capable. This is as expected based on molecular weight and indicates that fructose is both an optimal and commercially convenient primary OA sugar.

Initial sugar OA comparisons were accomplished using 500 ml of OA at a known starting concentration (Figure 26). Following this initial comparison dry fructose was used to determine total water recovery potential and rates (Figure 27). Note that greater than 90% of the total water recovery possible for a given OA draw solution concentration was achieved by 9 hrs in all case for fructose.

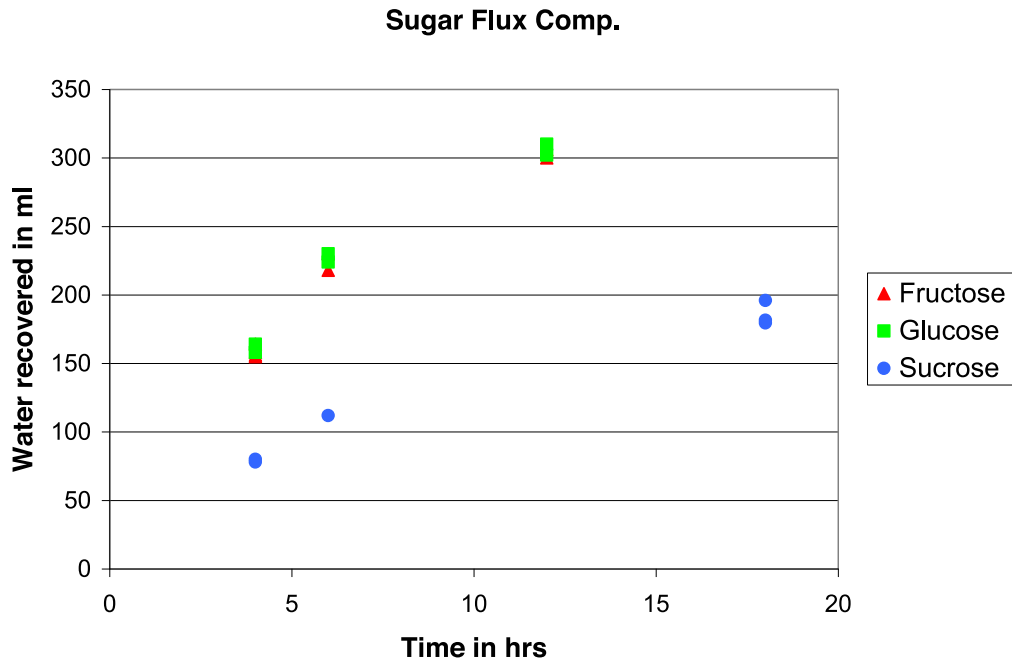


Figure 26: Comparison of sugar based OA solutions using 5.2 g/l NaCl urine ersatz, 90 g/l sucrose, and 80 g/l fructose and glucose.

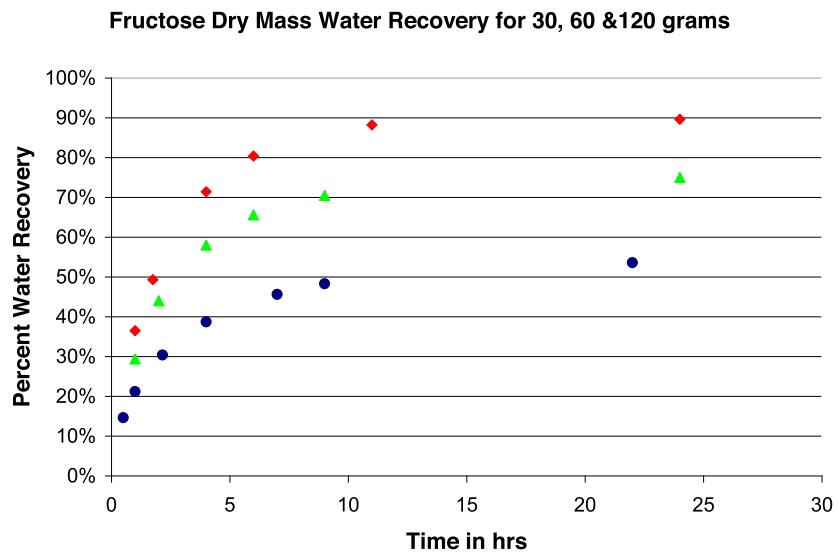


Figure 27. Percent water recovery as a function of time for fructose OA at 30 (blue), 60 (green), and 120 g (red) starting dry mass.

1.2.1 FO Rejection of Urine Salts

NaCl rejection was measured during the sugar OA flux testing and resulted in Na⁺ levels below 250 mg/l in the total OA product produced. Urine has a Na⁺ level of around 2000 mg/l. A comparison of water and Na⁺ flux (Table 12) appears to indicate that it is more time dependent than water flux related. Ion rejection is the primary function of the FO membrane. It is a characteristic of the membrane formulation. The data provided in Table 12 is from a commercially available membrane manufacturer. This manufacture has the ability to provide membranes with higher and lower ion rejection rates. Typically flux rate and ion rate are inversely proportional. The lower the flux the better the ion rejection. Table 13 show data generated from a NASA contract to evaluate modifying the membrane formulation to control ion flux.

1.2.2 NH₄ and Urea Rejection at the Membrane

NH₄⁺ simple ion rejection/retention at the membrane was also measured using reagent grade NH₄Cl and urea. NH₄⁺ rejection was better than 90%. Urea rejection was approximately 50%, which corresponds to previous data for the cellulose triacetate membrane used [Beaudry, 1999]. NH₃ rejection is assumed to be low and thus all ammonia nitrogen retained by the system will be NH₄⁺ or urea. Ammonia nitrogen fate will depend strongly on speciation at the membrane at the time of harvest and is not completely characterized at this time.

Table 12: Inorganic ion (salts) removal measured as a function of NaCl removal during sugar based OA flux/rate of yield testing (i.e. Fast vs. Slow Flux Test)

Na Flux Data Individual FO Bag Designation	T (hrs)	Total Flux Volume (ml)	Na+ Concentration in Total OA (mg/l)
SF1 Slow Sucrose Flux	12	N/A	73.9
SF1 Slow Sucrose Flux	18	182	127.1
SFLD1 Slow Sucrose Flux	18	196	116.4
SFLD2 Slow Sucrose Flux	18	180	140.1
SF1 Fast Sucrose Flux	6	N/A	39.4
SFLD2 Fast Sucrose Flux	6	112	34.2
NH4-1 Fast Sucrose Flux	6	191	59.3
NH4-2 Fast Sucrose Flux	6	202	114.5
NH4-1 Fast Fructose Flux	6	N/A	36
NH4-2 Fast Fructose Flux	6	348	82
UR-1 Fast Fructose Flux	6	372	118
UR-2 Fast Fructose Flux	6	393	101

Table 13: Results of reformation of FO membranes to adjust ion rejection characteristics. Feed was 10g/L NaCl		
Membrane	Flux	Permeate Passage, g NaCl/H
Commercially available	14.5	0
Reformulation #1	14	0.
Reformulation #2	10.2	0.
Reformulation #3	5.7	0.

1.2.3 Total Organic Carbon (TOC) Rejection

NASA is currently developing a new generation of FO membranes that have improved organic rejection over commercially available membranes. These membranes are being developed by third party private companies that are working with NASA. NASA has been working with some of these companies since the mid 90's and the results of this investment in advanced membranes is currently paying off. NASA currently has a new generation of biologically inspired membranes that have superior organic rejection, specifically urea rejection, over commercially available membranes.

NASA has a patent on a FO system to treat urine. This system utilizes a granular activated carbon (GAC) to pretreat the urine. This pretreat removes urea. About 50% of urea in urine is rejected by commercially available membranes. When this urea gets into the product and decomposes, hydrolyzes, it will produce ammonia. A membrane with better urea rejection would be beneficial in that it will improve the quality of the product and reduce or eliminate the need for GAC. As a result NASA has been developing a new class of membranes that have higher urea organic rejections. Table 14 shows a sample of an experiment, where NaCl 2M was used as osmotic agent and where the feed contained DI water with 3g/L of urea (3000 ppm). The results show that membrane is capable of reject 89.9% of urea.

Table 14: Results of testing of high urea rejection membrane Feed is DI water with urea added			
Measurement	Jv, incremental (LMH)	urea feed (ppm)	urea brine (ppm)
1	0.00	0.0	0.0
2	8.99	2855.0	18.0
4	-	2908.7	73.9
8	-	3102.0	125.10
15	12.47	3198.6	127.1
16	5.42	6022.4	139.3

LMH = L/m²h

The data in Table 14 is just an example of results from one run with one type of membrane. A complete set of results of our membrane development program are not provided as they are highly proprietary and have not been published. In general we currently have access to three different types of membranes that have improved urea rejection over the current state of the art. We are working with these vendors to improve their membranes and develop the capability to produce them in commercial scales. As a result the base line approach used in the WW concept it to eliminate the carbon bed in our design and use the advanced membranes.

However, at this time the bulk of our testing of the water treatment bags has been completed using the original GAC bag approach covered in the NASA patent. The following section provides a summary of the results of this testing. Most of the results are relevant for the advanced membranes as the total system performance is very similar for the GAC and advanced membrane approaches.

1.2.4 Initial GAC Treatment for TOC

Initial TOC analyses for GAC treatment is shown in Table 15. All Table 15 data utilized the Persulfate – UV Method (Method 5310 C). Initial data for GAC treatment indicates that activated carbon appears to be capable of treating urine to TOC levels between 50 mg/L and 100 mg/L when averaged for the total treatment volume. A 1hr contact time provided better than 90% of the TOC removal observed in 3 hrs during initial testing and subsequently a minimum 1hr contact time was adopted for all GAC treatments.

Table 15: Initial activated carbon treatment of TOC GAC (Stage 1) Urine Treatment					
Date	2/14	2/28	5/24	6/14	6/21
Column Volume	100 ml	100 ml	1 L	1 L	1 L
Raw Urine TOC (Average)	4018	5590	2358	4489	5369
Hour 1	N/A	N/A	87	44	85
Hour 2			106	37	81
Hour 3			93	36	89
Hour 4	67	59	91	35	89
Hour 5			88	58	104
Hour 6				115	106
Hour 7				129	111
Average TOC			93	55	95

1.2.5 Initial GAC and FO Membrane Treatment for TOC

The initial test indicated final TOC values between 25 mg/l and 30 mg/l could be achieved. However, two follow on tests using large amounts of urine collected from an uncontrolled and mixed population resulted in substantially higher apparent final TOC levels. These later tests results were also less self consistent between duplicate samples, indicating analytical scatter. Chloride levels in these samples were outside the acceptable range for the Persulfate – UV method, and it is also likely that humic and other organic acids are as well. Initial results are given (Table 16) as probable worst case only. Initial combustion TOC analysis was more than 10% below Persulfate – UV Method values for the same samples. As a result future data for total treatment will require method development.

Table 16: Initial TOC values for full treatment GAC & FO membrane.			
Cell #	1	2	3
Raw Urine TOC (Average)	4,490	5,370	5,370
Full Treatment TOC	26	70	76

1.2.6 Biological Testing

The X-Pack also provides an effective method for removing pathogens from water. The membrane is rated in independent testing by Pacific Analytical Lab, Corvallis, OR, and was non-detect for coliform, E. coli and anthrax antigen. The results of this testing are provided in Table 17. The testing was conducted in accordance with EPA methods and demonstrated better than 6-log (99.9999%) reduction of bacteria and 4-log (99.99%) reduction in viruses. This testing was funded by the Seapack® vendor.

1.2.7 Total Mass Per Liter Processing Rate

The WW bag water recycle system can produce 1 kg of drink from urine using about 250 g of equipment, dry weight (GAC+bag). The LWC urine recycle system achieves about a 75% water recovery. However, in the WW system a solid waste treatment system is provided which recovers about 99% of the remaining 25% of the water. Since urine production is only about 93% of drinking water requirements [Wieland, 1994] it is assumed that humidity condensate is used to make up the difference.

1.2.8 Concept Development Consideration

One of the interesting aspects of this process is that it produces a food grade sports drink and not drinking water. Logically this should result in different treatment and process performance goals. This is particularly true for ammonia nitrogen (and also TOC discussed later).

In drinking water all NH_4^+ , NH_3 , and urea, as well as some nitrogen containing simple organic acids (that have a tendency to spontaneously degrade and/or hydrolyze) are counted as if it was all ammonia nitrogen. All nitrogen is effectively counted against the 10 mg/l MCL used as the control for nitrate nitrogen in drinking water [Olin, 1999]. However, this standard is

inapplicable for food products (which are by definition nitrogen and carbon rich), particularly when a large percentage of the ammonia nitrogen is present as urea.

Table 17: Results of Pacific Analytical Labs Biological Rejection Testing ³		
Test Description	1 hr sample	24 hr sample
Anthrax Permeation		
1,200,000/ml	nt	nd
Pigment Ink Dilution		
0.4-1.0 micron	nd	nd
E. Coli Permeation		
Colony counts 1,000,000/ml	nd	nd
Colony counts 1,000,000,000/ml	nd	nd
M 13 phage Permeation		
Colony counts 10,000,000/ml	nd	nd
Colony counts 1,000,000,000/ml	nd	nd
MS2 phage Permeation		
Colony counts 1,000,000/ml	nd	nd
Colony counts 1,000,000,000/ml	nd	nd
M13 phage DNA Permeation		
2mg in 4 liters	nd	nd

nt – not tested, nd – no CFU detected

Urea is a normal component of food products, particularly dairy products. The Food and Drug Administration (FDA) lists over 230 approved formulations for human consumption where urea is a specific additive at concentrations from 0.01% up to 10% by weight. Consumption of urea is associated with chewing gum, and human testing has shown a safe oral consumption rate in excess of 300 mg/day. Urea is naturally produced as a component of saliva at a normal value of 200 mg/l, and is thus an essential part of digestive fluids (Geigy, 1981). Urea is a non-bioavailable form of nitrogen, is poorly absorbed, and is for the most part promptly re-excreted with no deleterious effects even in infants (the most vulnerable section of the population to total nitrogen levels in drinking water).

Research specifically addressing the effects of addition of organic nitrogen to sports drinks in the form of protein (which is rapidly degraded to urea among other things early in the digestion process) indicates that it improved fluid retention during exercise stress (Seifert, 2006). In contrast, moderate increases in Na⁺ levels in sports drinks consumed during exercise showed little improvement in water uptake in the upper gastrointestinal tract.

Toxicity levels for urea are well established (Archer and Robb, 1925) and are extremely high. Initial metabolic effect detection in blood urea requires 0.250 mg/kg (or approximately 20 mg/hr

for a 170 lb individual), and this level is not harmful, clearing in under 3hrs. This would indicate that 480 mg of urea in 24 hours would be acceptable. Using a required rehydration rate of 1.62 L/day (Wieland, p., 1994) this would give a safe urea level of 296 mg/l. Also, the total daily dietary load of urea is the value that must not be exceeded, so the contribution of other foods should not be negated when setting a safe contribution from the hydration liquid alone. For these reasons, it may be more conservative to set the standard based on a low estimate for background levels in saliva. This still allows 200 mg/l of urea in the food grade product. Off the shelf membranes and GAC should be capable of reliably achieving this level of performance based on current data.

1.2.9 Considering Necessary Product TOC Levels

TOC level in the product should be considered based on food grade requirements rather than drinking water MCLs. The WW approach uses an osmotic draw solution such as sugar. The product is something similar to a sports drink or food product. As a result, measuring total organic carbon of the product is not useful. The primary components of TOC in the recovered product that came from the feed will be urea.

The NASA drinking water TOC standard is set for cabin humidity condensate and combined crewmember urine recycle. This is because of the potential for toxic organics and/or endocrine disruptive chemical (EDC) in a combined waste system. Volatile and semi-volatile toxic organics from plastics and other sources are present in substantial quantities in humidity condensate water (Verostko, C., 2004). Some of these compounds are also EDCs. Pharmaceuticals in urine are another source of EDC's.

The fact that the WW water recycling process is personal/individual in nature eliminates the sharing of pharmaceutical EDCs. Also, since only urine is treated there will not be any toxic chemicals present, such as would be the case if the humidity condensate was treated.

1.2.10 Water Process Theory Summary

Initial testing of the WW Urine Recovery System at a component concept level was highly encouraging. Inorganic dissolved solids removal is better than 90% and TOC removal is better than 99%. Water recovery rates are in the range of 75% for the total system (83% for Stage 1 ,GAC, and 90% for Stage 2, the bag) are possible based on urine ersatz NaCl levels for input and hydration fluid simulative fructose draw solutions for output.

Inorganic rejection analysis is compatible with drinking water methods and standards, and can meet drinking water requirements. Both Na^+ and NH_4 specific testing indicate that the system has the potential to meet all inorganic urine constituent removal requirements to at or near current drinking water MCLs.

The logical method and standard development associated with acceptable levels of nitrogen and TOC flux is potentially the largest outstanding issue left over from the LWC Urine Recovery System concept development. All other technical development issues are incremental hardware improvements at this time.

Based on preliminary total nitrogen and TOC testing the product potentially can meet food grade hydration fluid standards. It appears based on preliminary testing that 25 to 80 mg/l TOC does cross the off the shelf FO membrane during treatment, though some method issues remain with this data. The majority of the dissolved solids that pass through the system to emerge and contribute to the nitrogen and TOC in the final product appear to do so in the form of urea.

Assessment to improve urea removal is ongoing, but due to the acceptability of the urea levels present in food grade liquid terms these improvement efforts should be accompanied by a

reassessment of necessary urea removal requirements and improved analysis method development for a product, which is a liquid food product from an ELS system, rather than drinking water. Within this context initial feasibility seems quite promising, and is worthy of future development.

Additional advanced WW design will likely add algae reactor components that are covered later. These will directly feed on and benefit from the urea and this actually has the potential to elevate nitrogen constraints on algae based CO₂ recycle.

The results of this work have shown that the LWC Urine Recycle System, using only off the shelf technology, can reduce the weight of providing water and urine handling by 85%. This means that the system can act as a fully independent and separate redundant water supply system at a mass of 250 g/l. Optimization of off the shelf components and elimination of the carbon bed may increase this savings even further. In addition, innovative utilization of the LWC Urine Recycle System within the space craft architecture may also increase the mass savings.

1.2.11 Baseline Theoretic on Sizing Constraints Provided by the WW from Water Processing Bag elements

The water processing FO bag elements provide the basic/core sizing element for WW. They provide bulk of the initial radiation shielding effect, both while providing active water solids treatment as well as during their function as water and treated solids storage. They are the critical first (start up) step in developing a mass balance by handling the water recycle primary treatment. Thus, they are the baseline sizing element for the whole system, and must be kept in balance as more advanced elements are integrated into the architecture. Air/algae elements as well as biological fuel cell based power will be balanced to compliment the water and solids treatment and storage/radiation protection function of these units. For this reason the water and solids dictated area of 5 cm FO bags will work as the core area function of WW design architecture math development, to which the advanced elements must be balanced as added.

Based on this testing it has been calculated that the WW bag could reliably process 4 L/hr per square meter of wall area, or 96 L/m² - day. This indicates that based on an early planetary base wastewater production rate, which is projected at 11.85 kg/crewmember-day. 8 crewmembers would be served by 1 m² of active membrane wall area. Assumed transit volumes would not include substantial amounts of hygiene water input and, as set by the same referenced operations research, would be closer to 3.53 kg/crew day. Thus, 1 m² of membrane wall area treating transit mission water (or any long-term free space habitat wastewater) could service a maximum of 27 crewmembers.

It is unlikely that 27 crewmembers will be housed in a space habitat in the foreseeable future, so this overcapacity will be used to extend system life. At this rate of use, an active membrane would last 10 to 20 cycles depending on the solids loading rates, based on commercial product use data and recommendations. Bag sizing and distribution would be organized so that the service life of any given bag would not exceed one month, and would correspond to approximately 10 cycles for transit/free space mission wastewaters and 20 cycles for planetary base habitats.

Cycles are dictated not by membrane life but reject accumulation rate. This in turn is dictated by water recovery rates of 90% for urine dominated transit wastewater and 95% for hygiene waste dominated wastewater (soapy gray water). These recovery rates are projected based on urine treatment testing results for transit scenarios and FO element hygiene water recovery rates for planetary base assumptions. The reject brine in both cases would be forced back into the previously exhausted membrane bags and the rate at which these expended bags

filled to capacity with reject brine would dictate the rate of progression (rather than membrane life which would never be approached).

This process would leave stabilized, concentrated salt water brine residual in the wall 5 cm (2 inches) thick after treatment. Filled with stabilized brine at the end of the active water treatment phase, the bag would contain approximately 0.51 m³ or 510 liters of water/reject brine weighing 510 kg total (water and bag construction). Bags could be layered to provide thicker water walls (10, 15 or 20 cm) as required, but all other conditions would remain the same (Table 18). The reject accumulation rate would be 0.35 kg/crew day for transit and 0.59 kg/crew day for planetary habitats. This results in an area use rate of 1400 crew days per m² for transit and 860 crew days per m² for planetary habitats. It should be noted that bags could then be layered to any desired thickness.

The extremely low rate of accumulation of reject volume is a result of the water being effectively treated and conserved, and the fact that up mass investment for the supply of fresh water is fully utilized. Water recovery rates of 95% to 99% are achieved. However, over long periods of continuous occupation the 100% utilization rate dictates that a substantial shielding layer of low cost volatile resources based on the 5% to 1% reject will be accumulated, and no further cost for down mass or waste handling will be incurred.

Table 18: Per Layer Membrane Wall Specifications.		
Type of Mission	Transit	Long Term
Wastewater Volume Requiring Treatment (kg/Crew day)	3.53	11.85
Active membrane area required (m ² /Crewmember)	0.036	0.12
Active area treatment capacity required at a 4 L/hr production rate (Crewmember days/m ²)	1400	860
Cycles per bag	10	20
Water recovery rate	90%	95%

The most substantial benefit of taking this approach from a near term mass and volume perspective is the FO membrane element mass and volume advantages, particularly when used in inflatable habitats. Prior to treatment, in a packed inflatable habitat bundle, 1 m² of membrane bag area would weigh approximately 1.7 kg and have a packed volume of 0.082 m³ per square meter of membrane area (0.082 m³/m²). Packing volumes are based on the of the shelf FO bag hardware and indicate a first stage FO treatment return of 850 crew days per kg or 2,990 kg of wastewater treated per kg of membrane bag launched. This does not include the second stage RO or MF and any final processing step, but it does indicate that the cost of primary treatment (done by FO) becomes an insignificantly small mass penalty in comparison to more mechanical ELS system elements.

These values are arrived at using the commercially available FO bag as follows:

Area = 15 cm X 27 cm X 2 sided membrane bag = 0.081 m² per bag
 Bag weight is ≈ 140g
 1 m² = 1/0.081 bags which weighs 12.3 X 140 g
 This gives 1.7 kg/ m²

Dry packed volume per bag is:

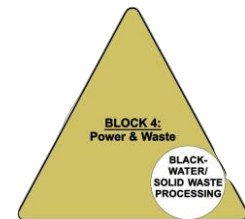
$$12.3 (30 \text{ cm} \times 17 \text{ cm} \times 1.3 \text{ cm}) \times 10^{-6} = 0.0082 \text{ m}^3$$

RO and other post processing are not included but would be a small addition if necessary (prior to integrating algae based post processing of water and air) because the bulk of the contaminant removal will be accomplished in the FO process. This means the mass and volume for the RO and polishing steps will be highly optimized.

This initial theoretical calculation for water process bag element sizing is based on the LWC-WRS emergency urine recycle testing, which always used new bags. This resulted in the use of 4 L/m² hr flux rates at all times. Initial 10 use full life cycle testing related degradation of this flux rate, and thus up sizing of the bag area requirement, is covered later, but will be effectively a 2X expansion to the optimal performance theoretical values given here, based on this NIAC Phase I initial testing.

1.3 *Solid Waste Processing Units as Components*

Solid waste treatment is accomplished using FO and a variant of the X-Pack bag. Using this approach, solid wastes and concentrated water recycling brines will be mixed and placed in an X-Pack type bag. These solid waste treatment bags will be the WW water recycling bags that have reached the end of their useful life recycling wastewater. They will be repurposed to treat solid waste. Laboratory scale testing has been complete and solids samples have been sent out for radiation protection testing.



1.3.1 Initial FO Sizing for Post Dewatering Solids/Residuals Processing in Membrane Walls

Once the wastewater and brine sequestration role of the membrane bag system is fully utilized, the solids sequestration advantages of the bags should be investigated and optimized for advantages over conventional solid waste treatment and disposal systems. This would be the most obvious opportunity to investigate the conversion of wastewater residuals into biologically stable and useful materials. Within this context the treatment strategy and fate of water treatment residuals is highly influenced by the waste stream origin and composition.

Mature space habitats will process hygiene water and feces, as well as humidity condensate and urine. These habitats will produce wastewater process solids that will be quite different from short-term transit habitats [10]. This is because these short-term transit habitats will have waste streams that are dominated by urine and humidity condensate wastewater. The composition of long term habitat wastewater will be larger in volume and contain a large and better metabolically balanced organic dominated solids load. The transit waste will be dominated by the dissolved solids (salts) in urine, be metabolically imbalanced in terms of the carbon to nitrogen ratio, and contain trace toxic organics from condensate. Based on these fundamental differences, both the conversion process and the product fate of these two residual waste streams must be different and are treated separately.

What follows is a rigorous analysis of the digestion mass balances and products for solids handling for both planetary base and transit mission wastewater. This discussion is intended to give a credible theoretical basis for considering and sizing the membrane water wall as a wastewater residual solids bioreactor for the conversion of these solids into useful building material within the same physical space (i.e. an FO membrane bag style element).

This part of the analysis is based on known wastewater treatment design principles as they would be applied to FO elements at the end of their useful life as water treatment elements. Also, the biological treatment, particularly for the urine dominated transit mission wastewater, may be amenable to purely physical (thermal) or chemical process treatment within the same design envelope, though likely with less optimal results for the final solid product.

However, the real function of this analysis is to give the space system architect the feel for how the processing of solids would work based using off the shelf materials and well understood engineering techniques from established municipal and industrial wastewater treatment engineering. Actual performance will vary based on variations in waste streams (and thus mission assumptions), but the principles of the water wall and its inclusion in system architecture concepts will remain the same.

Thus, the analytical sections to follow should be read as a rigorously presented example, rather than as an exact engineering solution at this time. Also it is good to see the full analysis to get a feel for the probable relative magnitude of product based on mass balance, while showing that those rough comparisons are based on defensible logic rather than poorly supported speculation.

1.3.2 Composted Biosolids for Hydrocarbon Wall Shielding Area and Volume Calculation

For hygiene water rich long term habitat wastewater, once treatment has moved on from a wall bag the remaining wastewater would be drained and mixed with concentrated biosolids from the feces collection and advanced (secondary) water treatment process (RO salts, spent activated carbon, and biodegradable trash) then re-injected into the imbedded bag for biological treatment. Under proper temperature and pH control these cells would undergo methanogenic composting, thus producing CO₂, CH₄, water vapor, and humus (organic soil). The CO₂ and CH₄ could be harvested for use as habitat makeup gas and water.

It should be noted that the gas resources recovered in this way are not interpreted as potentially large in terms of total volatile mission mass balance requirements like rocket oxidizer/fuel for primary propulsion. This element of the process is mentioned to indicate the possibility of retaining a limited and valuable resource that is a byproduct of the waste stabilization process to balance minor volatile requirements like attitude control and atmospheric leakage.

Composting accumulation rates should be dictated by the dry mass fraction of the treatment residuals. Total mass balance for a spacecraft habitat is given in Table 19. The Table 19 values following are approximations based on [Wieland, 1994]. However, mission scenarios range from as low as 2.67 kg/day to as high as 27.58 kg/day.

Examining only the wastewater side of the data and removing laundry water from the waste stream we get the following water and wastewaters solids inputs to the membrane system:

Water (in liters or kg):

Urine	1.50
Feces water content	0.09
Respiration/perspiration	2.28
Flush water	0.50
Hygiene water	<u>12.58</u>

Total water per crew day = 16.95

On a dewatering only basis the area requirement would be:

$$(4 \text{ days} \times 16.95 \text{ L/crew day}) / 510 \text{ L/m}^2 = 0.133 \text{ m}^2/\text{crew day}$$

However this is an in work dewatering area that does not correspond to the consumption rate of the membrane which at 95% recovery would be 20 X less, or 0.006 m²/crew day. Thus the active solids dewatering area is governing in this step. Solids calculation thus only relate to balancing mass throughput rather than area required. In reality some indigestible shredded garbage solids would likely be added to bring the dally solids volume up to match the FO water treatment bag area retirement rates giving in Table 20, at an effectively water and/or hydrocarbon based plastic thickness and volume dictated by the 510 L/m² accumulation rate.

Table 19: Daily mass balance for human life support varies with mission scenario.			
DAILY INPUTS in kg/day		DAILY OUTPUTS in kg/day	
Oxygen	0.84	Carbon Dioxide	1.00
Food Solids	0.62	Respiration and Perspiration	2.28
Water in Food	1.15	Urine	1.50
Food Prep Water	0.76	Feces Water	0.09
Drink	1.62	Sweat Solids	0.02
Hand/Face Wash Water	4.09	Urine Solids	0.06
Shower Water	2.73	Feces Solids	0.03
Clothes Wash Water	12.50	Hygiene Water	12.58
Dish Wash Water	5.45	Clothes Wash Water	11.90
Metabolized Water	0.35	Clothes Wash Latent Water	0.60
		Food Prep. Latent Water	0.04
Flush Water	0.49	Flush Water	0.50
Totals	30.60		30.60

1.3.4 Composted Biosolids for Hydrocarbon Wall Shielding Metabolic Mass Balance Calculation

Volume accumulation of residuals at 95% recovery gives 0.848 L/crewmember day (Table 10). Similarly for solids:

Solids:

Urine solids	0.062
Sweat solids (into hygiene)	0.02
Feces solids	0.03
Hygiene solids (soap)	<u>0.021</u>

Total 0.133 kg
Or: 133 g/crewmember day

Concentration is given by [12]: 133 g/0.848 L =157 g/L

Table 20. Area function for FO elements undergoing 4 day dewatering.				
Area Based on Dewatering	Corresponding Water Processing FO Area		Water to solids multiplier for active bags	
			Transit/ Urine	Long Term/ Gray
0.133 m ² / crew day	0.036 m ² /crew day Transit	0.12 m ² /cre w day	0.27	0.90

Table 21: Outputs per crewmember day prior to drying and/or digestion		
Water processed	Brine volume accumulated	Solids accumulated (dry weight)
16.95 L	0.848 L	0.133 kg

Hygiene solids are primarily body soap. The value used above is extracted from the work of Verostko et al., [Verostko, 2004] which functions as the currently available published ersatz for hygiene water. Within this ersatz concentrate mix prescribed for testing, 33 g/L organic solids in a 20X dilution is used. Of this 33 g/L, 30 g/L is soap, with acetic acid, urea, ethanol and lactic acid comprising 90% of the remaining organic solids by mass. This gives:

$$(33/20)\text{g/L}(12.58 \text{ L/d}) = 20.8 \text{ g/crewmember day dry mass of soap dominated organics}$$

Using an organic loading rate of 133 g/L organics is shown to give a mixed – liquor suspended solids (MLSS) loading rate of 156 g/L. Of course actual day to day loadings will probably vary wildly, but this will not effect the stoichiometric or average mass balance associated with treatment, and totals should average fairly close to the values given for long term accumulation based on wastewater design experience.

Conversion process calculations and values for wet activated sludge treatment are well documented [Tchobaoglous, 1991; Madigan, 1997; Maier 1999] for aerobic carbon reduction and nitrification (Stage 1 aerobic treatment), and anaerobic denitrification and methanogenesis (Stage 2 anaerobic treatment). Detailed stoichiometry and mass balance calculations for the municipal wastewater model are as follows.

1.3.5 Aerobic Digestion

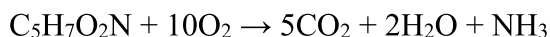
Aerated reactors can be expected to remove greater than 80% of the biologically available carbon in wastewater as measured by the total available biological oxygen demand (BOD₅). Biodegradable mass fraction varies substantially but 65% is used in text references for municipal wastewater prior to BOD testing for a specific waste stream. Oxygen to biomass consumption mass ratio is approximately 1.42 mg O₂/mg of biomass consumed. This and other values in biomass conversion are generally based on biomass stoichiometry relationships for C₅H₇O₂N [Tchobaoglous, 1991]. Using these values:

$$(0.8)(156 \text{ g/L})(0.65 \text{ BOD fraction})(1.42 \text{ O}_2 \text{ req/mg of bio}) = 115.2 \text{ gO}_2\text{/L residual concentrate stabilized}$$

$$156 \text{ g/L} (0.65)(0.8) = 81.1 \text{ g/L biomass converted to CO}_2$$

$$156 \text{ g/L} - 81.1 \text{ g/L} = 74.9 \text{ g/L biomass retained as sludge}$$

Using the stoichiometric relationship for aerobic biomass conversion [Madigan, 1997 & Maier 1999]:



Then:

$$115.2 (5\text{CO}_2/10\text{O}_2) = 115.2 (220/320) = 79.2 \text{ g/L CO}_2 \text{ production}$$

$$115.2 (2\text{H}_2\text{O}/10\text{O}_2) = 115.2 (36/320) = 12.9 \text{ g/L water production}$$

$$115.2 (\text{NH}_3/10\text{O}_2) = 115.2 (17/320) = 6.1 \text{ g/L ammonia nitrogen production}$$

If properly managed the aerobic digestion batch process will also nitrify the ammonia nitrogen [Madigan, 1997 & Maier 1999]:



This process should convert the majority of ammonia nitrogen to nitrate nitrogen, which is moved on to the anaerobic digestion step (Stage 2) as part of the wet solids rather than becoming a volatile ammonia problem. Please note that the discrepancy in hydrogen between NH_3 in one equation and NH_4^+ is a matter of pH adjustment and is fairly trivial from a mass balance perspective. It tends to be neglected in the available municipal sludge digestion calculation. However, it will probably be supplied by acetogenesis in the wastewater prior to treatment (i.e. the stored wastewater will become acidic and supply the necessary excess H^+). The impact on mass balance in Stage 1 of nitrification is as follows:

$$6.1(2\text{O}_2/\text{NH}_4^+) = 6.1(2(16)/18) = 5.4 \text{ g O}_2 / \text{L additional O}_2 \text{ required for denitrification}$$

$$6.1(\text{NO}_3^-/\text{NH}_4^+) = 6.1((14+3(16))/18) = 21.0 \text{ g nitrate/L produced}$$

$$6.1(2\text{H}^+/\text{NH}_4^+) = 6.1(2/18) = 0.7 \text{ g hydrogen produced}$$

$$6.1(\text{H}_2\text{O}/\text{NH}_4^+) = 6.1((2+16)/18) = 6.1 \text{ g H}_2\text{O produced}$$

This completes the aerobic Stage 1 treatment of the waste solids. Stage 2 will proceed with denitrification first followed by methanogenesis [Madigan, 1997 & Maier 1999].



$$21.0 \text{ g/L } (5\text{H}_2/\text{NO}_3^-) = 21.0(5/62) = 1.7 \text{ g/L hydrogen required}$$

2H^+ is balanced with the nitrification calculation and is canceled

$$21.0 \text{ g/L } (\text{N}_2/\text{NO}_3^-) = 21.0(28/62) = 9.5 \text{ g/L nitrogen produced}$$

$$21.0 \text{ g/L } (6\text{H}_2\text{O}/\text{NO}_3^-) = 21.0(18/62) = 6.1 \text{ g/L water produced}$$

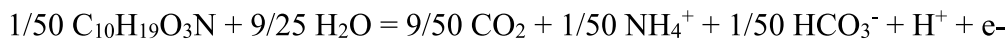
74.9 g/L of biosolids is moved forward to the anaerobic composting stage. Methane (CH_4) production rates are calculated based on the remaining 20% of the BOD_L not removed by aerobic digestion [Madigan, 1997]. The stoichiometry of the remaining BOD₅ is even more variable and unpredictable than it is for the initial waste stream, but a text reference for municipal sludge digestion [Tchobaoglous, 1991] uses a 4 to 1 mass ratio as a design estimate prior to specific waste stream testing/analysis. Using this admittedly rough estimation:

$$156 \text{ g/L } (0.2)(0.65) = 20.3 \text{ g/L BOD}_5 \text{ remains for methanogenesis (any biomass production for denitrification neglected)}$$

This will produce approximately 5g/L methane, but will proceed through various metabolic pathways simultaneously in a complex organic waste, and will consume a small amount of water

as well as convert it variously into H₂, HCO₃⁻, CO₂, and intermediate organic products such as acetate. All of the above in some relative proportion will likely occur based on waste stream composition [Madigan, 1997]. Although, the gas extracted will be predominantly methane, with a trace of hydrogen and CO₂.

A complete carbon and nitrogen formula is available for municipal wastewater solids [Grady, 1999]:



However, this strategy is not carried through (with O₂) because the difference between municipal wastewater and spacecraft wastewater is significant. It is not enough to warrant return to first principles when developing actual observed stoichiometric relationships through testing, rather than referencing normal wastewater engineering parameters.

Complete two stage mass balance per liter of wastewater residuals stabilized is as follows:

Input values per liter:

156 g/L solids input

O₂ requirements 115 g/L (carbon reduction) + 5.4 g/L (denitrification) = 120.4 g/L total aerobic O₂ requirement

1.3.6 Anaerobic Denitrification

Anaerobic denitrification will require 1.7 g/L hydrogen at a minimum but it is likely that the aerobic to anaerobic transition of the bag will be accomplished by purging the O₂ bag with an excess of H₂. For this reason, hydrogen use of 20 g/L or more should be allocated to the process. Mixed hydrogen and methane (with O₂) burning in an attitude control system should be investigated so that combined biogas (methane, nitrogen, hydrogen and trace CO₂) and hydrogen purge gases from the long term anaerobic stage digestion process could be used without further processing.

Output values per liter:

- 74.9 g/L sludge is produced in the aerobic stage with roughly another 5 g/L reduced by methanogenesis. This gives a residual stabilized organic solid recovery of approximately 70 g/L.
- Aerobic gas output would be 79.2 g/l CO₂.

Anaerobic gas production would amount to approximately 9.5 g/L nitrogen mixed with 1.7 g/L hydrogen, hydrogen purge gas as required, and 5 g/L methane and trace CO₂. Trace water production of 12.9 g/L water during aerobic digestion and 6.1 g/L water during denitrification would also occur but is small compared to the total water still available in the residual concentrate. From a mass/cost perspective, the oxygen and hydrogen gas inputs and CO₂ gas output represent the primary potential costs, which could make the process uncompetitive with simple disposal of solids and brines. However, the inclusion of algal growth cells in the habitat could recover much of the oxygen and the fate of the gas as leak rate makeup gas.

Also, algae biomass inputs could be used to balance the over capacity of the solid reactors in comparison to the water process membrane area consumption rate. In this mode the unusable biomass from food and energy (biological fuel cell) bags could easily be incorporated into the

cover capacity of FO bag based solids processing bags. Thus, between a slightly better than 1/1 (gray/long term habitat water) and 4/1 (urine/transit water) over capacity of solids digester capacity could be generated with careful management on the human waste side, and this capacity would be dedicated to algae biomass management in future habitats, though this would require the reduction of indigestible garbage to be balanced.

Finally, this mass balance requires no system upset and 95% water recycle. More often than not real world systems have failed to live up. So the 4 to 1 overcapacity of solids production bag can also correspond to lower the water recovery to 80% in early operation. This institutes a large safety factor into early system operations. Thus a 1/1 solids/reject processing bag area to water processing area provides a large margin of safety early in operation and a good balance once hygiene water use matures in the habitat. Due to the variability of real world human waste this 2X multiplier will not be refined further until actual human testing is possible. As with wastewater flux rate and area requirements, this initial theoretical set of values will be modified later to account for the roughly doubled time for full dewatering of human waste simulant experienced due to membrane flux decline in Phase I NIAC testing.

1.3.7 Experimental Testing to Determine Life Cycle Flux Decline and Related Design Area Expansion

To this point sizing has been accomplished using the rough ideal flux rate for urine treatment of 4 L/m² day and the initial human waste solids testing using distillation urine processing brine, which took 4 days to get to 90%. Both values were modified by Phase I NIAC testing to account for 10 cycle water processing decline followed by human waste simulant following solids dewatering. These values both came out to a rough 0.5 multiplier on both performance parameters and thus a rough 2X multiplier on both the solids and water processing areas determined above in the theoretical mass balance from the urine process.

The results of experimental flux testing for three bags are presented in Figures 27. Figure 28 shows the production rate or the flux of water through the internal membrane of the bag, in units of liters per meter square per hour (L/m² hr), as a function of time. The flux rate decreases with time, which is due to the increase in concentration of the feed and the dilution of the osmotic agent solution over time. The flux rate declines slightly due to fouling of the membrane. The spike in flux at about 5 hours is an artifact of the recharge of the NaCl draw solution during the run. Error bars range from 5% to 33%.

1.3.8 Water Processing Summary

This wastewater testing demonstrated the ability to treat simulated ersatz wastewater in an X-Pack™ bag with a water recover ratio of 90%. When mixing the resulting concentrated brine with simulated fecal material, and returning the mixture to the bag, another 95% of the water in the solid ersatz was removed. Therefore, the combined water recovery ratio that can be achieved is over 99%.

The testing also measured flux rate. Flux rates are the rate at which water crosses the FO membrane and is equal to the production rate. It is important as it defines the amount of membrane required to treat the wastewater on a given mission. The maximum flux of water in the X-Pack™ is 3.5 L/m²hr when treating wastewater and 0.3 L/m²hr when treating the solid ersatz. It is important to note that flux rates decrease as a function of time. This is because during a run, the feed is concentrating and the OA is becoming diluted. As a result, the osmotic potential difference across the membrane decreases during the run. A run is complete when the

osmotic potential equalizes and water no longer flows across the membrane. Area values in a conservative baseline design are as shown in Table 22.

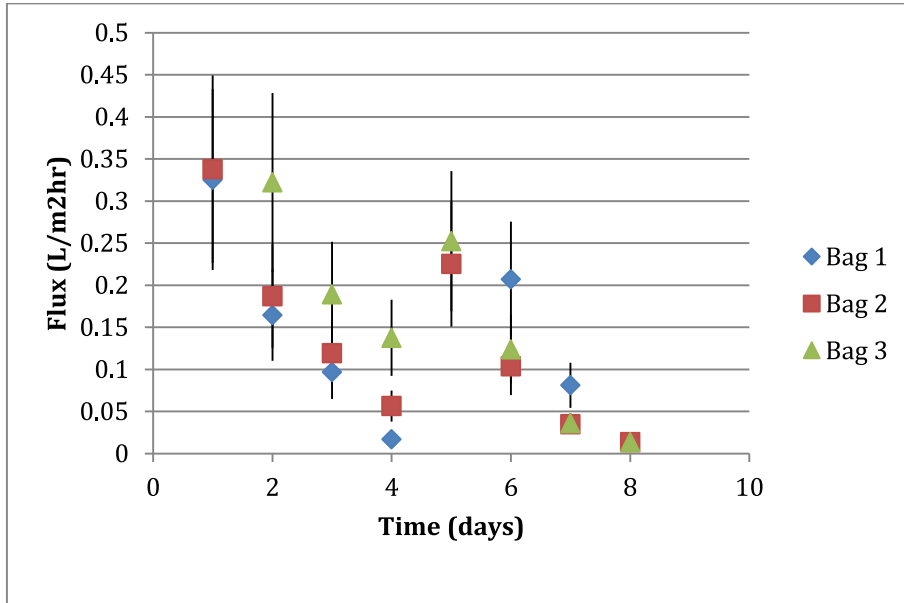


Figure 27. Flux testing for solid ersatz. Each data point is the average of 8 runs in each bag.

Figure 28 present the results of the water recovery ratio calculations for the same tests presented in Figures 27. The water recovery ratio is the ratio of the mass of water in the feed to the mass of water produced. The Figure shows that after 8 days of contact, a recovery ratio of approximately 95% is possible for the solid ersatz.

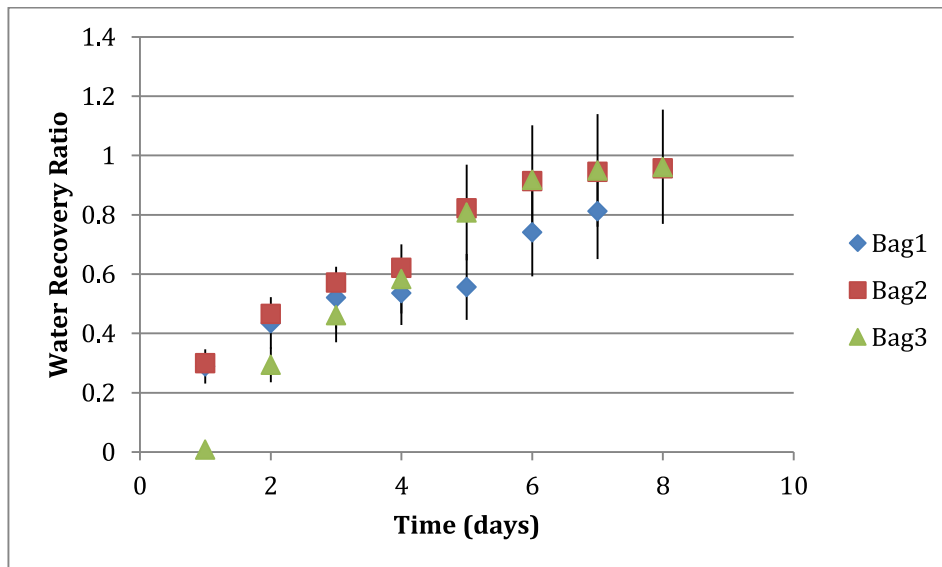


Figure 28. Water Recovery Ratio as a function of time for solid ersatz. Each data point is the average of 10 runs in each bag. Error bars are 20 %. Note that this is an 8 day test with human waste simulant as opposed to a 4 day test to 90% recovery for a 1st use membrane on urine brine.

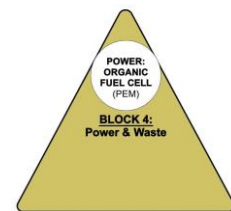
Table 22. Modified Area Values for Water Processing FO Bags
in m²/Crewmember/day

Water Process; Start-up (i.e. urine and condensate based)	Water Process; Based on a Mature Habitat (i.e. hygiene water based)	Solids; Start-up Habitat	Solids; Mature Habitat
0.072	0.24	0.019	0.22

The results of this experimental testing demonstrate that the concept of a membrane based FO water treatment system integrated into the walls of a spacecraft as a Water Wall is feasible. The system will treat wastewater and achieve a high water recovery ratio. The FO membranes are reusable but their life will be limited as the flux rate decreases with every reuse. Product water purity and post treatment requirements were not evaluated in this work but have been previously evaluated in Gormly et al. [Gromly, 2007].

1.4 Microbial Fuel Cells as Life Support Components

Microbial fuel cells (MFC) offer great promise to provide both blackwater/solid waste pre-processing and the concurrent generation of electricity. For the implementation of MFCs to succeed in WW as an intrinsic part of the Life Support Architecture, it is necessary to understand and master their properties, potential, advantages and disadvantages. This section addresses the relevant issues for MFCs as components in the Bioelectrochemical Subsystem of the Power and Waste Process Block 4. Development of MFC for space flight applications is currently funded by the STMD Synthetic Biology Program and the PI for this NIAC grant is a CoI on that project. The STMD MFC project is currently constructing a MFC for space flight application with a milestone to have an operational system by the end of FY13. Figure 29 is a CAD drawing of the STMD MFC which is currently being constructed in the Ames machine Shop. Figure 30 is an exploded view of a single cell of the same MFC.



MFCs exploit biological functions for the catalysis of electrochemical reactions. MFCs specifically utilize microbial functions to produce an electrical current, or to catalyze a reaction with the addition of an electrical current. While there are many configurations for the functionality of BESs, the classic design, as illustrated in Figure 31, involves two electrode chambers, an anode and a cathode, that are commonly separated by a proton exchange membrane (PEM). The design and components of each electrode chamber are dependent on the desired result or product of the overall system, and can involve microbial cultures or communities, electrolytes, electrochemical reactions, and water.

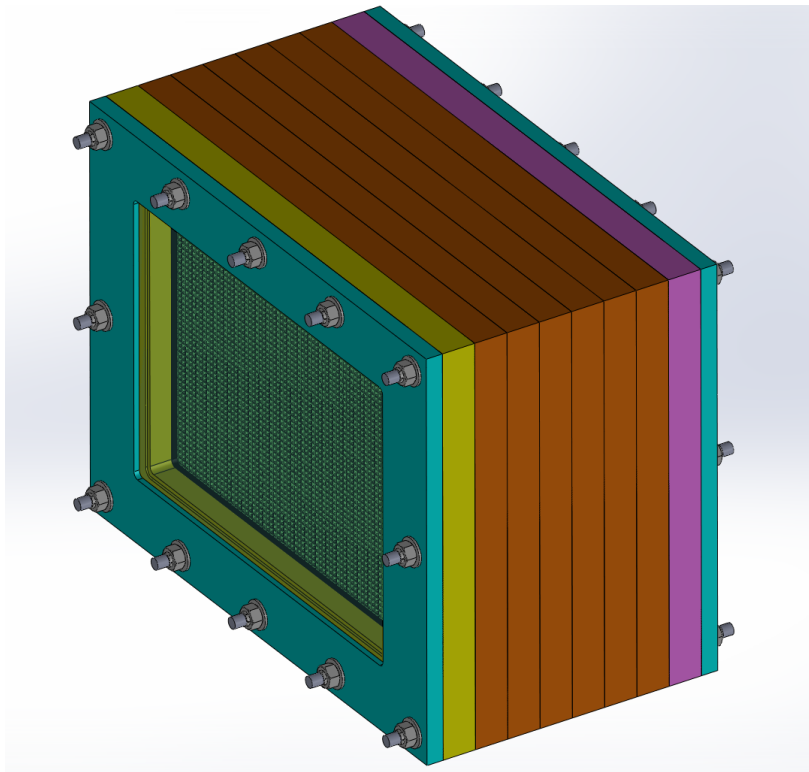


Figure 29: CAD drawing of STMD Synthetic Biology NASA MFC test system

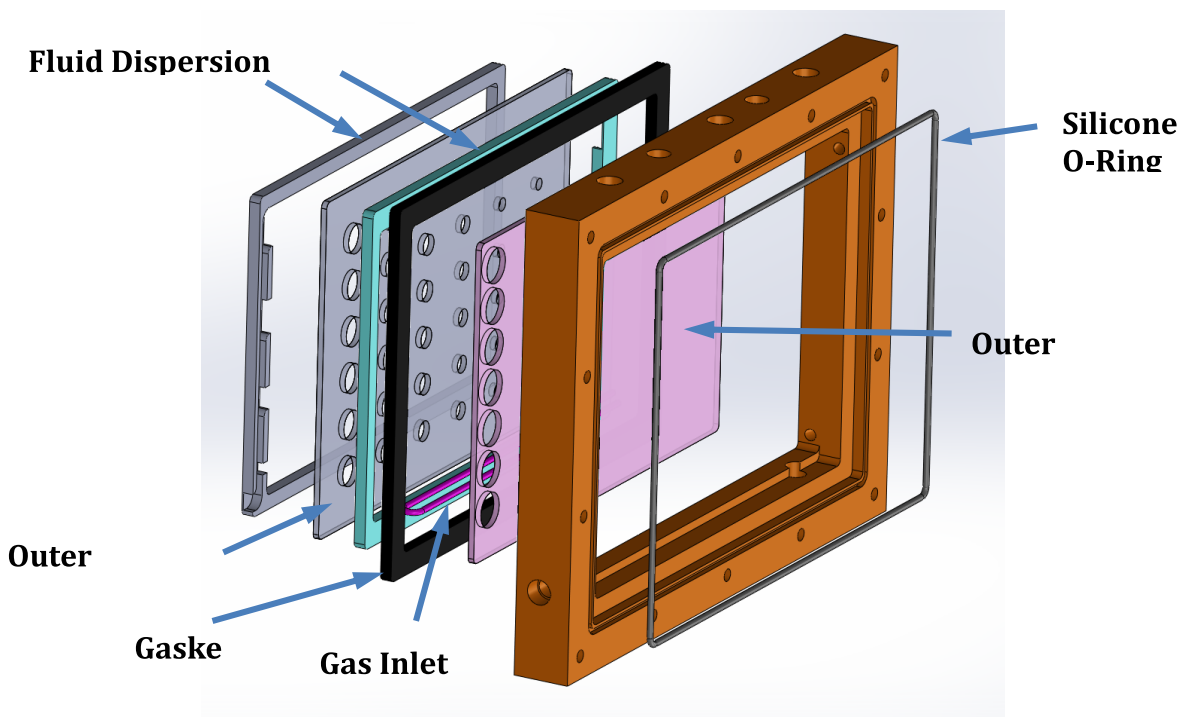


Figure 30: Explode view of single cell of NASA MFC

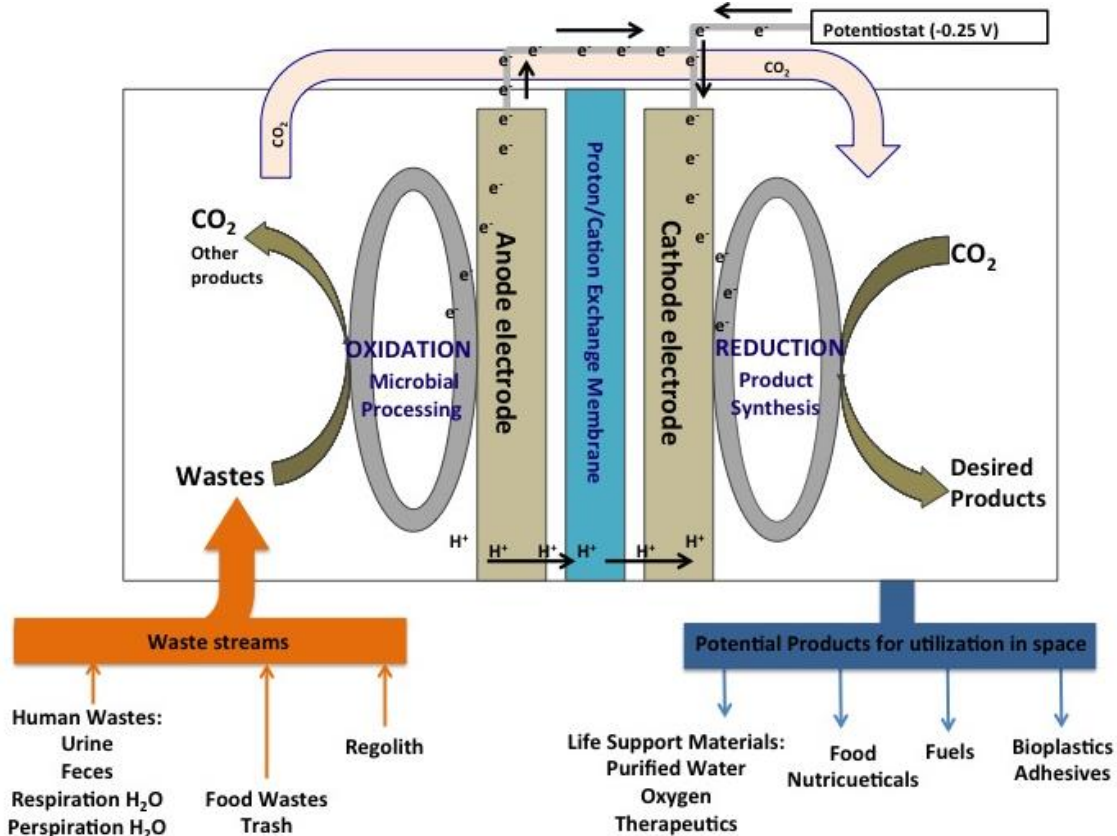


Figure 31: Schematic of potential BES application for space exploration. The Figure illustrates the potential inputs and products that are targeted for BES use during space exploration. The synthesized product is dependent on the waste stream used as an input, and the species or community of organisms used within the system.

1.4.1 Extracellular Electron Transport

A small number of organisms, known as exoelectrogens, can utilize extracellular electron transport (EET) to move electrons from an electron donor to an extracellular electron acceptor, and occasionally involves intermediates⁶. It is this novel capability that allows MFCs to operate. The exoelectrogens utilize reduced and oxidized molecules to move electrons across the cellular membrane. The movement of electrons via EET generates energy to fuel metabolic processes that occur amongst microbial communities. There are three mechanisms that can be utilized in order to perform EET: direct electron transport, hydrogen production/consumption, and redox mediators [Logan, 2006 & Rabaey, 2009]

Direct electron transport methods require contact or to be in close proximity to the surface to which the electrons are being transferred, and requires membrane associated compounds to assist the transfer. Direct electron transport does not allow for electron transfer across long distances. There are a minimal number of species that are able to perform direct electron transport. Recent discovery of bacterial nanowires, conductive appendages that extend from the bacterial

membrane, has shown a naturally occurring adaptation to the limitations of distance and proximity for direct electron transfer^{2,3,6}. [Logan, 2006; Ghangrekar, 2006 and Snider, 2012]

The hydrogen production/consumption method, also called hydrogen transfer, utilizes the conversion of protons to H₂ as an electron transport mechanism between cell surfaces [Lovley, 1996]. Acids act as temporary electron acceptors, or intermediates, and shuttle electrons between systems. The most common examples of hydrogen transfer methods of EET are reported to occur in humic environments [Lovley, 1996 & Stams, 2006]

The third method of EET involves the use of redox mediators. Redox mediators can be naturally occurring in the system, such as the production of quinones and flavins by *Shewanella spp.* [Stams, 2006] or they can be added to the system. Redox mediators act similarly to that of the hydrogen production/consumption method, wherein the mediators act as a shuttle for electrons being transferred [Marsili, 2008]. The lack of restriction of an electron shuttle allows electrons to be transported across larger distances than that of direct electron transport methods [Rabaey]. The use of redox mediators has been seen in electron transport both intracellularly and extracellularly, but the internal or external location and environment in which the mediators can be used is dependent on the species and type of mediator [Babanova, 2011] Many studies have found that EET mechanisms that rely solely on redox mediators are overall less efficient than direct EET⁷.

1.4.2 The Biology of MFCs

Only certain microorganisms can be exploited to perform the bioelectrochemical reactions necessary to run a MFC. The selection of which microorganisms to use is most often dependent on the desired result or product, wherein a single organism is selected to perform the desired reactions [Torres, 2009] Selecting a single organism allows more control over the specific reactions, and can influence the reactor design. Alternatively, a microbial consortia, or a community of mixed organisms, can increase efficiency via working collaboratively towards a desired goal or product [Ghangrekar, 2006]. Reactor systems run by communities of organisms are commonly seen using self-selecting communities directly extracted from their natural environment. For example, sludge samples isolated from sewage run off can be used to inoculate MFCs designed for water treatment [Kim, 2007].

When working with consortiums of microorganisms, the issue of competition for resources must be considered. Selective pressures may assist in the reduction of competition when applied to selected field samples [Korotkevych, 2011]. Genomic analysis of the samples will allow characterization of key organisms. Selective pressure through the use of organism-specific media, temperature specifications, or pH adjustments to the media will amplify the survival of target organisms, while excluding others.

The advent of synthetic biology has improved the capabilities of MFCs by enabling the “customization” of gene sequences and organismal function [Montague, 2012]. Redox reactions are not a static occurrence in every organism. The methods of EET naturally utilized by a target organism indicate the method of interaction between the organism and the electrode surface, and will directly affect the design of the MFC. An issue may arise if, for example, the organism only utilizes direct EET methods, but will not adhere to the electrode surface in order to perform the transfer. Genetic manipulation may influence the organism to be able to use redox mediators as an EET shuttle instead, performing the desired reaction [Montague, 2012 & Colin, 2011]. Some organisms may have the capability to perform certain reactions or synthesize a complicated and desired product, but are also impossible to accommodate in a MFC environment. For example, the temperature requirements or gas environment requirements for an organism of interest may

be unreasonable to reproduce in a laboratory setting, while organisms like *E. coli* thrive well in universal conditions but are unable to perform the desired reaction. Synthetic biology and genetic engineering are potential solutions, as key genes identified to be critical for the completion of a desired reaction could be inserted into an organism that is easy to manipulate and maintain, such as *E. coli*. Some laboratories have had success with influencing organisms to perform alternative EET mechanisms, whether through environmental changes or genetic manipulation and engineering¹⁸. Additionally, synthetic biology can be used to override negative controls that naturally limit the productivity of the organism in response to nutrient availability or other environmental factors. Productivity and recovery rates serve as critical data for justifying the use of MFCs for many applications, especially for use in space.

1.4.3 Anode and Cathode Configuration

An anode is the positively charged electrode by which the electrons leave a device. In the parlance of MFCs, an anode is the negatively charged electrode of a device supplying current. The efficiency of an anode is assessed through endeavored optimization of its design and material. For example, an increase in anodic surface area has shown to be positively correlated to electrode efficiency [Park, 1999 & Gil, 2006]. By increasing the region of interaction between electrode material and microorganisms utilized within the system, there exists a greater opportunity for electrons to congregate and increase a charge gradient on the PEM, thus increasing the current furthering efficiency. Anode efficiency can also be increased through the application of redox mediators [Park, 1999]. Redox mediators carry the electric charge from the production site to the anode, and facilitate larger congregations of electric charge.

A cathode is an electrode used to transfer electrons into or out of a device. The polarity of the cathode determines the direction of the electron flow. Optimization of cathode efficiency is done through the use of electron acceptors such as ferricyanide or oxygen, which have a high oxidation potential [Park, 1999]. Regular catholyte replenishment has also been shown to increase power density by a factor of three and operation longevity by a factor of seven [Hou, 2012].

As in all energy production systems, a loss of efficiency exists due to inherent internal resistance. In MFC systems, the current produced is degraded by the resistance of electrons and protons flowing through their respective composite material [Hoogers, 2003]. This phenomenon, Ohm's Law, can be modeled via classical electric circuit theory as:

$$V = IR$$

Where, V = difference in electrical potential (or voltage, measured in Volts), I = current (or amperage, measured in Amperes) and R = electrical resistance, measured in Ohms.

Optimizing the electrode spacing, membrane resistivity, redox mediator potential, and surface contact between organism and electrode³³ can minimize ohmic loss.

1.4.4 Membranes and membrane-less systems

Membranes are used in various technologies for spaceflight for filtering, insulation and other barrier needs [Hanford, 2004]. PEMs, also called cation exchange membranes (CEMs), assist in the selective movement of excess protons from the anode chamber to the cathode chamber, wherein the protons are often sequestered for a target product or byproduct of the system [Kim, 2007]. In most instances, an accumulation of protons will contribute to an inhospitable environment for the microorganisms through the increase in acidity of the medium. The proton selectivity of the PEMs allows the dual chamber design to control the pH through minimizing unnecessary proton build up, while maintaining separate culture environments in the

cathode and anode [Li, 2011], which limits the risk of fluid exchange or contamination. The flow of protons from one chamber to the next may also contribute to the generation of desirable products in the cathode.

1.5 Radiation Protection

The ionizing radiation affecting human operations during spaceflights comes from three different sources and consists of every known particle including energetic ions formed from stripping the electrons from all of the natural elements (Figure 32). The three sources of radiations are associated with their different origins identified as:

- Particles of galactic origin (Galactic Cosmic Rays, GCR)
- 3. Particles produced by the acceleration of the solar plasma by strong electromotive forces in the solar surface and propagating through coronal mass ejection (Solar Energetic Particles, SEP often referred to as solar storms)
- 4. Particles trapped within the confines of the geomagnetic field (Van Allen Belts).

The radiation environment in space is dynamic. The GCR intensity is constant outside the solar system while at the Earth's orbit undergoes a modulation over the solar cycle (usually to an average 11 – *years* cycle) and according to changes in the interplanetary plasma which excludes the lower energy galactic ions from the region within several AU of the sun.

The SEP are unpredictable both in timing and intensity. They are associated with some solar flares, which produce intense burst of high energy plasma propagating into the solar system along the confines of the sectorized interplanetary magnetic field. The SEP are accelerated within this transition region.

The trapped radiations consist mainly of protons and electrons within two bands centered on the geomagnetic equator reaching a maximum at 3,600 *km* followed by a minimum at 7,000 *km* and by a second very broad maximum at 10,000 *km*.

In early space habitat missions, the GCR has been considered negligible because mission durations were relatively short and/or where below the Van Allen Radiation Belts. In these missions the main radiation concern was the very intense SEP events which can rise unexpectedly to high levels and deliver a potentially lethal dose in a few to several hours if precautions are not taken. The trapped radiations become relevant for spacecraft's flying from LEO to interplanetary space if the passage time is more than several minutes. ¹

¹ Shielding Strategies for Human Space Exploration

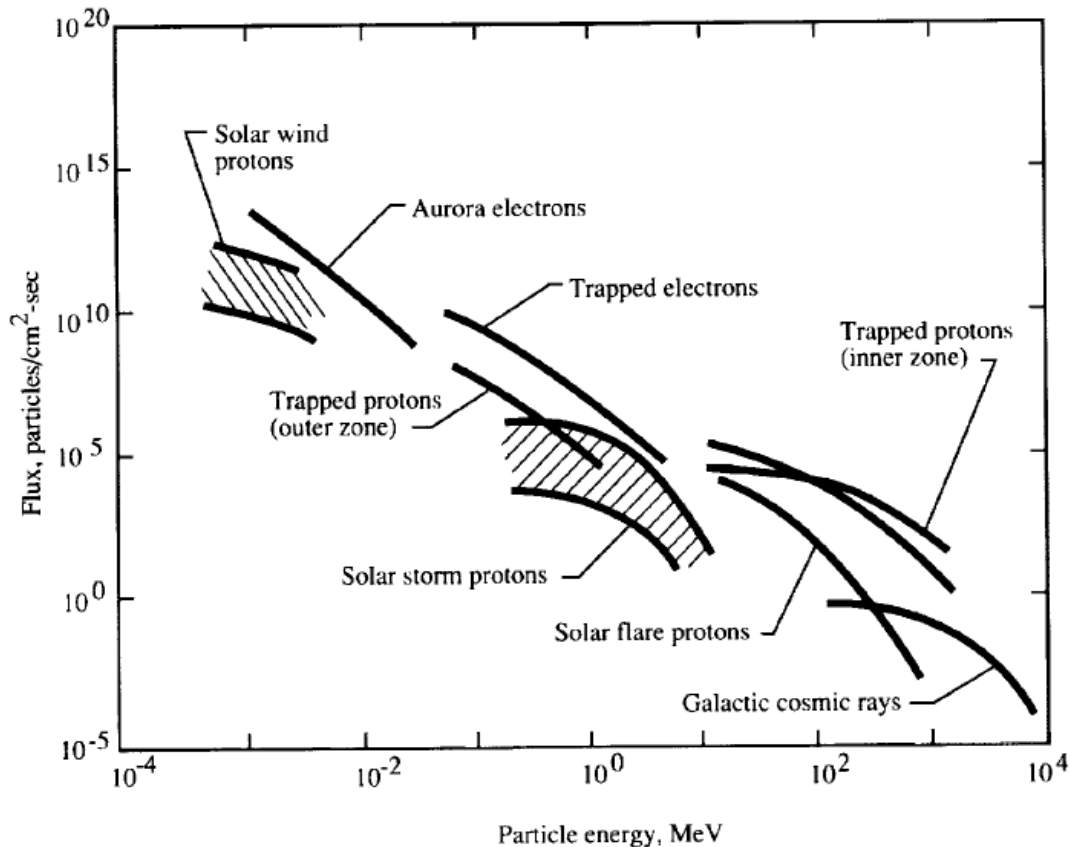


Figure 32 - Free-space radiation environment

Occupational radiation exposure from the known space environment is sufficiently severe that it may increase cancer morbidity or the mortality risk in astronauts. A long-term human mission to Moon or Mars will not be feasible unless improved shielding is developed and/or transit time is decreased. In fact, the major obstacle to human space exploration at this time is the limitation imposed by the adverse effects of long-term radiation exposure in the space environment. The Human Research Program (HRP) has developed and is continuously updating research and technology requirements and standards regarding the maintenance of human health and performance, which will define acceptable risks for each type, and duration of exploration mission. These elements form the basis of NASA's research and technology development in safeguarding human health by reducing medical and environmental risks for long-duration spaceflight and they must be incorporated into future exploration mission planning and vehicle designs. The HRP utilizes a criticality metric to determine the weight of each risk. The criticality metric is based on the level of the current state of knowledge about a risk, whether existing standards are met, and the degree to which the level of understanding of the risk may prompt one not to undertake a mission. Three mission scenarios are taken into account in the HRP analysis: a Lunar Outpost mission of a 180-days' duration, a NEA mission of a 1-year's duration and finally a 3-years' long Mars mission. Each risk has a separate criticality rating for each of the previous mission scenarios. Four different levels describe the criticality rating:

- The *unacceptable* rating level is related to a risk, which has one or more attributes (i.e. consequence, likelihood, uncertainty) that are well understood but at the same time are characterized such that it will not meet existing standards, making it necessary to reduce one or more of these attributes prior to a mission. Otherwise, it causes the delay of a

mission even if all other elements of the mission were ready (e.g. launch systems, Extravehicular Activity (EVA) systems, landing and life support systems).

- The *acceptable* rating level is assigned to a risk if all of its risks are well understood and meet existing standards but are not fully controlled. In this case it is important to reduce one or more attributes prior to a mission, even if the risk is not expected to preclude a mission.
- The *controlled* rating level is ascribed to a risk if one or more of its attributes are well understood and mitigation exists to control it at an accepted cost. It is still helpful to reduce one or more of these attributes prior to a mission even if the risk will not preclude a mission, while some additional work could further reduce the risk's consequence and increase engineering or operational efficiencies.
- A risk is deemed to have a rating of *insufficient data* if one or more of its attributes are poorly understood and inadequately characterized to assess whether it has the potential to preclude any mission. Standards do not exist and current state of data regarding the impact of the risk to a mission is grossly inadequate.

Finally, the Verification Status classifies a risk as *verified* if it is substantiated by strong evidence either from spaceflight incidents, spaceflight or terrestrial data. If the risk is a concern that cannot be supported or refuted by available information, and for which further evidence to substantiate the risk is required, the risk is *unverified*.²

Among all the risks identified by the HPR, *Table 23* takes into account only those, which are strictly related to space radiation exposure

Table 23 - Radiation space exposure risks identified by HPR

Risk	Criticality Rating			Verification Status
	Lunar	NEA	Mars	
	(180 days)	(1 year)	(3 years)	
Risk of Radiation Carcinogenesis	Acceptable	Unacceptable	Unacceptable	Verified
Risk of Acute Radiation Syndromes Due to Solar Particle Events	Acceptable	Acceptable	Acceptable	Verified
Risk of Acute or Late Central Nervous System Effects from Radiation Exposure	Acceptable	Insufficient data	Insufficient data	Unverified
Risk of Degenerative Tissue or other Health Effects from Radiation Exposure	Acceptable	Insufficient data	Insufficient data	Verified

Astronauts are exposed to ionizing radiation quantitatively and qualitatively different from the terrestrial one. The space environment includes protons and High-Z high-Energy (HZE) ions together with secondary radiation, including neutrons and recoil nuclei produced by nuclear reactions in spacecraft materials. Crewmembers on missions to the ISS, to a Lunar Outpost, to a NEA or to Mars are understood to be exposed to ionizing radiation with effective doses in the range of 50 to 2000 mSv (milli-Sievert) if unsheltered. Similar doses from terrestrial radiation

² Human Research Program Requirements Document (revision May 2012)

sources, such as γ -rays and X-rays, are associated with an increased risk for development of cancer. Therefore, occupational radiation exposure from the space environment may increase cancer morbidity or mortality risk in astronauts.

A major Solar Particle Event (SPE) may increase the risk for Acute Radiation Sickness (ARS) (e.g., nausea, vomiting, anorexia, and fatigue) such that the mission or crew survival may be placed in jeopardy. Beyond LEO, the protection of the Earth's magnetosphere is no longer available, such that increased shielding and protective strategies are necessary in order to safeguard the astronauts' health and performance. Given the inability to accurately predict the occurrence of SPE, there is the possibility the crew will suffer from ARS, skin damage and hematological changes, which can result in a potential loss of mission. The primary data available at present are derived from medical analysis of patients accidentally exposed to high doses of radiation. However, data more specific to the space environment must still be compiled to quantify the magnitude of increase of this risk.

GCR and SPE can damage the Central Nervous System (CNS) leading to acute and/or late changes in motor function, behavior, or neurological disorders. CNS risks are a documented concern for space environment, which may affect either the success of a mission because of altered cognitive function and reduced motor function of crewmembers or late human health including Alzheimer's disease, dementia and premature aging. Although detrimental CNS changes are observed in humans exposed to high dose radiation and are supported by experimental evidence showing behavioral and neurological effects in animal models, the significance of these results on the morbidity to astronauts has not been elucidated yet. There is a lack of human epidemiology data on which to base CNS risk estimates and therefore risk projection based on scaling to human data, as done for cancer risk, but is not possible for CNS risks. Research specific to the space environment using animal and cell models must still be compiled to quantify the magnitude of this risk and to establish validity of the current Permissible Exposure Limits (PEL).

Degenerative effects following exposures to terrestrial radiation sources such as γ -rays and X-rays are well documented and include cardiac, circulatory, digestive diseases as well as cataracts. However, the mechanisms and the magnitude of influence of radiation leading to these diseases are not well characterized. Long exposures to ionizing radiation in the form of GCR or SPE and, possible degenerative tissue effects (non-cancer or non-CNS) are highly expected during space travels beyond LEO. However, data specific to space environment must still be compiled to quantify the magnitude of degenerative disease risks, to decrease the uncertainty in current PELs, and to determine if additional protection strategies are required to safeguard crewmembers' health.

7.5.1 Current NASA permissible exposure limits

The astronaut career exposure to radiation is limited to not exceed 3% of the Risk of Exposure-Induced Death (REID) from fatal cancer. This value is based on several criteria, including a comparison to dose limits for ground radiation workers and to rates of occupational death in less safe industries. NASA policy is to assure that this risk limit is not exceeded by the cumulative effective dose (in units of *Sievert*) that is received by an astronaut throughout his or her career. These limits are applicable to missions of any duration in LEO and to short lunar missions. The relationship between radiation exposure and risk is both age- and gender-specific due to latency effects and differences in tissue types, sensitivities, and life spans between genders. These relationships are estimated using the methods that are recommended by the

National Council on Radiation Protection (NCRP). *Table 24* lists examples of career effective dose limits for an $REID = 3\%$ for missions that are of ≤ 1 year duration.

Age [yr]	E[mSv] for 3% REID	
	Males	Females
25	520	370
30	620	470
35	720	550
40	800	620
45	950	750
50	1,150	920
55	1,470	1,120

Table 14 - Career effective dose limits

1.5.1 Evaluating career limits

Radiation exposures are often described in terms of the physical quantity absorbed dose, D , which is defined as the energy deposited per unit mass. Dose has units of *Joule/kg*, which defines the special unit, 1 *Gray* [Gy], which is equivalent to 100 *rad* ($0.01 Gy = 1 rad$). The number of particles per unit area is called fluence, F , with units of *particle/cm²*. As particles pass through matter, they lose energy at a rate dependent on their kinetic energy, E , and charge number, Z , and approximately the average ratio of charge to mass (Z/A) of the materials they traverse. The rate of energy loss is called the linear energy transfer (LET), which for unit density materials such as tissue is given in units of *keV/μm*. The dose and fluence are related by $D = \rho F LET$, where ρ is the density of the material (e.g., 1 *g/cm³* for water or tissue).

Cancer risk is not measured directly but is calculated using radiation dosimetry and physics methods. The absorbed dose D is calculated using measurements of radiation levels that are provided by dosimeters (e.g., film badges, thermo-luminescent dosimeters, spectrometers such as the tissue-equivalent proportional counter, area radiation monitors, biodosimetry, or biological markers) and corrections for instrument limitations. The limiting risk is calculated using the effective dose and risk conversion life-table methodologies.

The body is divided into a set of sensitive tissues, and each tissue, T , is assigned a weight, w_T , according to its estimated contribution to cancer risk, as shown in *Table 25*.

The absorbed dose, D_T , delivered to each tissue is determined from measured dosimetry. Different types of radiation have different biological effectiveness, depending on the ionization density that is left behind locally (e.g., in a cell or a cell nucleus) by the passage of radiation through matter. For the purpose of estimating radiation risk to an organ, the quantity characterizing this ionization density is the LET (in units of *keV/μm*). For a given interval of LET, the dose-equivalent risk to a tissue $H_T(L)$ is calculated as

$$H_T(L) = Q(L)D_T(L)$$

where the quality factor $Q(L)$ is obtained according to the International Commission on Radiation Protection (ICRP) prescription shown in *Table 26*.

The average risk to a tissue T , due to all types of radiation contributing to the dose, is given by

$$H_T = \int D_T(L) Q(L)dL$$

The effective dose is used as a summation over radiation type and tissue using the tissue weighting factors

$$E = \sum_T w_T H_T$$

For a mission of duration t , the effective dose will be a function of time, $E(t)$, and the effective dose for mission i will be

$$E_i = \int E(t) dt$$

The effective dose is used to scale the mortality rate for radiation-induced death from the Japanese survivor data, applying the average of the multiplicative and additive transfer models for solid cancers and the additive transfer model for leukemia by applying life-table methodologies that are based on U.S. population data for background cancer and all causes of death mortality rates.

Ti /organ	w
Gonads	0.
Bone marrow	0.1
Colon	0.1
Lung	0.1
Stomach	0.1
Bladder	0.0
Breast	0.0
Liver	0.0
Esophagus	0.0
Thyroid	0.0
Skin	0.0
Bone surface	0.0
Remainder	0.0

Table 25 - Tissue weighting factors

LET [keV/μm]	Q(LET)
<10	
10 to 100	0.32 LE
>100	300/√(LET)

Table 26 - Quality factor- LET relationship

Age [yr]	NCRP report #98		NCRP report # 13	
	Males [Sv]	Females [Sv]	Males [Sv]	Females [Sv]
25	1.5	1	0.7	0.
35	2.5	1.75	1	0.
45	3.2	2.5	1.5	0.
55	4	3	3	1.

Table 27 - Career dose limits for 10-year careers as a function of age and sex, as recommended by the NCRP

1.5.2 Evaluation of cumulative radiation risks

The cumulative cancer fatality risk (%REID) to an astronaut for occupational radiation exposures, N , is found by applying life-table methodologies that can be approximated at small values of %REID by summing over the tissue-weighted effective dose, E_i , as

$$Risk = \sum_{i=1}^N E_i R_0$$

where R_0 are the age- and gender-specific radiation mortality rates per unit dose. The effective dose limits that are given in the *Table 24* illustrate the effective dose that corresponds to a 3% REID for missions with a duration of as long as 1 year. Values for multiple missions or other occupational exposure are estimated using the previous formula or directly from life-table calculations.

Table 27 provides examples of career radiation limits for a career duration of 10 years, with the doses assumed to be spread evenly over the career. The values from the previous report are also listed for comparison. Both of these reports specify that these limits do not apply to deep-space missions because of the large uncertainties in predicting the risks of latent effects from heavy ions. The decreased rate of fatalities in the so-called less safe industries (e.g., mining, agriculture) because of the large improvements that had been made in ground-based occupational safety, would suggest a limit below the 3% fatality level today as compared to that in 1989. However the social and scientific benefits of space flight continue to provide justification for the 3% risk level for astronauts who are participating in LEO missions. In comparison to the limits that have been set by NASA, the U.S. nuclear industry uses age-specific limits that are gender-averaged, which is of sufficient accuracy for the low doses received by nuclear workers. Here career limits are set at a total dose-equivalent that is equal to the individual's age multiplied per 0.01 Sv. It is estimated by the NCRP that ground workers who reach their dose limits would have a lifetime risk of about 3%, but note the difference in dose values corresponding to the limit is due to differences in how the radiation doses are accumulated over the worker's career. The short-term (30 days and 1 year) dose limits set by NASA are several times higher than those of terrestrial workers because they are intended to prevent acute risks, while the annual dose limits of 50 mSv, which are followed by U.S. terrestrial radiation workers, control the accumulation of career doses. The exposures that are received by radiation workers in reactors, accelerators, hospitals, etc. rarely approach dose limits with the average annual exposure of 1 to 2 mSv, which is a factor of 25 below the annual exposure limit and significantly less than the average dose for a 6 month ISS mission (100 mSv). Similarly, transcontinental pilots, although they are not characterized as radiation workers in the U.S., receive an annual exposure of about 1 to 5 mSv, and enjoy long careers without approaching the exposure limits that are recommended for terrestrial workers in the U.S. Under these conditions, ground-based radiation workers are estimated to be well below the career limits. As space missions have been of relatively short duration in the past, thereby requiring minimal mitigation, the impact of dose limits when space programs actually approach such boundaries, has not been explored.

Whole body doses of 1 to 2 $\frac{mSv}{day}$ accumulate in interplanetary space, and approximately half of this value accumulates on planetary surfaces. Radiation shielding is an effective countermeasure for solar SPE, which are chiefly made up of protons with energies that are

largely below a few hundred MeV , with intermediate dose-rates $< 500 \frac{mSv}{hour}$. The energy spectrum of GCR peaks near $1,000 \frac{MeV}{nucleon}$; consequently, these particles are so penetrating that shielding can only partially reduce the doses that are absorbed by the crew. Thick shielding poses obvious mass problems to spacecraft launch systems, and would only reduce the GCR effective dose by no more than 25% using aluminum, or about 35% using more efficient polyethylene. Therefore, with the exception of SPE, which are effectively absorbed by shielding, current shielding approaches cannot be considered a solution for the space radiation problem. In traveling to Mars, every cell nucleus within an astronaut would be traversed by a proton or secondary electron every few days, and by an HZE ion every few months. The large ionization power of HZE ions makes them the major contributor to the risk, in spite of their lower cell nucleus hit frequency compared to protons.

1.5.3 Radiation attenuation strategies

A radiation exposure reduction is essential to enable a Lunar Outpost, a NEA or Mars mission. The attenuation measures can be managed by optimizing operational parameters such as:

- 1) Length of space missions
- 2) Crew selection for age and gender
- 3) Adequate radiation shielding application
- 4) Biological countermeasures (medicine) application

1.5.4 Radiation shielding approach

SPE shielding problems are readily solved by existing technologies, yet they require that optimization analysis to reduce mass and ensure other material requirements for spacecraft structures are satisfied. However, it is unlikely that there can be a technology solution to GCR risk from a shielding approach because of their high energies and limitations due to very high costs to launch large masses of shielding materials. In addition, active shielding devices require significant power sources or are exceptionally massive to achieve significant GCR risk reduction. Material selection and optimization of topology are major considerations for both GCR and SPE. Spacecraft volumes may be constrained when considering shielding retrofits or design augmentations, which further complicates shielding approaches. More importantly, the extra fuel required to launch such shielding compounds the mass dedicated to shielding. Also, a competition exists between shielding mass relative to other necessary resources or flight safety factors. Dual-use shielding approaches, such as water, fuel, and food stowage, are useful in this regard.³

The following pages analyze the radiation exposure dose in deep space flight for the three mission scenarios previously described by using the WW-based shielding technology within a theoretical water-wall radiation shielding architecture.

1.5.5 Shielding of SPE radiation

SPE occur about 5 to 10 times per year. Although the composition of the released energetic particle type varies slightly from event to event, on average these particles consist of 96% protons, 4% helium-ions, and a small fraction of heavier ions. The intensity and the energy

³ Evaluating Shielding Approaches to Reduce Space Radiation Cancer Risks

spectrum of an SPE vary throughout the course of the event, which lasts from a few hours to several days. The intensity of the event can be described by particle fluence, $F > E$, which is the number of ions per unit area with energy greater than E , expressed as $MeV/nucleon$. The energies of the protons are important because the range of penetration of these protons increases with energy. Protons with energies above $30 MeV$ have sufficient range to penetrate an EVA spacesuit, and are used as a simple scaling parameter to compare different SPE. However, each event has distinct temporal and energy characteristics. The majority of SPE are relatively harmless to human health, with doses below $10 mGy$ for minimal shielding protection; but the SPE that have the highest fluence of particle of energies above $30 MeV$ are a major concern for future missions outside the protection of the magnetic field of the Earth.

Figure 33 shows data that were collected in the modern era for the $F > 30 MeV$ proton fluence from large SPE and the solar modulation parameter Φ . The solar modulation parameter describes the strength of the Sun's magnetic field with solar maximum where $\Phi > 1,000 MV$. The various SPE shown in *Figure 33*, which are characterized as large SPE ($F_{>30 MeV} > 10^8 \frac{particles}{cm^2}$), would contribute doses of 10 to $500 mGy$ for average shielding conditions. Of the nearly 400 SPE observed in the space age since 1955, only 41 have $F_{>30 MeV} > 10^8 \frac{particles}{cm^2}$. The majority of SPE with $F_{>30 MeV}$ below this level lead to small doses ($< 0.01 Gy$) in tissue. Although the dose resulting from the majority of SPE is small, SPE nonetheless pose significant operational challenges because the eventual size of an event cannot be predicted until several hours after the particles are initially detected. Extraordinarily large SPE were recorded in November 1960, August 1972, and October 1989. In general, SPE occur more often near solar maximum, but the correlation between event frequency and solar conditions is not precise.

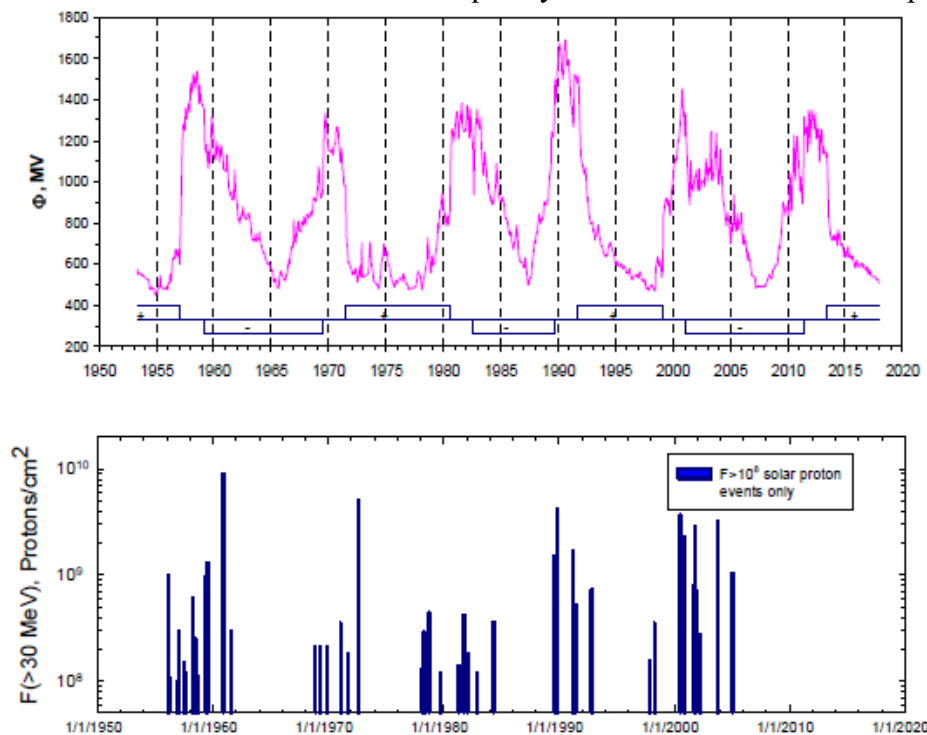


Figure 33 - Historical data on fluence of protons above 30 MeV per cm² from large SPE relative to solar modulation

In contrast to the constant presence of GCR in space, SPE exposures are sporadic and occur with little warning. Without sufficient shielding protection, a large SPE may result in a whole-body dose of over 0.5 Gy received over a period of several hours. Humans who are exposed to γ -rays or X-rays at doses ≥ 0.5 Gy are known to experience Acute Radiation Syndromes (ARS). ARS can be classified clinically as hematopoietic syndrome, gastrointestinal syndrome and neurovascular syndrome. Based on the time of appearance, ARS can be divided into:

- III. Prodromal phase (0 – 24 hours)
- IV. Latent phase
- V. Manifest illness phase
- VI. Recovery phase.

The most probable ARS effects from SPE exposure in space flight that can potentially affect mission success include prodromal effects (nausea, vomiting, anorexia, and fatigue), skin injury, and depletion of the Blood-Forming Organs (BFO), possibly leading to death. Shielding is an effective countermeasure to SPE inside spacecraft, making ARS extremely unlikely except in EVA or combined EVA and intravehicular activity scenarios. The operational impacts of ARS on space flight crew members could affect crew performance and lead to the possibility of mission failure.

Dose limits for deterministic effects, which are given in units of Gray-equivalent (Gy-Eq), are listed in *Table 28*. The unit of Gray-equivalent is distinct from the unit of Sievert that is used to project cancer risk because distinct radiation quality functions occur for ARS and cancer. The Gray-equivalent is calculated using the RBE values that are described in NCRP Report No. 132, Sievert instead by using the LET-dependent radiation quality function.

Organ	Dose limits [mGy-eq]		
	30-d limit	1-yr limit	Career
Lens	1,000	2,000	4,000
Skin	1,500	3,000	6,000
BFO	250	500	N.A.
Heart	250	500	1,000
CNS	500	1,000	1,500

Table 28 - Dose Limits for non-cancer radiation effects

ARS appears in various forms and has different threshold onset doses for the possible effects. The threshold whole-body dose for ARS is about 0.1 to 0.2 Gy for radiation that is delivered under acute conditions where dose-rates are more than $1 \frac{\text{Gy}}{\text{hr}}$ occur. Doses that are in the range of 0.5 to 1 Gy cause minor acute damage to the hemopoietic system and mild prodromal effects (nausea, vomiting, anorexia, and fatigue) in a small number of irradiated persons. In the dose range of 1 to 2 Gy acute, prodromal effects and injury to the hemopoietic system increase significantly. Most victims will probably survive, however, with only 5% lethality in a population after doses of about 2 Gy. Survival is possible within the dose range of 2 to 3.5 Gy; As the dose reaches about 3.25 Gy, 50% may die within 60 days if appropriate medical care is not administered. From 3.5 to 5.5 Gy, symptoms are more severe, affecting nearly all who are exposed. If untreated, 50% to 99% of those who are affected may die primarily. Survival is almost impossible to doses ≥ 5.5 Gy.

Figure 34 shows the energy spectra of the January 2005 SPE, which is one of the most recent large events. At that time, there was a sudden increase in proton flux, especially in particles with energies that were greater than 50 MeV. Protons with energies greater than 100 MeV increased by as much as four orders of magnitude after they declined following the major pulse.

A detailed temporal analysis of dose-rate and cumulative dose equivalent for the August 1972 King SPE is illustrated in Figure 35. This event, which was one of the largest SPE in the modern era, had the highest dose-rate at its peak. The temporal behavior suggests that significant biological damage would occur in a crew if adequate shielding is not provided.

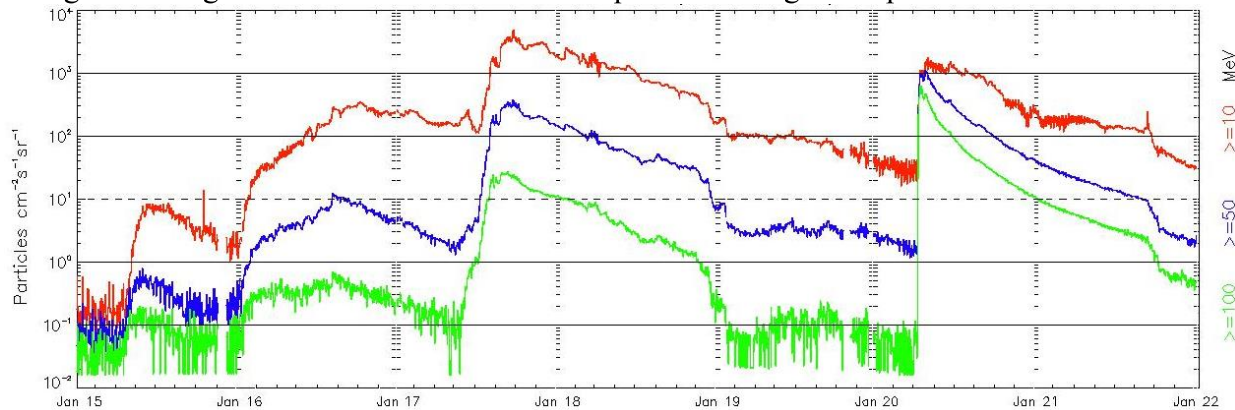


Figure 14 - Proton flux measured during January 2005 SPE by GOES 11 satellite⁴

To avoid placing unrealistic mass on a space vehicle while at the same time increasing safety factors for the astronauts, one solution for shielding against SPE would be to select optimal materials for the vehicle structure and shielding. To this end it has been shown that materials that have lower atomic mass constituents have better shielding effectiveness. Overall exposure levels from this specific event have been estimated to be greater than 100 mSv (10 rem) at sensitive sites. Those from other large SPE that have been recorded in the modern era can be reduced to below 0.1 Sv when heavily shielded “storm shelters” are added to a typical spacecraft. Optimizing mass through material selection and topological considerations are the focus for SPE shields. Because SPE last only several hours at the peak exposure rates, localized shielding approaches using crew sleep quarters as storm shelters are considered to be sufficient for SPE protection. FO-CTBs could be used as portable shielding blankets both on orbit and on moon surface, filled in-situ for the SPE occasion. A personal radiation safety haven made of FO-CTBs is described later.

Such a localized shielding strategy requires an effective operational procedure with an SPE warning or alert system. This system does not exist at the current time, and near-term forecasts estimating the probability of an event within the next few hours to days are limited. New capabilities for deep-space mission forecasting will be needed prior to a NEA or Mars mission because the alignment of the Earth and Asteroids or Mars does not allow all SPE on non-Earth orbits to be observed from Earth (as explained in SPE chapter).

⁴ National Oceanic and Atmospheric Administration

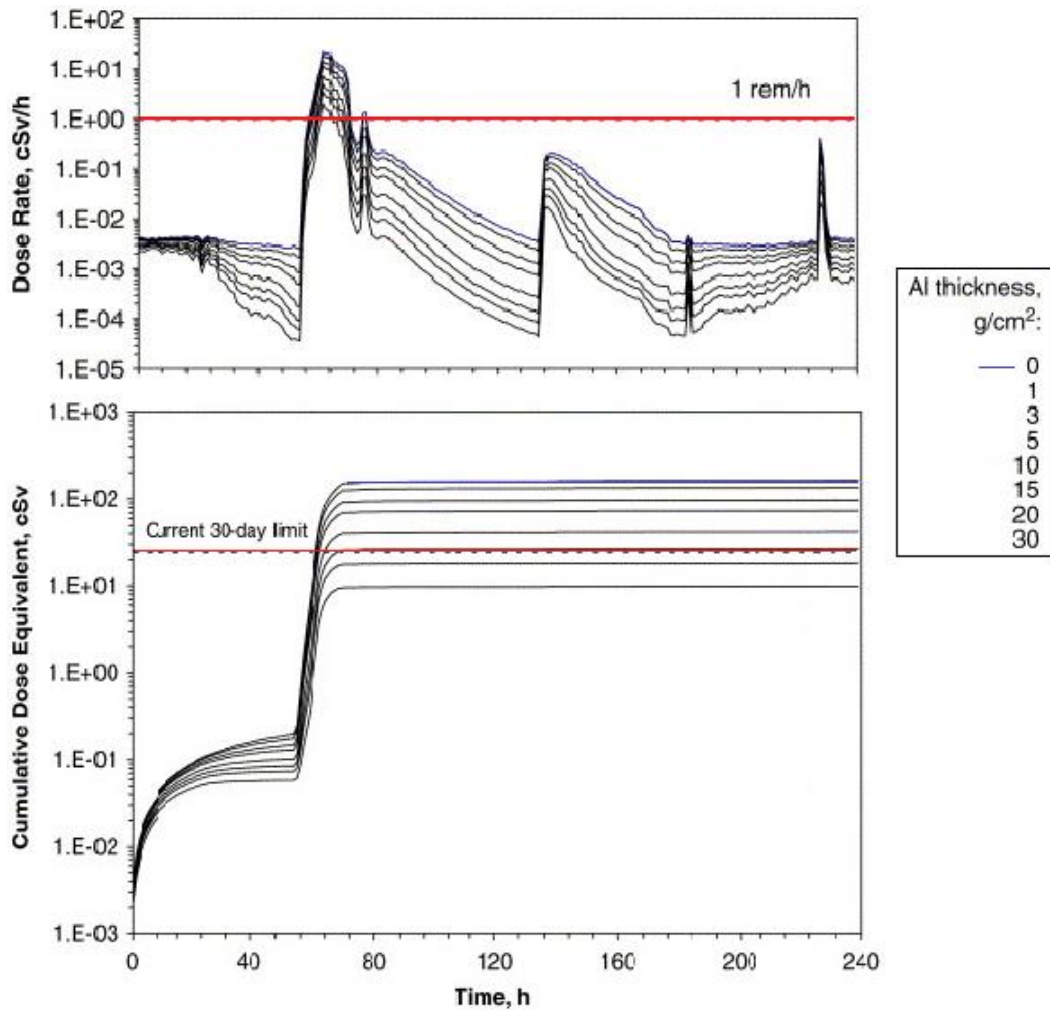


Figure 35 - Dose rate and cumulative dose rate during August 1972 SPE⁵

Nowcasting is another tool attempting to forecast the energy spectrum and time evolution of the expected flux based on currently measured conditions. Its technology is based on the fact that the light-weight electrons in SPE can travel at a speed close to that of light, so can deliver an earlier warning signal of the imminent arrival of its bulk protons. Detection of relativistic solar electrons may enable as much as a 1 *hour* warning of SPE proton events, as well as prediction of the integral number of protons that can be expected. *Figure 36* shows the distribution of 31 to 50 *MeV* proton onset delays over relativistic electrons. The histogram uses 48 SEP events from 1996 to 2002 with their observed delay times. The distribution appears to have two peaks, the early one is found at a delay of 20 to 30 *min*, whereas another shallow peak is observed at about 1 *hour* delay. Connection longitude information is also shown, with well-connected events with longitude distances between flare and observer of up to 30 *degrees* shown in the red fraction of the histogram. Well-connected events have proton delays of approximately

⁵ Mean occurrence frequency and temporal risk analysis of solar particle events, Kim, Cucinotta and Wilson, 2006

1 hour. On the other hand, not well connected events can also have relatively short proton delays.

With these tools and an appropriate communication asset with various space weather satellites, astronauts will have sufficient forewarning to go to a radiation safe havens for sheltering from SPE ions. At last, *Figure 37* displays radiation dose reduction as a function of area density of equivalent aluminum shielding calculated in the Crew Exploration Vehicle radiation analysis. The assumed SPE situation is the August 1972 King SPE. The plot corresponds to a simplified analysis where aluminum shielding is distributed around a human model.

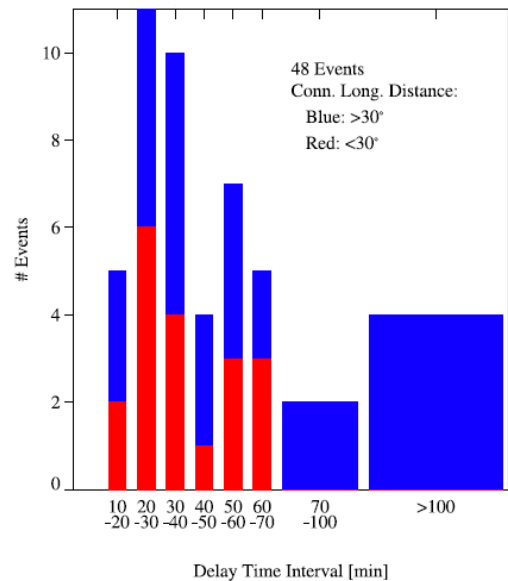


Figure 36- Delay time of 31-50 MeV protons over relativistic electrons during 48 SPE⁶

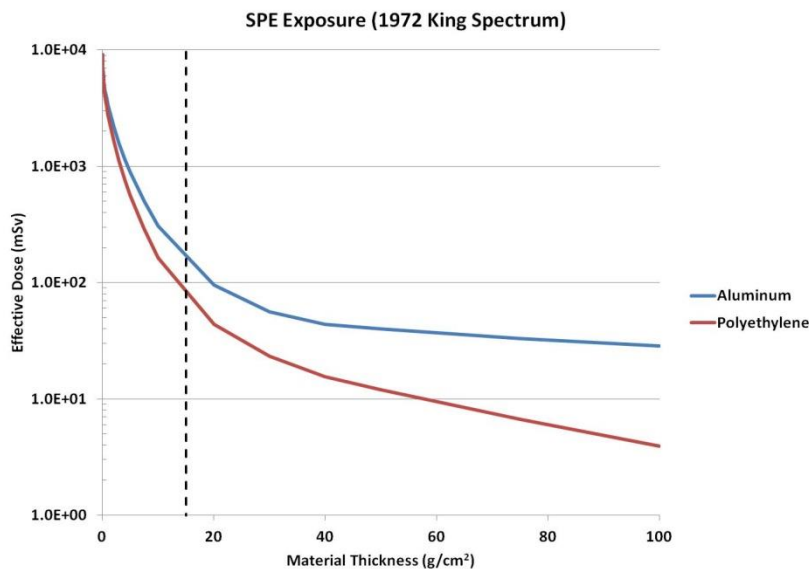


Figure 37 -Effective dose depth curve for aluminum and polyethylene shields⁷

⁶ Up to 1-hour forecasting of radiation hazards from solar energetic ion events, Posner, 2007

⁷ Space Radiation Protection, Space Weather and Exploration, Lee et al., 2012

1.5.6 Shielding of GCR in deep space

The high energies associated with the GCR are distinct in that the energy absorbed in astronaut tissues is at best unchanged by typical spacecraft shielding configurations and use of some materials in spacecraft construction will even increase the energy absorption by the astronaut. For GCR, one must abandon the concept of "absorbing" the radiation by use of shielding. The protection of the astronaut in this case is not directly related to energy absorption within their body tissues but rather depends on the mechanism by which each particle type transmitted through the shield results in biological injury. Even though the energy absorption by the astronaut can be little affected, the mixture of particle types is strongly affected by the choice of the intervening shield material. Knowledge of the specific biological action of the specific mixture of particles behind a given shield material and the modification of that mixture by choice of shield materials is then a critical issue in protecting the astronaut in future human exploration.

The GCRs of interest have charge number $1 \leq Z \leq 28$ and energy from less than $1 \frac{\text{MeV}}{\text{nucleon}}$ to more than $10 \frac{\text{GeV}}{\text{nucleon}}$ with a median energy of about $1 \frac{\text{GeV}}{\text{nucleon}}$. The GCRs with energies less than about $2 \frac{\text{GeV}}{\text{nucleon}}$ are modulated by the 11 year solar cycle, with more than twice higher GCR flux at solar minimum when the solar wind is weakest compared to the flux at solar maximum. The most recent solar minimum was in 2008-2009, and the next one will occur in 2019-2020.

Materials with the smallest mean atomic mass are usually the most efficient shields for both SPE and GCR. The composition of the radiation field changes as particles lose energy and suffer nuclear interactions in traversing structural materials, instruments, and the tissues of astronauts. Both the energy loss and the changes in particle fluence are related to the number of atoms per unit mass in the traversed material, which, in turn, is proportional to Avogadro's number divided by the atomic mass number, A , for each element of the material. The energy loss by ionization of a single component of shielding material with atomic number Z is proportional to the number of electrons per atom and thus proportional to Z/A . However, the energy lost per gram of material and per incident fluence (e.g., in units of $\frac{\text{particles}}{\text{cm}^2}$), the "mass stopping power," is also inversely proportional to the density ρ (e.g., in $\frac{\text{g}}{\text{cm}^3}$) of the material, so that the energy lost by one incident particle per cm^2 per unit mass is proportional to $\frac{Z}{\rho A}$.

The number of nuclear interactions per unit mass and per unit incident fluence is proportional to $\frac{\sigma}{A}$, where σ is the total nuclear reaction cross section. To a first approximation, σ is proportional to $A^{2/3}$, so that the nuclear transmission is proportional to $\frac{1}{A^{1/3}}$.

The ratio of electronic stopping power to nuclear interaction transmission is therefore proportional to $\frac{Z}{\rho A^{2/3}}$. Materials with small atomic mass have the highest number of electrons per nucleon (e.g., Z/A is 1 for hydrogen, 0.5 for carbon, 0.48 for aluminum, 0.46 for iron, and 0.40 for lead). Light mass materials have smaller nuclei and therefore more of them can fit into a given mass so that there can be more nuclear interactions. Furthermore, the ratio of ionization energy loss to nuclear interactions is also dependent on the material density. For liquid hydrogen ($\rho = 0.07 \frac{\text{g}}{\text{cm}^3}$), the ratio is approximately 14, whereas for aluminum ($\rho = 2.7 \frac{\text{g}}{\text{cm}^3}$) the ratio is only 0.5, and for lead ($\rho = 11.3 \frac{\text{g}}{\text{cm}^3}$) the ratio is 0.2. Thus, an electron plasma would provide the best shield from GCRs. A shield made of liquid hydrogen, which has the highest ratio of electrons to nuclei per atom and produce minimal secondary radiation (e.g., mesons), is the

second-best choice (*with respect to the electron plasma*). Hence, interest grows in polyethylene and hydrogen embedded nanofibers. The character of particle interactions and the secondary nuclei produced through both projectile and target fragmentation is important in shielding considerations. Lighter nuclei have fewer neutrons to release and some nuclei (e.g., carbon) can break into three Helium nuclei without releasing any neutrons. In tissue, the release of three helium atoms is much more biologically damaging than that of neutrons; however, if produced within spacecraft shielding materials, neutrons are a higher concern because of their longer ranges than slow helium particles. For very thick shields, lighter nuclei are also more effective in shielding against the built-up neutrons. For these and related reasons, detailed knowledge of the actual composition of the radiation fields (and of the biological consequences of exposure to them) is required to evaluate the net effect of shielding materials.

In terms of dose equivalent for a shield of thickness x , $H(x)$, we find that aluminum structures attenuate radiation effects over most of the range of depths used in human rated vehicles (2 to 10 $\frac{g}{cm^2}$) as shown in *Figure 38*. Thus, dose equivalent reduction may be a misleading indicator of astronaut safety. In contrast, track structure models show markedly different attenuation characteristics and, in fact, show that cell transformation, $T(x)$, is more likely to result by increasing the aluminum shielding in spite of the decreasing dose equivalent.

As a further example of the issues we face, the dose equivalent behind three shield materials is shown in *Table 29* for an annual GCR exposure at 1977-solar minimum. The first shield is aluminum, typical of many constructions including ISS. The 1.5148 $\frac{g}{cm^2}$ thickness is that of the JSC TransHab wall design for a combination of polymers and fillers. The 5 $\frac{g}{cm^2}$ thickness is typical for an area within a human-occupied vehicle loaded with equipment. The value in parenthesis is the performance index, which is the ratio of dose equivalent in Al to dose equivalent in another material M

$$P_H(x) = \frac{H_{Al}(x)}{H_M(x)}$$

and represents the performance advantage of the given material compared to aluminum. A similar performance metric for Harderian gland tumor induction, $HG_M(x)$, is shown in the second column. If unshielded, the dose equivalent would be 120 cSv and the excess tumor risk would be the 2.23%. Polyethylene is 16% more effective than aluminum in controlling dose equivalent with only 1.5148 $\frac{g}{cm^2}$ of material and a larger gain is achieved at 5 $\frac{g}{cm^2}$ thickness. On the other hand, a substantial increase in Harderian tumor risk, $HG(x)$, is found for both thicknesses of aluminum while a very light improvement results only for the 5 $\frac{g}{cm^2}$ polyethylene shield.

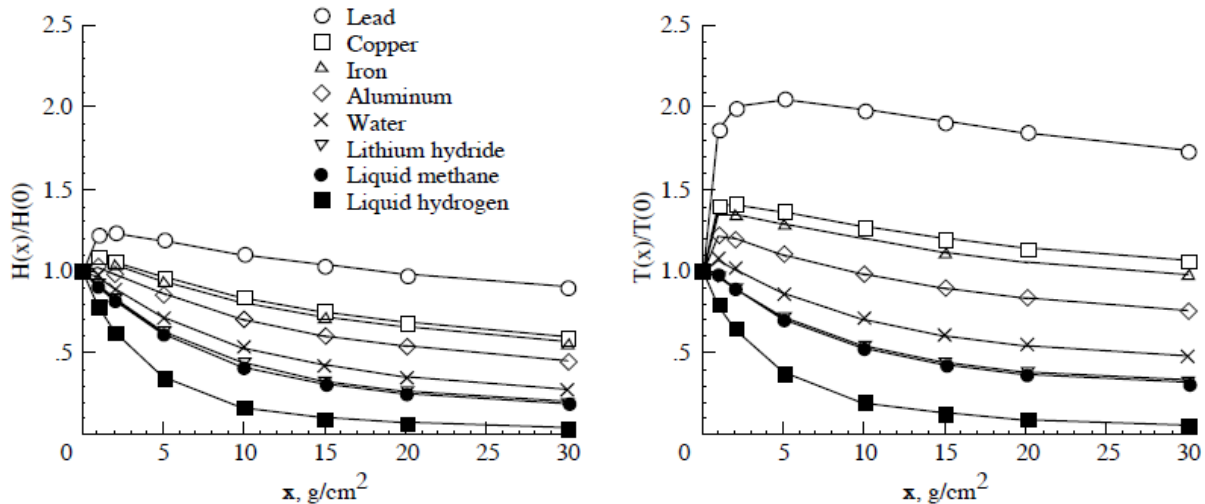


Figure 38 - Attenuation of dose equivalent and cell transformation for a 1-year GCR exposure at solar minimum behind various shield materials⁸

Shield		Dose equivalent [cSv]	Excess tumor risk [%]
Unshielded		120	2.23
1.514 g/cm ²	Aluminum	130.9(1.00)	3.57(1.00)
	TransHab	121.6(1.08)	3.07(1.16)
	Polyethylene	113.1(1.16)	2.64(1.35)
5 g/cm ²	Aluminum	113.9(1.00)	3.37(1.00)
	TransHab	99.4(1.15)	2.74(1.24)
	Polyethylene	86.4(1.32)	2.20(1.54)

Table 29 - Annual GCR exposure behind various shields at 1997 solar minimum⁹

Energy loss by cosmic rays is through ionization and excitation of target atoms in the shielding material or tissue. The ionization of atoms leads to the liberation of electrons that often have sufficient energy to cause further excitations and ionizations of nearby target atoms. These electrons are called δ -rays and can have energies $\geq 1 \text{ MeV}$ for ions with $E > 1 \frac{\text{GeV}}{\text{nucleon}}$. For HZE particles, about 80% of a particle's LET are due to ionizations leading to δ -rays. The number of δ -rays created is proportional to $\frac{Z^{*2}}{\beta^2}$, where Z^* is the effective charge number that adjusts Z by atomic screening effects important at low E and high Z . The lateral spread of δ -rays is the track-width of the particle and dependent on β but not Z , being determined by kinematics. At $1 \frac{\text{MeV}}{\text{nucleon}}$, the track-width is $\sim 0.1 \mu\text{m}$ and at $1 \frac{\text{GeV}}{\text{nucleon}}$ the track-width is $\sim 1 \text{ cm}$. A phenomenological approach to describing atomic ionization and excitation is to introduce an empirical model of energy deposition. To apply the model, some definition of a characteristic target volume is needed. A diverse choice of volumes are used in radiobiology, including ones

⁸ Approach and issues relating to shield material design to protect astronauts from space radiation, Wilson, 2001

⁹ Materials for shielding astronauts from the hazards of space radiation, Wilson et al., 1997

with diameters $< 0.01 \mu m$ to represent short DNA segments, and of diameters from a few to $\sim 10 \mu m$ to represent cell nuclei or cells. Energy deposition is the sum of the energy transfer events due to ionizations and excitations in the volume, including those from δ -rays. For large target volumes, energy deposition and energy loss (LET) become approximately the same. Two particles with different Z and identical LET will have different values for E and therefore different track-widths.

The particle with lower Z will have a narrower track-width and more localized energy deposition and, in many experiments, has been shown to have a higher biological effectiveness than a particle with higher Z . However, in tissue, the higher Z nuclei often have a larger range and can traverse more cell layers than a lower Z nuclei at the same LET.

The biological effects of different types of particles are usually compared using the ratio of doses that lead to an identical effect. This ratio is the RBE factor. Human data for low LET radiation such as γ -ray or X-ray exposures leading to increased cancer risk has been studied in the survivors of the atomic-bombs in Japan during World War II, medical patients exposed therapeutically to radiation, and nuclear reactor workers. However, there is no human data for high LET radiation such as cosmic rays to make risk estimates. Therefore, RBEs where the dose in the numerator is that of γ -rays and the dose in the denominator of a nuclear particle being studied, is often used to compare results from biological experiments with nuclei created at particle accelerators to results of epidemiological studies in humans exposed to γ -rays or X-rays.

RBE's vary widely with the biological endpoint, cell or animal system, type of radiation and doses used in experiments. Traditionally, it has been the role of advisory panels to make a subjective judgment of available RBE data to make estimates for human risk. Such judgment is used to define a radiation quality factor. For terrestrial radiation exposures, quality factors Q have been defined uniquely by LET, $Q(LET)$. Values of Q from 1 to 30 have been used in the past for different LET values with $Q = 1$ below $10 \frac{keV}{\mu m}$ and $Q = 30$ at $100 \frac{keV}{\mu m}$ used at this time. However, for the more complex radiation environments in space, the inaccuracy of LET as a descriptor of biological effects has been a long-standing concern. In the NASA 2010 model, radiation quality factors are redefined to have a dependence on two particle physical parameters, E and Z , rather than LET alone. As particles penetrate through shielding materials or tissue and lose energy or undergo nuclear interactions, they produce secondary particles that then can have higher or lower quality factors than the primary particle.

Figure 39 illustrates this situation where the NASA radiation quality factor for solid cancer is plotted for different Z and E . Two examples that illustrate the complexity of the problem can be considered. First, if an Fe particle with energy above $800 \frac{MeV}{nucleon}$ loses energy its Q -value will increase. Thus, shielding has made the situation worse. However, if the starting energy of Fe is below about $500 \frac{MeV}{nucleon}$, the shielding material can lower the cancer risk. A second example is for a fragmentation event of an Fe particle. When an Fe particle fragments, new particles of lower Z and E are produced that could be more biologically effective than the primary particle. Also, high energy neutrons, protons, and other light particles are produced in the same fragmentation event, thereby increasing the number of nuclear particles in the radiation field. For this reason, the understanding of the effectiveness of shielding materials and amounts is incomplete until the radiation quality factors and particle flux spectra are accurately defined.

The multiplication of the absorbed dose by the quality factor is referred to as the dose equivalent, $H = Q(LET)D$, in units of Sv . For calculating cancer risks, radiation transport codes are used to describe the atomic and nuclear collisions that occur inside spacecraft shielding and

tissue, and resulting particle spectra averaged over the tissues of concern for cancer risk (e.g., lung, stomach, colon, bone marrow, etc.) to describe the organ dose equivalent, H_T .

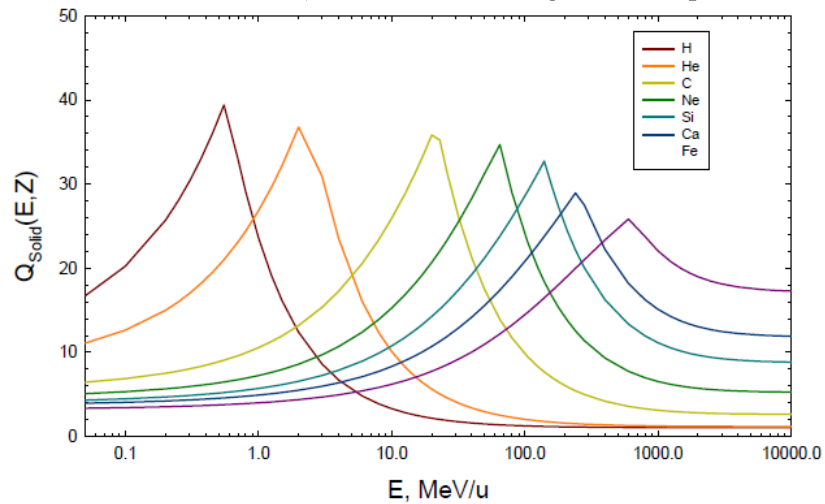


Figure 39 - Dependence of the NASA radiation quality factor on particle kinetic energy for several GCR particles

Nuclear collisions within the shielding material lead to heavy ion fragmentations, two models of which are shown in *Figure 40*. Low energy evaporation products including heavy ion target fragments are high LET events. Knockout products from proton or neutron reactions and projectile fragments from GCR nuclei are typically of low to moderate LET; however, their large ranges lead to radiation buildup through further reactions.

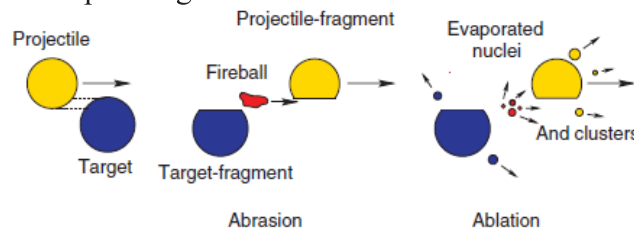


Figure 40 - Abrasion-ablation model¹⁰

Nuclear plastic track detectors were used for fragmentation cross-section measurements directly from projectile interactions with target atoms. The NASA Space Radiation Laboratory (NSRL) made extensive ground-based measurements of the Bragg ionization curve for several defined beams of HZE nuclei in thin and thick polyethylene or aluminum shielding targets and compared them with a recently developed Monte Carlo based transport code, the GCR event-based risk model (GERMCODE). An excellent agreement between the code and the NSRL experimental measurements is seen at all depths in *Figure 41* for ^{28}Si , ^{37}Cl , ^{48}Ti , and nuclei.

¹⁰ New Journal of Physics, Gunzert-Marx et al., 2008

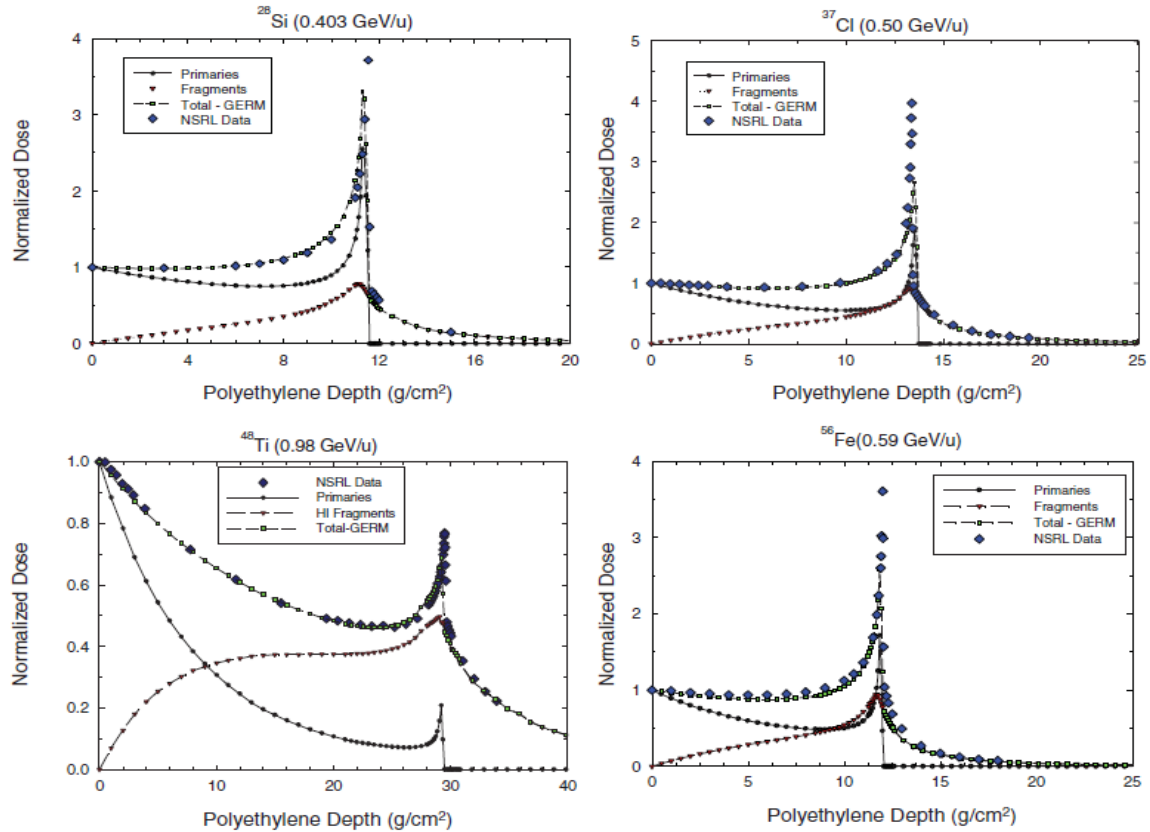


Figure 41 - Comparisons of the GERM CODE to NSRL measurements for depth dose for ^{56}Fe , ^{48}Ti , ^{37}Cl , ^{28}Si nuclei¹¹

Estimation of total radiation dose in deep-space missions

For estimating radiation doses in a typical spacecraft, an equivalent aluminum areal density is assumed. Areal densities of existing spacecraft are listed in *Table 30*.

Spacecraft	Areal Density (g/cm ²) <i>Aluminum-equivalent</i>
Apollo Command Module	2.5
Space Shuttle (STS-66 cargo bay)	15
ISS US Lab	10
ISS (average)	5.26
Skylab crew sleep compartment	1.6
Space suit	1.22

Table 30 - Areal densities in typical spacecraft

An areal density of $5.26 \frac{\text{g}}{\text{cm}^2}$ of aluminum equivalent is assumed and used by NASA in many radiation shielding tests because this value is the average areal density available as a combined aluminum hull plus all consumables and internal components within the Space Shuttle and the ISS.

¹¹ Nuclear interactions in heavy ion transport and event-based risk models, Cucinotta and Plante, 2011

As emerged in the previous chapters, a thin or moderate shielding is generally efficient in reducing the equivalent dose but, as the thickness increases, shield effectiveness drops. This is the result of the production of a large number of secondary particles, including neutrons that are caused by nuclear interactions of the GCR within the shield. These particles have generally lower energy, but they can have higher quality factors than incident cosmic primary particle. Radiation shielding effectiveness depends on the atomic constituents of the material that is used. Shielding effectiveness per unit mass, which is the highest for hydrogen, decreases with increasing atomic number. In contrast to the highly penetrating GCR, radiation from SPE can be effectively reduced, as shown in *Figure 42* where dose equivalent under increasing shielding depth for both solar minimum GCR and August 1972 SPE is presented for a variety of shielding materials calculated by NASA's HZETRN/BRYNTRN codes. For hydrogen shielding, the GCR effective dose is larger than the point dose because target fragments in tissue contribute about 50% of the effective dose, even though very little secondary radiation is produced directly in the hydrogen shield. Clearly, calculations or measurements of point dose equivalents misrepresent the effectiveness of shielding because of the role of secondary radiation produced in tissue.

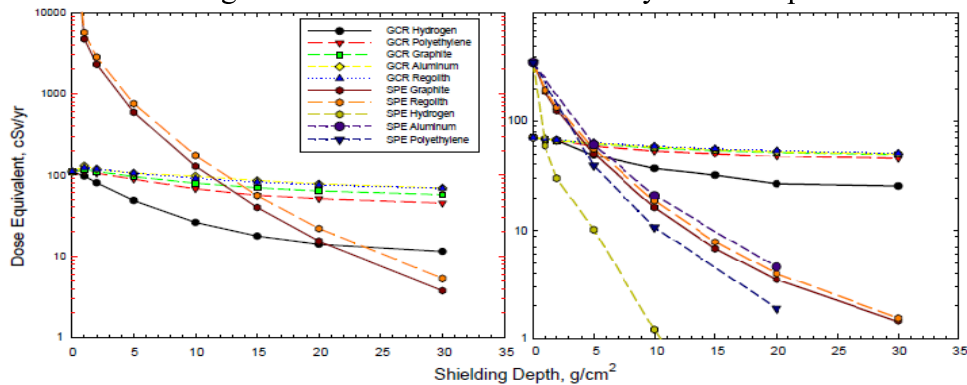


Figure 42 - Comparison between GCR and SPE dose equivalent for different materials' depths¹²

A lot of disaccording data was found in the literature related to the same space events, particularly for the doses measured during the 1972 King SPE and during the 1977 solar minimum. Sometimes such disaccording data are due both to experimental errors, to different quality factors and to different boundaries used within NASA's and ICRP's code models, as showed in *Figure 43*. The values taken in consideration during the next estimates and calculations are based on their frequency of comparison in the literature. Their reliability was verified comparing them to the distribution of experimental data available from the history of spaceflights, such as data collected in *Table 31* and *Figure 44*. *Table 31* shows the average and individual effective dose-rates, respectively, for all astronauts from all NASA Missions (through 2004). These results use records of passive dosimetry worn on all NASA missions, and estimates of tissue absorption and average quality factors from flight spectrometers and radiation transport codes. Also *Figure 44* shows effective dose -rates recorded from 1965 to 2004 for all NASA missions. Dose-rates increase at higher altitudes are due to longer sampling of the Earth's trapped radiation belts, with the highest dose-rate occurring on the Hubble telescope launching and repair missions with altitudes near 600 km. Average quality factors range from about 1.6 to 3.5 with the highest values occurring for GCR dominated missions such as the Apollo missions.

¹² Evaluating Shielding Effectiveness for Reducing Space Radiation Cancer Risks, Cucinotta et al., 2006

For the deep space Apollo missions, the GCR dominated astronaut doses with a small contribution from the trapped belts. The International Space Station (ISS) and Mir missions were in a 51.6 *degree* inclination with altitudes ranging from about 340 to 400 km have led to effective dose-rates will range from 0.4 to about 1 *mSv/day*. Organ dose equivalents are made-up of more than 80% contributions from GCR for most missions. US participation on the Mir missions occurred near solar minimum, while ISS Expeditions 1-10 are at or near solar maximum resulting in a lower dose-rate.

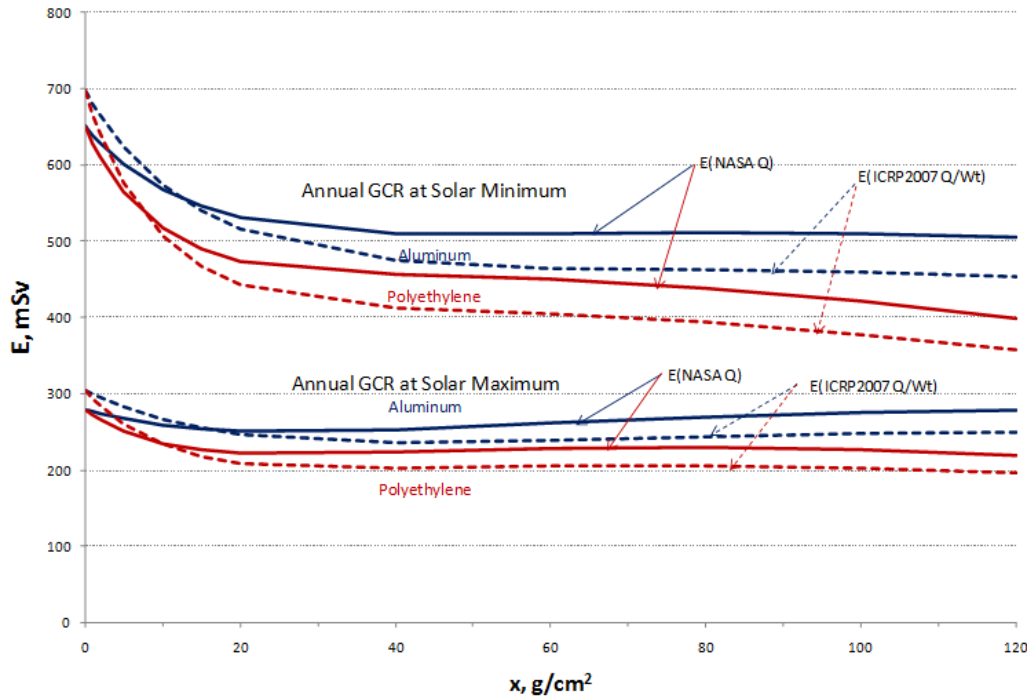


Figure 43 - Effective dose for male behind shielding¹³

NASA program	# crew	D [mGy]	E [mSv]	D-rate [mGy/d]	E-rate [mSv/d]
Mercury	6	0.1	0.15	0.3	0.55
Gemini	20	1.3	2.2	0.49	0.87
Apollo	33	4.1	12	0.43	1.2
Skylab (50°, 430km)	9	40.3	95	0.71	1.4
STS (28.5°, >400 km)	85	9.5	17	1.2	2.1
STS (28.5°, < 400 km)	207	0.9	1.6	0.1	0.18
STS (40°)	57	1.1	2.4	0.1	0.21
STS (>50°, >400 km)	10	2.2	5.2	0.44	1.1
STS (>50°, <400 km)	190	1.7	3.8	0.2	0.45
Mir (51.6°, 360km)	6	50.3	115	0.37	0.84
ISS (51.6°, 380km)	13	26	68	0.16	0.4

¹³ What's New in Space Radiation Research for Exploration?, Cucinotta, 2011

Table 31 - Average dose and dose-rate recorded by dosimetry badge and estimates of the effective doses received by crews in NASA programs through 2004¹⁴

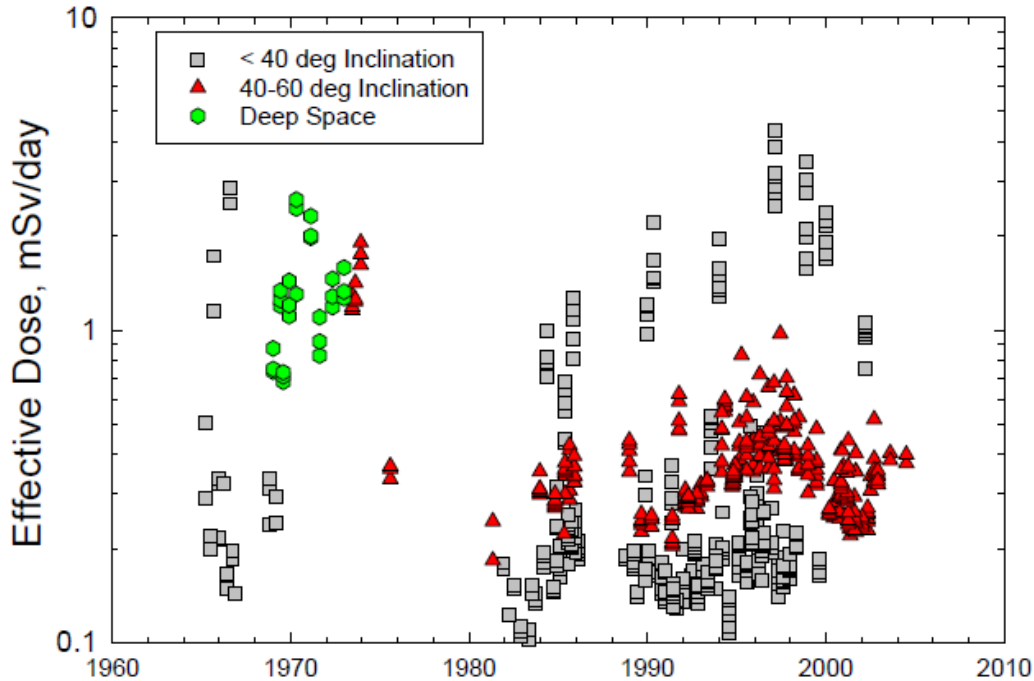


Figure 44 - Effective dose-rates recorded from 1965 to 2004 for all NASA missions¹⁵

The worst cases for both GCR and SPE exposures were considered simultaneously in the following calculations even if it's nearly impossible that such a condition of space weather would ever occur because maximum GCR intensity is associated with solar minima while SPE happen by definition within solar maxima. Anyway, conservative estimates were made for both deep space flight scenarios and for LEO missions at the ISS 's altitude.

In deep space, an annual GCR dose equivalent of 1200 *mSv* related to the 1977 solar minimum is assumed in the unshielded case, while a dose of 1139 *mSv* has been measured for a $5 \frac{g}{cm^2}$ aluminum equivalent shield. A total SPE exposure dosage of 1200 *mSv* in the unshielded case and of 885 *mSv* with a $5 \frac{g}{cm^2}$ Al equivalent shield was assumed corresponding to year 1972, during which occurred the King SPE. GCR and SPE exposure doses corresponding to different flight durations were proportionally calculated. The radiation doses for a single crossing through the Van Allen Belts are estimates as follows:

- 5.7 *mSv* dose equivalent from protons
- 0.047 *mSv* dose equivalent from electrons.

Two crossings through the belts are assumed for the considered missions and the total dose for different flight duration is considered constant.

The estimates of radiation exposure doses from GCR, SPE, trapped-ion radiation, and total radiation in deep space for the three considered mission scenarios are shown in *Plot 45*. Although the total radiation dose is below the 30 *days* allowance limit of 250 *mSv*, the annual radiation dose will be exceeded after about 88 days of deep space flight. Obviously, the current shielding technology is not adequate for a Lunar, NEA or Mars mission.

¹⁴ Space Radiation Organ Doses for Astronauts on Past and Future Missions, Cucinotta, 2007

¹⁵ Space Radiation Organ Doses for Astronauts on Past and Future Missions, Cucinotta, 2007

In LEO, an annual GCR dose equivalent of 650 mSv related to the 1977 solar minimum is assumed in the unshielded case, while a dose of 650 mSv has been measured for a $5\frac{\text{g}}{\text{cm}^2}$ aluminum equivalent shield. A total SPE exposure dosage of 3300 mSv in the unshielded case and of 610 mSv with a $5\frac{\text{g}}{\text{cm}^2}$ Al equivalent shield was assumed corresponding to year 1972, during which occurred the King SPE. GCR and SPE exposure doses corresponding to different flight durations were proportionally calculated. Crossings through the Van Allen Belts do not occur. The estimates of radiation exposure doses from GCR, SPE, and total radiation in LEO for different spaceflight durations are shown in *Plot 46*. Although the total radiation dose is below the 30 days allowance limit of 250 mSv , the annual radiation dose would be exceeded after about 151 days of space flight, which is less than the average 180 days period of duration of a mission onboard the ISS.

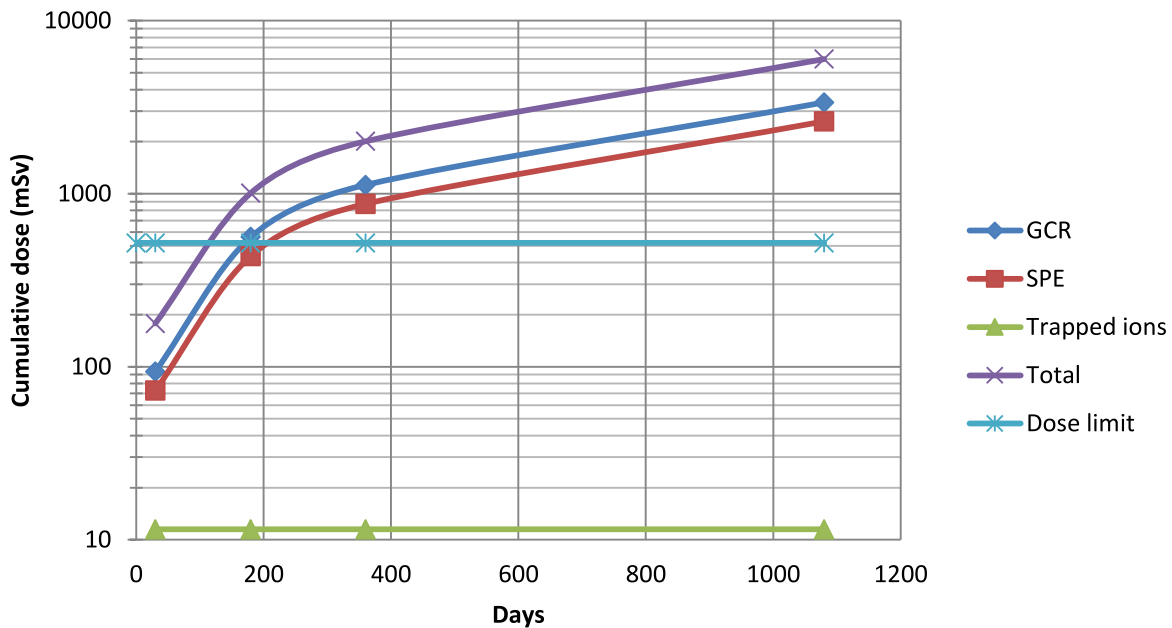


Figure 45 - Cumulative doses in deep space for 5 g/cm^2 Al-*eq* case

Estimation of Astronaut Radiation Exposure Doses onboard the ISS with Radiation Safety Haven Made of personal Water Wall Radiation Shield

Let's consider a conventional mission onboard the ISS during which a large SPE similar to the 1972 King SPE happens. The crew would have about half an hour to reach and build a safe haven thanks to the new forecast technologies explained before. The realization of personal elliptic-cylindrical (with an oval section that adapts to the shape of a human body) shelters could be obtained by joining together six FO-CTBs per person for minimal protection or twelve FO-CTBs per person for a double layer-augmented protection, after having completely filled all of them with water taken from the onboard hygiene water reserve. Each FO-CTB should be nominally filled with 22 L of water and so the astronaut could stay within an about 3.5 cm shelter in the first case or within a 7 cm shelter in the second case. The minimum number of unfolded FO-CTBs needed to completely cover a human body, considering the ergonomic factors of a 95th percentile American man, who is 1860 mm tall and whose top maximum section is 318 * 592 mm, is six. As showed in the following Solidworks model, two series of

three unfolded FO-CTBs joined one to the other along their long edges are connected together to form a big rectangular blanket which will be bent by the astronaut to form a cylinder with elliptical base similar to a camping sleeping bag. The astronaut is then supposed to stay within this haven for all the duration of the SPE.

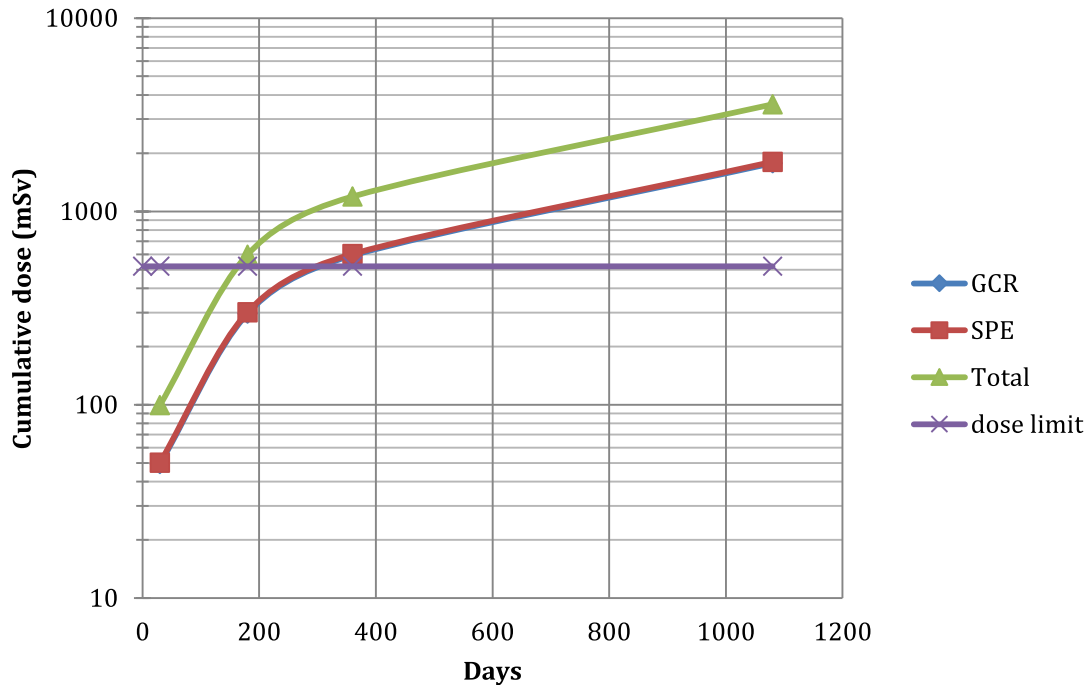


Figure 46 - Cumulative doses in LEO for 5 g/cm² Al-*eq* case

Dose reduction to GCR exposure is expected to be negligible for both a 3.5 and a 7 cm water-wall, while the capability against SPE dose absorption should be more effective. An average areal density 5 $\frac{g}{cm^2}$ of aluminum equivalent is available onboard the ISS as a combined aluminum hull plus all consumables and internal components.

The GCR radiation attenuation is calculated using the following formula, proved during tests performed at Lawrence Berkeley National Labs, where beams of 1 $\frac{GeV}{nucleon}$ ^{56}Fe were used as representatives of the heavy ion component of the GCR. A wide variety of targets were placed in the particle beams, and the spectra of particles emerging from the targets were measured using a stack of silicon detectors. Results are presented primarily in terms of dose reduction per $\frac{g}{cm^2}$ of target material, and support the conclusions that performance improves as the shield's mass number decreases, with hydrogen being by far the most effective. The data also show that, as depth increases, the incremental benefit of adding shielding decreases, particularly for aluminum and other elements with higher atomic mass numbers.

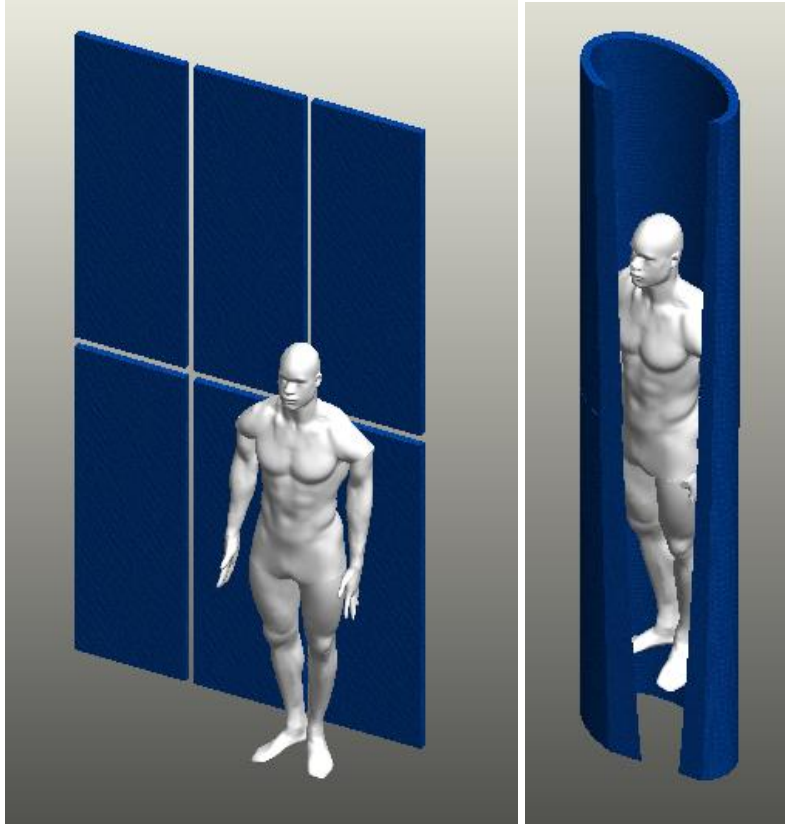


Figure 47 – Personnel radiation protection formed from 6 CTBs

The relationship between dose reduction and the depth of heavy ion radiation passage is:

$$\delta D_n = a e^{-bx}$$

where $\delta D_n = \frac{\delta D}{x}$ is the normalized dose reduction, δD is the dose reduction, a and b are constants characteristic of shielding material and x is its thickness.

Since water has a very similar molecular structure to the polyethylene monomer, the a and b constants are approximately equal and their values are defined in *Table 31*.

Material	a	b
Al	0.0234	0.0235
H2O / CH2	0.0507	0.0289

Table 31 - a, b constants¹⁶

Even if the a and b constants indicated above were directly found only for polyethylene, many experimental tests proved that the behavior of water targeted by different radiation particles is very similar to that of polyethylene, and the variation of dose reduction between the two materials is almost negligible.

Using the above formula, dose reduction from typical GCR radiation, represented by ^{56}Fe ions has been calculated for the 3.5 cm and 7 cm FO-CTBs shelters (without taking into account the contribution of the Nomex cloth, the plastic liner and the membrane) and results are summarized in *Table 32*. A 3.5 cm water-based shelter realized with six FO-CTBs and employing about 130 L of water adds about 14% of GCR dose reduction to the attenuation of

¹⁶ Measurements of Materials Shielding Properties with 1 GeV/nuc ^{56}Fe , Zeitlin et al., 2006

the average $5.26 \frac{g}{cm^2}$ aluminum hull available onboard the ISS and so its benefit is negligible for GCR radiation. A 7 cm shelter realized with twelve FO-CTBs would led to an overall GCR dose reduction of about 36% inside an ISS module but it requires more than 260 L of water.

Shielding material	δD	Daily GCR dose
5.26 g/cm ₂ Al equivalent	0.1087	1.587246575
5.26 g/cm ₂ Al equivalent + single FO-CTB layer (3.5 g/cm ₂ H ₂ O)	0.251575	1.332810949
5.26 g/cm ₂ Al equivalent + double FO-CTB layer (7 g/cm ₂ H ₂ O)	0.367088	1.127103793

Table 32 - Dose reduction from GCR radiation

The SPE radiation attenuation is calculated by extrapolating data of interest from existing empiric data and graphs. Dose reduction for a 3.5 cm waterwall is estimated to be about the 72% while for a 7 cm waterwall it is estimated to reach about 93%. This means that behind a filled FO-CTB onboard an ISS module we will reach an overall dose reduction of about 95% while behind two overlapped FO-CTBs this value rises to more than 98%, as showed in *Table 33*.

Shielding material	δD	Daily SPE dose
5.26 g/cm ₂ Al equivalent	0.819	1.636438356
5.26 g/cm ₂ Al equivalent + single FO-CTB layer (3.5 g/cm ₂ H ₂ O)	0.9504718	0.447789041
5.26 g/cm ₂ Al equivalent + double FO-CTB layer (7 g/cm ₂ H ₂ O)	0.9885915	0.103145205

Table 33 - Dose reduction from SPE radiation

The personal FO-CTB-based shelters would provide a significant contribution of the necessary SPE dose reduction while its contribution to GCR dose reduction can be considered negligible. Considering the acute dose-rate of $500 \frac{mSv}{hour}$ calculated for the King SPE, which, if shielded only with the modulus's aluminum hull, would led to the annual dose exposure limit in less than six hours, a single layer personal shelter would extend this limit to about 21 hours by reducing the absorbed dose rate to $24.76 \frac{mSv}{hour}$. A double layered shelter, instead, would further reduce the absorbed dose rate to $5.7 \frac{mSv}{hour}$, extending the time exposure limit to almost four days. As such strong intensity events occur only for a few hours, the personal shelter can effectively mitigate the very severe effects of a SPE occurring during an ISS mission. Assuming a theoretical extension of the worst-case King SPE over a long term period and using the previously calculated values, dose reductions from its radiation with an FO-CTB-based water shelter would be those shown in *Figure 47*. Assuming the crew will spend 8 hours per day sleeping by using the personal FO-CTBs shelters instead of the conventional sleeping bags and the remaining 16 hours within the general spacecraft space. The estimates of radiation exposure doses from GCR, SPE, and total radiation in LEO using this strategy are shown in *Figure 48* for different spaceflight durations.

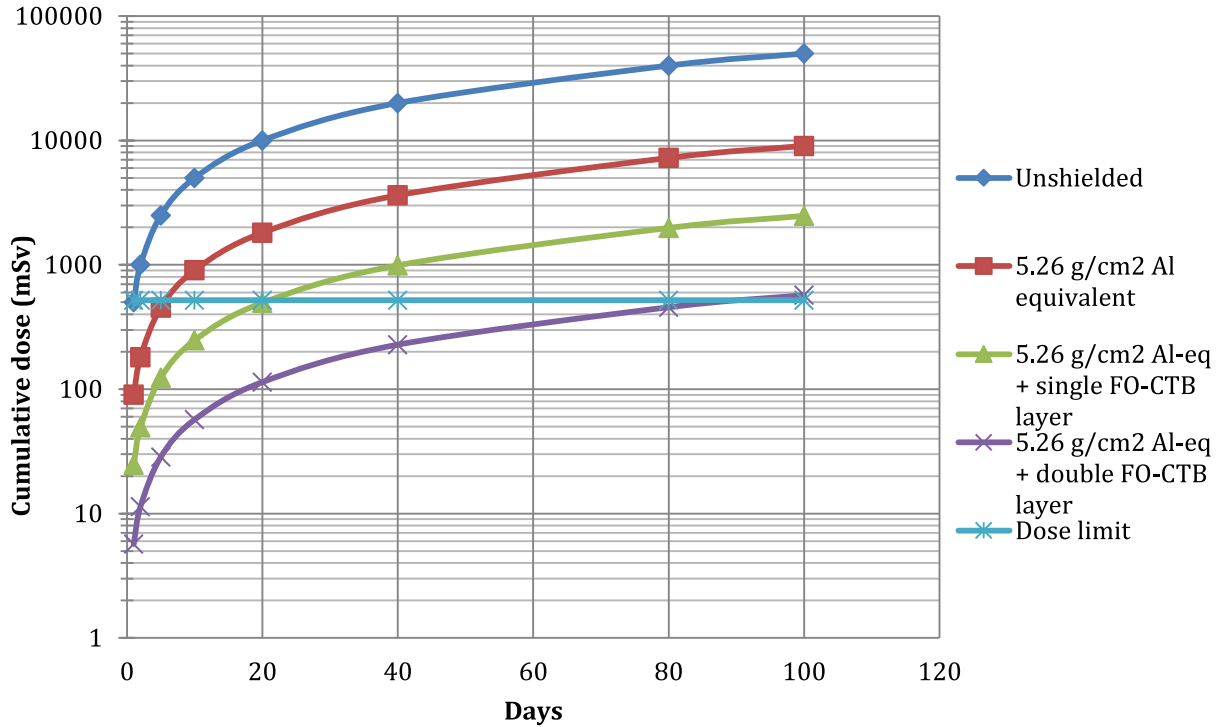


Figure 47 - Dose reduction from SPE radiation with FO-CTBs

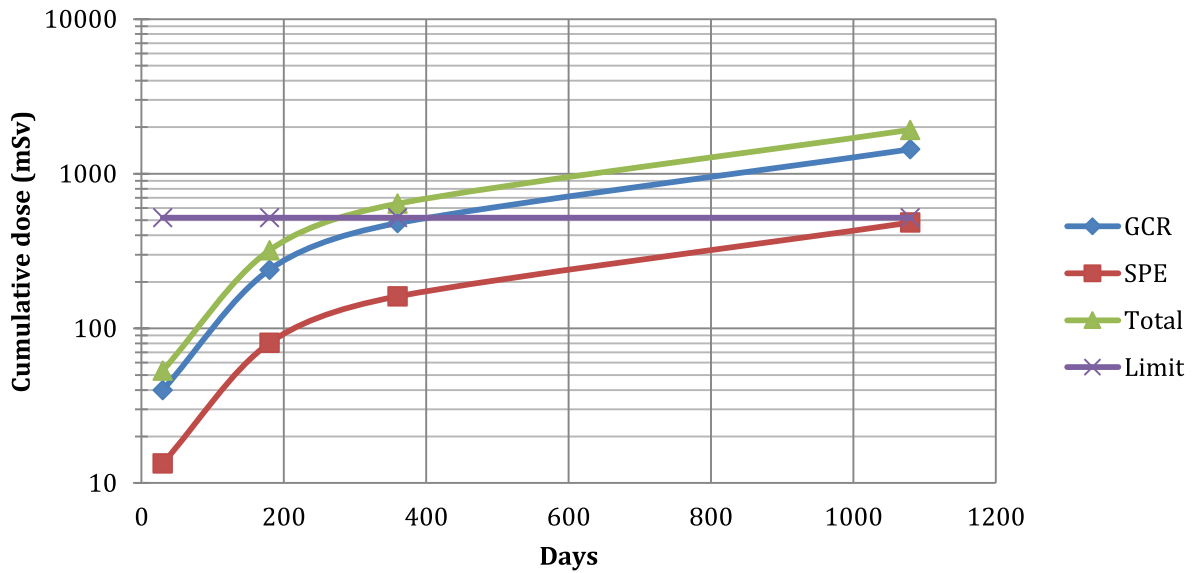


Figure 48 - Radiation exposure dose in LEO with FO-CTB sleeping bag

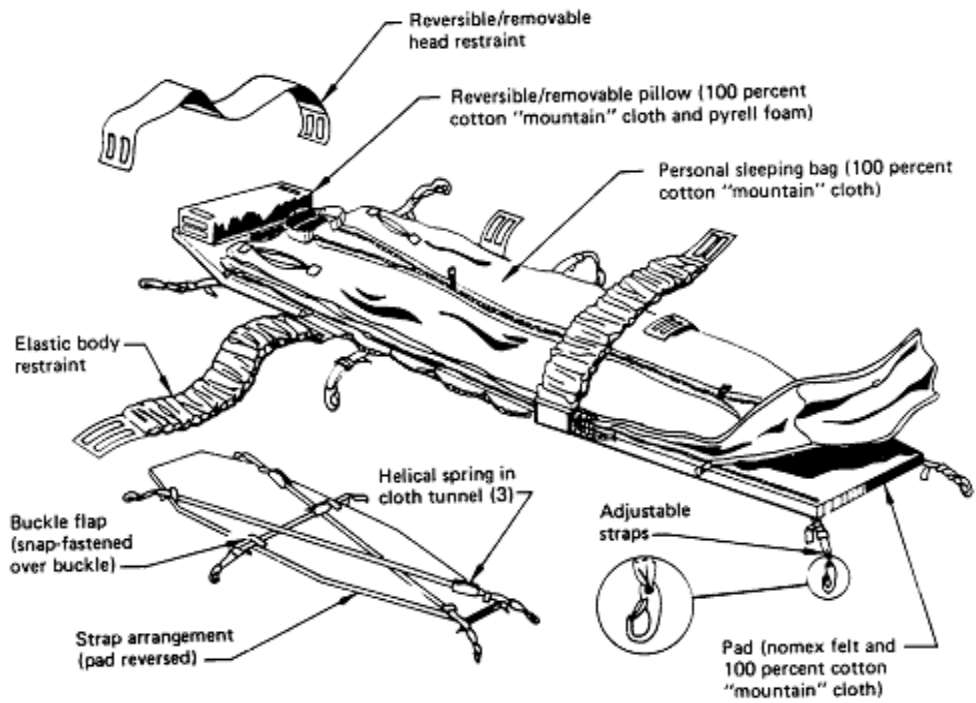


Figure 49 - Standard Sleep Restraint¹⁷



Figure 50 - Sleeping quarters located in the Japanese module of the ISS

¹⁷ NASA STD 3000, Volume 1, Section 11

As seen in *figure 48*, the exposure dose limit of $520 \frac{mSv}{year}$ would be reached more than four months later with respect to the case showed in the previous plot, allowing an increase of the duration of an astronaut's mission onboard the ISS of about 80%. This advantage is due mostly to SPE dose reduction and only in small portion to the GCR dose reduction.

At last, *Figure 49* shows a comparison among the overall dose exposure received in LEO by an astronaut in three different shielding modes: the first one occurs using simply a typical spacecraft wall supposed to be equal to the ISS $5.26 \frac{g}{cm^2}$ aluminum equivalent hull, the second one occurs using a personal sleeping bag composed by a 1 layer filled FO-CTB for 8 hours per day for the full duration of the mission within the previous aluminum hull, the third one is obtained using a double layer of filled FO-CTBs for the personal sleeping bag. The last case allows to extend a typical mission duration onboard the ISS of up to 14 months without reaching the dose career limit.

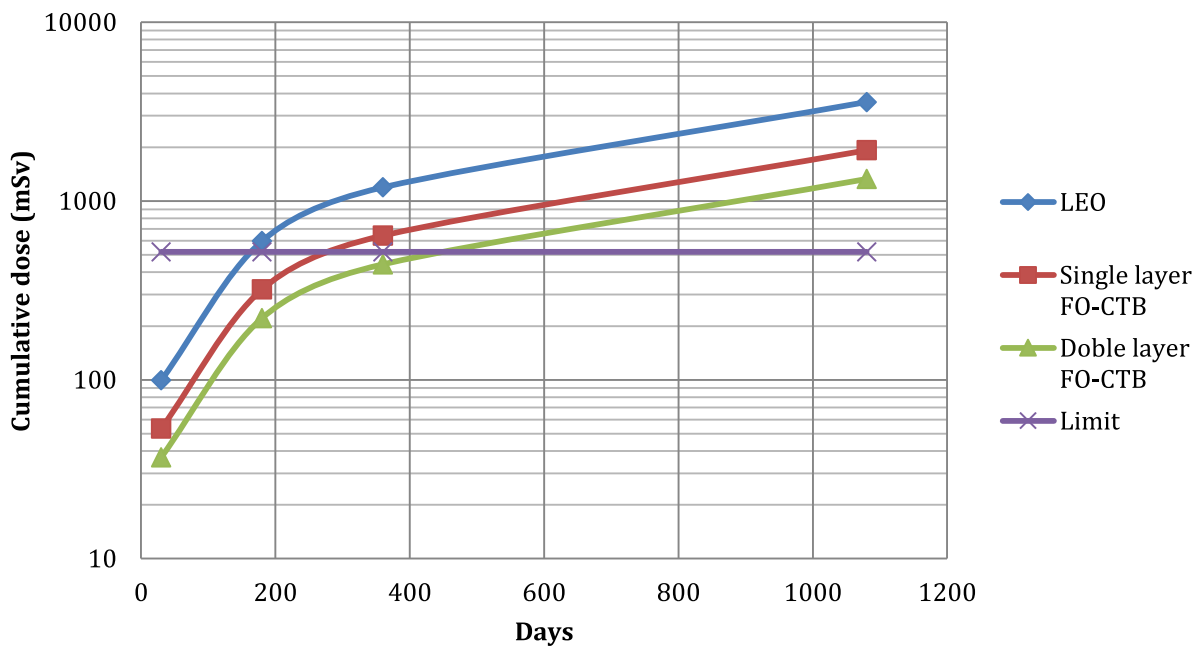


Figure 49 - Exposure dose in LEO with different shielding strategies

Summary and Sizing for Deep Space

When extending this 5 cm FO-CTB Water Wall storm shelter analysis to a deeper more mature water wall designs the effects of WW on a mature long term habitat become clear, and are substantial (Table 34). The GCR dose fall off frustratingly slowly and by 5+ layers is plateauing at a 50% range reduction that while not definitive, could be useful for deep space. In combination with other elements in the inflatable habitat wall (thick layers of Kevlar and other structural fabric and Mylar) 7 to 9 layers could protection that reduces dose to between 42% and 36% of the unshielded GCR dose. Thus, to say that the WW cannot have a strong and relevant effect is untrue, though allow it cannot entirely eliminate the problem.

This finding is not trivial and could work in concert with other countermeasures to drive the GCR does well into the acceptable rage within the inner solar system. Larger habitat could

provided water depth concentration in the sleeping and rest areas that by providing better than 50% dose reductions could change the calculus of radiation limitations on interplanetary travel.

Table 34: The radiation shielding effects of mature multi layer WW.				
Profile of layers, 3.5 cm each in depth, no Al, deep space	$\delta D/\text{layer}$	Daily SPE dose	$\delta D/\text{layer}$	Daily GCR dose
Unshielded	0.000	19.178	0.000	3.288
1 st layer H ₂ O 3.5 cm	83.711	3.124	0.160	2.760
2 nd layer	45.698	1.650	0.145	2.335
3 rd layer	31.359	1.136	0.131	1.995
4 th layer	23.902	0.842	0.118	1.730
5 th layer	19.318	0.654	0.107	1.528
6 th layer	16.228	0.505	0.096	1.379
7 th layer	14.009	0.371	0.087	1.276
8 th layer	12.345	0.237	0.079	1.209
9 th layer	11.056	0.096	0.071	1.174

As explained before, career dose limits vary in function of gender and age of the astronauts. However, while a 2 or 3 layer WW would guarantee to not exceed the current dose limits in LEO when severe solar events happen, especially if used in combination with the conventional shielding mass of the ISS's walls, a deep space mission would require a much thicker WW to meet the current requirements.

Considering a 500 days mission to Mars, even a 10 layer (35 g/cm²) WW would not guarantee a safe deep space mission for a 25 years old male astronaut. Considering the career dose limit of 620 mSv for a 30 years old male astronaut, an 8 layer WW, instead, would be enough to not exceed the previous limit during such a mission, especially taking into account that GCR maximum corresponds to solar minimum and vice versa. With such a thickness, the SPE dose will be almost neglected, leading to almost the 99% of dose reduction.

Radiation tests at NIRS HIMAC, May 2013

A stack of two forward osmosis bags containing a total of 2000 g (or 4.17 g/cm²) fecal simulant were exposed to particle beams representative of significant components of the space radiation field:

- 4 230 MeV/nucleon ⁴He
- 5 800 MeV/nucleon ²⁸Si (GCR)
- 6 160 MeV protons (SEP).

The change in dose after passage through the fecal simulant has been determined by measuring the energy deposition with and without the simulant target present on the path of the particle beams. Table 35 shows that the fecal simulant, if used in small amounts, increases dose.

Table 35: Exposure Data for the Fecal Simulant Target	
Particle Beam	Relative Dose
160 MeV protons	1.41
230 MeV/nucleon ⁴ He	1.13
800 MeV/nucleon ²⁸ Si	1.03

This results are perfectly consistent with the expectation: as explained above, use of some materials in spacecraft construction will even increase the energy absorption by the astronaut. The composition of the radiation field changes as particles lose energy and suffer nuclear interactions in traversing the simulant material. As particles undergo nuclear interactions, they produce secondary particles that can have higher or lower quality factors than the primary particle and so the new particles of lower Z and E could be more biologically effective than the primary ones, depending on their flux spectra. Also, high energy neutrons, protons, and other light particles produced in the same fragmentation event increase the number of nuclear particles in the radiation field: this is the main reason of the dose increase showed in the previous table. Increasing the thickness of the fecal simulant, the relative dose would have dropped down to values < 1 . However, in a WW architecture, the solid-waste layer will be only one of the many layers used in synergy as a shielding wall (and nothing forbids us to use a third forward osmosis bag): the combined effect of all these different elements must still be analyzed with tests similar to the HIMAC's one, but it is definitely expected to obtain results showing a hardly decrease of the relative dose.

2. Conclusion

The success of this work should be assessed in relation to objective a stated in the original proposal. The Water Walls proposal addresses five specific aims: Module Assembly, Functional Flow, Sizing, Reversible Power-CO₂ Sequestration, and Spacecraft Architecture

2.1.2 Specific Aim 1 – Module Assembly

Design a physical WW Module Assembly for the water walls system that provides the life support, dietary supplement, and radiation shielding capabilities.

Results. *An assembly design has been created that enables all the subsystem and component development to follow in later phases. CAD models of an entire WW system integrated into a Bigelow Aerospace BA 330 inflatable structure have been provided. All element of this Aim were completed except for the dietary supplement element. Progress on this element was delayed do the establishment of a STMD support Synthetic Food Development new start activity that will start up in FY 14. Research into this subject was therefore delayed to allow time to coordinate with this larger activity.*

2.1.3 Specific Aim 2 – Functional Flow Architecture

Design the functional and operational relationships and process flow among the FO bags and PEM (MFC) cells.

Results. *A functional flow diagram has been developed and is presented in the final report. It shows the interrelation of the “life support economy” in a space habitat. The functional flow diagram explains the regenerative and closed-loop aspects of the WW, showing how the effluent from one FO bag is the feed for another bag or MFC, which bags require surface air flow or light, and most important, where the output consumables (O, N, water, algae nutritional supplement) derive.*

2.1.4 Specific Aim 3 – Sizing

Size the number of FO bags and PEM cells for various mission scenarios. Design a physical assembly for the water walls system that provides the life support, dietary supplement, and radiation shielding capabilities. Table 8 shows the allocation of the five types of FO bags.

Significance. The sizing analysis establishes how many bags of each type will be required for parts of the WW system to work and for a complete system to operate. It estimates the range of variation and flexibility possible to enhance or decrease reliance on each of the FO processes.

Innovation. This approach to sizing recognizes that different mission types, durations, and crews may need different life support “economies.” It also allows calculation of a reliability and risk management model that may incorporate some stored consumables and buffer capacity to accommodate fluctuations in the process flows.

Approach. The approach begins from a “minimum functionality” paradigm of what are the basic numbers to enable the WW system to perform all its process functions. We posit a *minimum functionality* sizing model also shown in Table 8. These numbers do not fit exactly into the 20 bags that comprise the initial module assembly. Therefore, within this architectural matrix, the WW system integration is flexible. For example, if more nutritional supplement is desired, since the sizing of the algae growth bags is limited by the nitrate output from the graywater-urine/water FO bags and blackwater/solids FO bags, it is possible to seed more algae bags with nitrate fertilizer. This example would also increase the N₂ output.

Result. A sizing analysis was completed that establishes how many bags of each type will be required for parts of the WW system to work and for a complete system to operate. This approach to sizing recognizes that different mission types, durations, and crews may need different life support “economies.” The approach begins from a “minimum functionality” paradigm of what are the basic numbers to enable the WW system to perform all its process functions.

2.1.5 Specific Aim 4 – Organic Fuel PEM Cell

Design configuration for the PEM (MFC) Cell optimized for WW.

Results. *We are currently constructing the first NASA MFC system. This work is funded by the STMD. Through this proposal we have been using data generated in the STMD MFC project to size and define the integration parameters as well as power generation capabilities of a MFC in the WW system.*

2.1.6 Specific Aim 5 – Spacecraft Architecture

Design a WW system into a spacecraft for a long duration mission (e.g. asteroid or Mars).

Results. *A preliminary design of a fully integrated WW system with a BA 330 inflatable habitate has been developed. This design enables space architects to design the spacecraft “from the inside-out” for the first time to optimize the life support, habitability, and crew productivity. This application of WW is the first operational solution for “non-parasitic radiation shielding.” The spacecraft architecture would install the WW matrix to provide shielding around the crew cabin. It also offers new potential ways to design ventilation & air flow, lighting, and partition walls. An analysis of the shielding potential of this system is also provided.*

All of the specific Aims of this original proposal have been achieved, with the exception of the nutritional supplement element of Aim 1. In addition sizing and assumption data have been generated that have allowed us to complete the first feasibility sizing of the WW concept. Based on the sizing completed through this proposal, the WW system will require 362 m² of membrane area which can be correlated to the internal surface area. This sizing value assumes that semi-volatile removal function of the Contaminate Control functions are integrated into Air Revitalization and Climate Control subsystems. Therefore, if we assume that the BA will have a minimum of 2 layers of bags to provide for SPE protection then the WW functionality will completely cover the first layer of bags and about 35% of the second layer, resulting in a factor of safety in our sizing of 32%, meaning that the sizing could be off by 32% and still fit within the tow bag layer constraint of the BA 330. This configuration is shown in Figures 5, 6, and 7.

In addition, the total mass of the WW would be 19,000 kg, which is equal to the mass of the radiation protection water wall alone. This would displace about 16,642 (from 240 day Mars Transit Mission) of life support ESM using traditional ISS derived system. Thus the 19,000 kg WW system would displace a 36,000 conventional system with radiation protection and life support functions included (46% reduction in system mass). Note that these calculations are based on preliminary design data. In addition, it is possible to generate this 19,000 kg from waste residual brines generated on orbit by ISS crew or commercial crewed missions. The WW system is uniquely capable of treating these high solids wastes.

Future work will be needed to further define each element of the WW concept at the Functional Flow System, Process Block, Subsystem, and Component level (Bag/Membrane). One of the key future tasks will be the verification of the assumption that the semi-volatile removal function of the Contaminate Control functions can be integrated into Air Revitalization and Climate Control subsystems. These are some of the lowest TRL systems so additional development will be required to verify these assumptions. There is also a need to generically increase all of the Process blocks that are at low TRLs (TRL 3 and below) to verify sizing data. A better understanding of the flow of micro nutrients in the system is required and we still need to evaluate the generation of nutritional supplements and food production in general.

In addition, the objectives as defined in the Specific Aims of the original proposal we have also completed radiation exposure testing of key solid waste endpoint materials and completed extensive testing of new membrane materials. We have filed a patent on the WW concept and have been selected by the Inspiration Mars Foundation for evaluation in their privately funded Mars fly-by mission. We are also working to provide the Solar Impulse Aircraft, the first solar

powered aircraft to attempt a circumnavigation of the Earth, with water recycling bags and are negotiating a grant with the US Army for version of the water recycling aspects of WW for use in forward operating bases. In short this grant has been more than a success. It is a seed for a new way of thinking of sustainability and recycling. The ultimate impact of this on terrestrial and space mission is impossible to predict. We will just have to wait and see how this approach revolutionizes space flight and terrestrial sustainability research.

3. Appendix A – Hazardous Waste Handling

The WW project introduces a new set of risks to space exploration missions in regards to hazardous waste handling. Initiation of use of the WW system requires the transfer of wastes into the membrane-integrated bags. Transfer of wastes could occur manually, by directly urinating and defecating into the system bags, or through automated plumbing systems. Each transfer option provides unique opportunities for the introduction of risks. The manual method of waste transfer requires contact with human wastes (feces, urination, other trace bodily fluids), and increases the risk for the introduction of potential hazards into the spacecraft environment via condensation and aerosolization. While risks are increased with the manual methods of transfer, the materials required for use of the WW system are limited to the bags, a draw solution and the waste produced by the user. Automated transfer using a plumbing system would dramatically reduce the risks associated with contact and handling of wastes, but could present greater issues, such as clogging, leaks, contamination of the clean water produced, or system failure. Automated transfer requires a large amount of materials for use of the system, which will increase the flight mass of the system.

Wastewater reconstitution is a current practice for producing agricultural/irrigation water in the United States. The United States Environmental Protection Agency (USEPA) has set strict guidelines detailing the maximum allowable amount of fecal coliform bacteria in reconstituted wastewater used for agricultural purposes, in order to limit the contamination of crops, agricultural workers and natural water sources [Blumenthal, 2000]. Coliform bacteria density is used to determine the degree of pollution, which directly references the quality of sanitation of the sample [WEF, 1990]. The standard for crops that may be consumed raw has become stricter over time, increasing from 1000 fecal coliform bacteria per 100 milliliters of water in 1989 to 0 fecal coliform bacteria per 100 milliliters of water in 2000 [Blumenthal, 2000]. Actual standards and regulations are overseen by each state, with California requiring the strictest standards (< 2.2 total coliform bacteria per 100 milliliters of unrestricted spray irrigation, where other states have a maximum allowance of 200 total coliform bacteria per 100 milliliters of spray irrigation). While enteric disease is commonly transmitted through poor hygiene and sanitation rather than through wastewater reuse [Blumenthal, 2000 & WEF, 1990], strict guidelines must be in place for wastewater reuse during space exploration, as medical treatment will be limited.

Reuse of wastewater involves the risk of contamination by products that can move through the selectivity of the filtration membranes used. Forward osmosis (FO) membranes have repeatedly shown successful rejection of fecal coliforms and small proteins. While urine isn't considered a hazard, as it is considered a sterile waste, it could act as a transfer solution for many microbial species and other bodily secretions. Crewmembers are often required to consume a large number of nutritional supplements and medicinal therapeutics to ensure safety during spaceflight [NASA

Human Research Program, 2008 & Link, 1965]. Any substances from these supplements and therapeutics, as well as other proteins, sterols and mineral wastes that not used by the body are often expelled in the urine. Most of these secreted materials are not considered harmful to others, depending on the material. Many studies have researched the influence of synthetic hormones, such as those from contraceptive pills and hormone therapies, in wastewater and environmental systems, as the sterol hormones aren't easily dissolved in water and are expelled from the body through urination. Most data collected has shown that hormones accumulating in environmental water sources have an influence on the mating processes of other species [Hoffmann, 2012]. FO membranes have also shown rejection of 77 to 99% of natural hormones in solution, depending on pH, experimental duration, and feed solutions used [Cartinella, 2006].

Pathogens excreted in human wastes include viruses, bacteria and parasitic organisms. Enteric diseases, which are transmitted through the handling or consumption of human or animal wastes are a worldwide issue, and are often representative of the hygienic conditions and availability of clean water and proper sewage systems in an area. Diseases like typhoid fever, cholera, hepatitis, and dysentery are the some of the leading causes of death in developing countries [Obeng, 1983] . While most of these pathogenic threats will be screened for to determine the health of the crewmembers prior to spaceflight, other risks may be present. Researchers have shown recent interest in personal microbiomes and gastrointestinal microbiota research, and how individual microbiomes may be linked to common diseases, including cancer, diabetes and intestinal disorders [Li, 2013; Friedrich, 2013 & Wang, 2013]. Each microbiome is unique to the individual, and is indicative of their diet and overall health [Li, 2013; Friedrich, 2013 & Wang, 2013]. . Given the distinctiveness of each microbiome, membranes in the WW system must be able to reject microorganisms and proteins associated with symbiotic organisms from the digestive tract in order to avoid risks of possible ingestion.

Current membrane technologies have fine-tuned the range of size-based selectivity available for wastewater treatment and filtration. Fecal coliforms are most commonly found in a flocculated configuration, making it easier to reject them from moving across the FO membrane. Smaller proteins and molecules may pose an issue if included in the flux across the membrane, but may not be as concerning for the WW system as the possible flux of viruses and bacteria. Ultrafiltration membranes (UF) have pores small enough to reject macromolecules and viruses (typically 100nm to 1 nm in size) while allowing the passage of ions through the membrane¹¹. Nanofiltration (NF) and osmotic membranes (reverse osmosis (RO) and FO membranes) show pore selectivity for ions, depending on their size (typically ranging from 1nm to 1Å) [Liu, 2010].

Appendix B –Nitrogen Loop Balances

The crew cabin atmosphere is primarily nitrogen gas (N₂) and is a major reservoir of nitrogen in the system. There are only two mechanisms for N₂ to leave the atmosphere: 1) leakage to outside the spacecraft, or 2) Nitrogen fixation, that is, the conversion of N₂ to ammonium, nitrate or nitrite, by biological or non-biological means. This is the transfer of nitrogen from the cabin atmosphere reservoir to pools that exist in other reservoirs aboard the spacecraft (e.g., food (brought on board or plats grown on board), waste, plants, etc.). Non-biological means are extremely energy expensive and probably not done on a spacecraft (true?). N-fixing bacteria

such as cyanobacteria or other bacteria inhabiting certain plant nodules could perform biological nitrogen fixation. This biological fixation results in the formation of ammonium. The ammonium can be nitrified to nitrite and nitrate. Fixed nitrogen can also be found as organic nitrogen in form of food and human waste (fecal and urine). In a complete nitrogen cycle the N₂ is fixed into ammonium, nitrified to nitrate and nitrite, that is used as fertilizer for food that in turn transforms it into organic-N that is then microbially transformed back to ammonium, that is then again nitrified. For nitrogen to be returned to the atmosphere it must be denitrified (the transformation of nitrate/nitrite to N₂). To be able to determine the N-cycle we need numbers to do a mass balance.

Following is a more detailed summary of the nitrogen cycle of the Water Walls system.

NITROGEN ECONOMY of Water Walls

Nitrogen is found most commonly in pools consisting of N₂, N₂O, NH₄⁺/NH₃, NO₃⁻, NO₂-or organic-N. These pools are found throughout the various reservoirs (bags). Transformation reactions of N allow it to be transferred from pool to pool, as well as from reservoir to reservoir (bag to bag). These reactions constitute the N-cycle, or N₀-economy of the WW system.

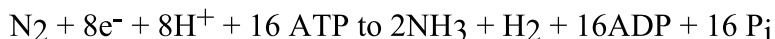
The total amount of N in a given reservoir (Bag) at any one time represents a balance between N gains and losses. For example, N can be added from one bag (reservoir) to another through active pumping, or by biological fixation of N₂. The loss of N from the bags through denitrification represents a gain of N to the gaseous atmosphere (as N₂ or N₂O), but a loss to the bags. The transfer of N among the various bags constitutes the nitrogen cycle, or economy of the system.

The transfer of nitrogen from one pool to another within a bag, such as occurs during ammonification (organic-N to □NH₃), represents a loss from one pool (organic-N) and a gain to another (NH₃), with no net change in either the total nitrogen in the bag (reservoir). These nitrogen transformation reactions constitute the nitrogen cycle at the bag (reservoir) level.

NITROGEN FIXATION

Nitrogen fixation in WaterWalls occurs biologically. Biological N-fixation refers to the ability of an organism to transform N₂ from an atmospheric gas into NH₃. The NH₃ is eventually attached to organic compounds and incorporated into. Only a select few organisms, all of which are prokaryotic, possess the ability to grow in the absence of fixed nitrogen (Mancinelli, R. L. Nitrogen Cycle, Encyclopedia of Microbiology 3:229-237; Academic Press; 1992.). Nitrogen fixers can be divided into autotrophs and heterotrophs, depending on their source of carbon. They can be further sub-divided and designated as free-living (e.g., cyanobacteria) or symbiotic (Rhizobia found in nodules on plant roots).

Nitrogen fixation is performed by Nitrogenase is a complex The overall reaction catalyzed by nitrogenase is:



Sixteen molecules of ATP are required to break the nitrogen to nitrogen triple bond in N₂ The requirement for such a large number of ATP molecules makes biological nitrogen fixation a very energy expensive process. Because of the high energy cost, organisms preferentially use fixed nitrogen when it is available and only fix nitrogen when the demand exceeds the supply. Because in the WW system there will be a plentiful supply of fixed nitrogen from the black water and grey water bags we anticipate that N-fixation rates will be low or non-existent.

AMMONIFICATION

Ammonification, the enzymatic process of organic-N conversion to NH_4^+ , is performed by numerous organisms. Because there is a wide array of N-containing organic compounds belonging to different chemical classes, a wide array of enzymes is required that break them down to produce NH_4^+ . In the WW bag system the greywater and black water bags will have active ammonification occurring constantly. The NH_4^+ (or NH_3) will be used as “fertilizer” for the algae bags. The algae used in this system will be species of *Chlorella*, a well characterized fast growing green alga.

N-ASSIMILATION

Nitrogen assimilation is the conversion of NH_3 or NH_4^+ to organic-N and that organisms use for the production of new organisms. The NH_3 produced by nitrogen fixation, or ammonification, is assimilated in a series of enzymatically catalyzed reactions. Some organisms, such as the algae used in the WW system have the ability to assimilate NO_3^- . In these organisms the NO_3^- is reduced to NO_2^- by an assimilatory nitrate reductase. This reaction is followed by the reduction of NO_2^- to NH_3 by an assimilatory nitrite reductase. The NH_3 that is formed is then used in proteins and nucleic acids, for example.

NITRIFICATION

Organisms capable of oxidizing NH_4^+ to NO_2^- and then the NO_2^- to NO_3^- (nitrification). Typically there are two distinct types of chemoautotrophic bacteria (autotrophs obtaining their energy from the oxidation of inorganic compounds), and related the metabolism of each to the two steps involved in nitrification, that is, step 1: NH_4^+ to NO_2^- (e.g., *Nitrosomonas*) and step 2: NO_2^- to NO_3^- (e.g., *Nitrobacter*). These nitrifiers synthesize all of their cellular constituents from CO_2 *via* the Calvin cycle and an incomplete tricarboxylic acid (TCA) cycle. Although nitrification in nature is principally carried out by these two types of chemoautotrophic bacteria, a variety of heterotrophic bacteria and fungi are also capable of nitrification.

DENITRIFICATION IN WaterWalls

Denitrification is the dissimilatory reduction of Nitrate (NO_3^-) to nitrous oxide (N_2O) or dinitrogen (N_2). It occurs among a diverse array of microbes. Because it is coupled to the production of adenine-tri-phosphate (ATP) and electron transfer occurs *via* the cytochrome system it constitutes a form of anaerobic respiration. The process usually occurs under anaerobic conditions, but can occur in primarily aerobic systems that contain anaerobic microsites (e.g., Mancinelli, R.L., Smernoff, D.T. & White, M.R. 1999. Controlling denitrification in closed artificial ecosystems *Adv. Space Res.* 24:329-334), such as may occur in the WaterWalls bags (e.g., black water and grey water bags). With few exceptions, denitrifiers preferentially use O_2 as their terminal electron acceptor and when respiring O_2 function as aerobes. It is only when O_2 is depleted and there is sufficient electron donors in the environment do they respire NO_x and become anaerobes, thus relegating the nitrogen oxides to a secondary level.

The organism generates cellular energy (ATP) by the transport of electrons *via* the cytochrome system from an organic or inorganic source to NO_3^- , or to a more reduced nitrogen oxide (e.g., NO_2^- , NO , N_2O) derived from NO_3^- . Nitrate serves as an electron acceptor in an electron transport chain. By accepting electrons, it becomes more reduced and forms a new acceptor of electrons. This process continues until N_2O or N_2 is formed. The nitrogen oxides that form

during the process serve as electron acceptors during denitrification and proceed along the following pathway: $2\text{NO}_3^- \rightarrow 2\text{NO}_2^- \rightarrow 2[\text{NO}] \rightarrow \text{N}_2\text{O} \rightarrow \text{N}_2$. An enzyme, catalyzes each step of this pathway; the enzyme is a nitrogen oxide reductase that transfers electrons from the chain to the particular intermediate of the denitrification pathway.

Heterotrophic denitrifiers use a wide variety of organic compounds (e.g., alcohols and organic acids) as initial electron donors for denitrification. The electrons are used to reduce NO_3^- to NO_2^- . This reaction is catalyzed by dissimilatory nitrate reductases, distinct from the assimilatory nitrate reductases in form and function. For example, neither the production nor the activity of the assimilatory reductases is affected by O_2 in most organisms, whereas dissimilatory nitrate reductases are usually not produced in the presence of O_2 , nor do they function properly under aerobic conditions. In addition, the presence or absence of NH_4^+ does not influence dissimilatory nitrate reductases, but does regulate the synthesis of assimilatory nitrate reductases. In fact, many denitrifiers can also assimilate nitrate and incorporate it into biomass while obtaining the energy for performing these reactions by denitrification. They produce two separate enzyme systems that are independently operated and regulated that both use NO_3^- as a substrate and reduce it to NO_2^- (e.g., Mancinelli, R. L. Nitrogen Cycle, Encyclopedia of Microbiology 3:229-237; Academic Press; 1992; Lam, P and M.M.M Kuypers (2011) Microbial Nitrogen Cycling Processes in Oxygen Minimum Zones Annual Review of Marine Science, 3: 317 -335)

A dissimilatory reduction of NO_3^- and NO_2^- to NH_4^+ may also occur when NO_3^- is used as an electron dump to fermentatively oxidize NADH. This phenomenon has been found in organisms grown in pure culture (Caskey, W. H.; Tiedje, J. M. The reduction of nitrate to ammonium by a *Colostridium* sp. isolated from soil, J. Gen. Microbiol., 119, 217-217-223; 1980. Cole, J. A.; Brown, C. M. Nitrite reduction to ammonia by fermentative bacteria: a short circuit in the biological nitrogen cycle, FEMS Microbiol. Lett., 7, 65-72; 1980), as well as in natural environment under extremely anaerobic conditions (e.g., Koike, I; Hattori, A. Denitrification and ammonia formation in anaerobic coastal sediments, Appl. Environ. Microbiol., 35, 278-282; 1978).

Nitrous oxide reductases reduce N_2O to N_2 and are found in most denitrifiers, but not all. The reaction is a single step reduction. Nitrous oxide reductase is an O_2 -sensitive labile protein. It is membrane bound and receives electrons from the electron transport chain *via* cytochrome *c*.

4. References

- Agrios, A.G. and Pichat, P. (2005) "State of the art and perspectives on materials and applications of photocatalysis over TiO₂," *Reviews in Applied Electrochemistry*, 58, 655-663. doi:10.1007/s10800-005-1627-6
- Anpo, M. and Takeuchi, M. (2003) "The design and development of highly reactive titanium oxide photocatalysts operating under visible light irradiation," *Journal of Catalysis*, 216, 505-516. doi:10.1016/S0021-9517(02)00104-5
- Archer, S., and Robb, G., (1925), "The tolerance of the body for urea in health and diseases," *Quarterly Journal of Medicine*, Vol. 18, pp. 274-287
- Babanova, S., Hubenova, Y., and Mitov, M. (2011), "Influence of artificial mediators on yeast-based fuel cell performance," *Journal of Bioscience and Bioengineering*, Vol. 112, No. 4, pp. 379-387.
- Beaudry, E., Herron, J., and Peterson, S., (1999), "Direct osmotic concentration of wastewater: final report," US Government Publication #NAS2-14069 Final Report
- Benefield, L., Judkins, J., and Weand, B., (1982) *Process Chemistry for Water and Wastewater Treatment*, Prentice-Hall, Inc. NJ, pp. 212-235
- Bloß, S.P. and Elfenthal, L. (2007) "Doped titanium dioxide as a photocatalyst for UV and visible light," *Proceedings International RILEM Symposium on Photocatalysis, Environment and Construction Materials*, Florence, 8-9 October 2007, 31-38.
- Blumenthal, UJ., Mara, DD., Peasey, A., Ruiz-Palacios, G., and Stott, R., (2000), "Guidelines for the microbiological quality of treated wastewater used in agriculture: recommendations for revising WHO guidelines," *World Health Organization*, Vol. 78, No. 9.
- Carp, O., Huisman, C.L. and Reller, A. (2004) "Photoinduced reactivity of titanium dioxide," *Progress in Solid State Chemistry*, 32, 33-177. doi:10.1016/j.progsolidstchem.2004.08.001
- Cartinella, JL., Cath, TY., Flynn, MT., Miller, GC., Hunter, KW. Jr., and Childress, AE., (2006), "Removal of natural steroid hormones from wastewater using membrane contactor processes," *Environmental Science and Technology*, Vol. 40, No. 23.
- Chen, D., Li, K., (2003), "Visible-light-responsive titania modified with aerogel/ferroelectric optical materials for VOC oxidation," EPA Grant R831276C004.
- Corbitt, R., (1990) *Standard Handbook of Environmental Engineering*, McGraw-Hill Inc. NY. pp. 9.25-9.26
- Davis, Wayne T., (2000) *Air Pollution Engineering Manual*, 2nd Ed., John Wiley & Sons, Inc.
- Demeestere, K., Dewulf, J. and Van Langenhove, H. (2007) "Heterogeneous photocatalysis as an advanced oxidation process for the abatement of chlorinated, monocyclic aromatic and sulfurous volatile organic compounds in air: State of the art." *Critical reviews in Environmental Science and Technology*, 37, 489-538.
- Devlin, J., Deshusses, M., and Webster, T., (1999) *Biofiltration for Air Pollution Control*, Lewis Publishers, FL pp. 13-15.
- Duffield, B., and Anderson, M.S, (2008) Exploration life support baseline values and assumption Document, JSC-64367, December 2008
- Flynn, M., Delzeit, L., Gormly, S., Hammoudeh, M., Shaw, H., Polonsky, A., Howard, K., Howe, A., Soler, M., Chambliss, J., (2011) *Habitat water wall for water, solids, and atmosphere recycle and reuse*, AIAA-2011-5018, 41st International Conference on Environmental Systems, Portland, Oregon, July 17-21, 2011

Fuerte, A., Hernandez-Alonso, M.D., Maira, A.J., et al. (2002) "Nanosize Ti-W mixed oxides: Effect of doping level in the photocatalytic degradation of toluene using sunlight-type excitation." *Journal of Catalysis*, 212, 1-9

Geigy, Scientific Table, 8th Edition, CIBA-GEIGY Ltd., Basel, Switzerland, Vol. 1, 1981, pp. 62-63

Ghangrekar, M. M., and Shinde, V. B., (2006), "Wastewater treatment in microbial fuel cell and electricity generation: A sustainable approach," *International Sustainable Development Research Conference*, April 6-8, 2006, Hong Kong.

Gil, G.C., et al., (2006), "Operational parameters affecting the performance of a mediator-less microbial fuel cell," *Biosensors and Bioelectronics*, Vol. 18, No. 4, pp. 327-334.

Gormly, S., and Flynn, M., (2007), "Lightweight contingency urine recovery cell concept development," SAE Technical Paper No. 2007-01-3036, 37th International Conference on Environmental Systems, July 2007.

Grady, L., Daigger, G., and Lim, H., (1999) *Biological Wastewater Treatment*, 2nd ed., Marcel Dekker, Inc. NY, pp. 68-69

Graham, L. E., Graham, J. M., Wilcox, L. W., (2009) *Algae* 2nd Ed, Pearson Benjamin Cummings, San Francisco, USA.

Grizzaffi, L., Lobascio, C., "Columbus condensate water characterization and wastewater revitalization," AIAA 2010-6297, 40th International Conference on Environmental Systems, 2010.

Hanford, A.J., (2004), "Advanced life support baseline values and assumptions document," *Lockheed Martin Space Operations*, NASA/CR-2004-208941.

Hoffmann, F. and Kloas, W., (2012), "The synthetic progesterone, Levonorgestrel, but not natural progesterone, affects male mate calling behavior of *Xenopus laevis*," *General and Comparative Endocrinology*, Vol. 176, No. 3.

Hoogers G., (2003), *Fuel Cell Technology Handbook*. CRC Press, Boca Raton, FL.

Hou H., et al., (2012), "A microfluidic microbial fuel cell array that supports long-term multiplexed analyses of electricigens," *Lab on a Chip*, Vol. 20, No. 12, pp. 4151-4159.

Ishii, S., et al., (2012), "Functionally stable and phylogenetically diverse microbial enrichments from microbial fuel cells during wastewater treatment," *PLoS One*, Vol. 7, No. 2, p. e30495

Kikuchi, Y., Sunada, K., Iyoda, T., et al. (1997) Photo-catalytic bactericidal effect of TiO₂ thin films: Dynamic view of the active oxygen species responsible for the effect. *Photochemistry and Photobiology A: Chemistry*, 106, 51-56.

Kim, JR., Cheng, S., Oh, SE., and Logan, BE, (2007), "Power generation using different cation, anion and ultrafiltration membranes in microbial fuel cells," *Environmental Science & Technology*, Vol. 4, No. 3, pp. 1004-1009.

Korotkevych, O., et al., (2011), "Functional adaptation of microbial communities from jet fuel-contaminated soil under bioremediation treatment: simulation of pollutant rebound," *FEMS Microbiology Ecology*, Vol. 78, No. 1, pp. 137-149.

Li, K., Bihan, M., and Methé, BA., (2013), "Analysis of the stability and core taxonomic memberships of the human microbiome," *PLoS One*, Vol. 8, No. 5.

Li, WW., Sheng, GP., Liu, XW., and Yu, HQ., (2011), "Recent advances in the separators for microbial fuel cells," *Bioresour. Technology*, Vol. 102, No. 1, pp. 244-252.

- Link, MM., (1965), "Space medicine in project Mercury: A chronology," *NASA Scientific and Technical Information Office*, NASA SP-4001, p. 143.
- Liu, Y. and Mi, B., (2010), "Combined organic and inorganic fouling of forward osmosis membranes," *25th Annual Water Reuse Symposium*.
- Logan, B. E., *et al.*, (2006), "Microbial fuel cells: methodology and technology," *Environmental Science and Technology*, Vol. 40, No. 17, pp. 5181-5192.
- Lovley, D. R., Coates, J. D., Blunt-Harris, E. L., Phillips, E. J., and Woodward, J. C., (1996), "Humic substances as electron acceptors for microbial respiration," *Nature*, Vol. 382, No. 6590, pp. 445-448.
- Madigan, M., Martinko, J., and Parker, J., (1997), *Brook Biology of Microorganisms*, 8th ed. Prentice Hall NJ, pp. 474-530
- Maier, R., Pepper, I., and Gerda, C., (1999) *Environmental Microbiology*, Academic Press, CA, 125-130
- Marshburn, T. H., (1999), "Spacecraft Minimum Allowable Concentrations: Determination, Application, and Contingency Situations," NASA Technical Reports Server (NTRS).
- Marsili, E., *et al.*, (2008), "Shewanella secretes flavins that mediate extracellular electron transfer," *Proceedings of the National Academy of Sciences*, Vol. 105, No. 10, pp. 3968-3973.
- Montague, M., *et al.*, (2012), "The role of synthetic biology for in situ resource utilization (ISRU)," *Astrobiology*, Vol. 12, No. 12, pp. 1135-1142.
- Morel, F., and Hering, J., (1993) *Principles and Applications of Aquatic Chemistry*, John Wiley & Sons, Inc. NY, 239-290
- Morse, A., Kaparthi, S., and Jackson, A., (2004) "Biological treatment of a urine-humidity condensate waste stream," Proceedings of the 34th International Conference on Environmental Systems, Colorado Springs, CO SAE Paper # 2004-01-2462
- NRC, Steering Committee for NASA Technology Roadmaps; National Research Council of the National Academies, (2012), *NASA Space Technology Roadmaps and Priorities: Restoring NASA's Technological Edge and Paving the Way for a New Era in Space*, National Academies Press.
- Obeng, LE., (1983), "The control of pathogens from human waste and their aquatic vectors," *Ambio*, Vol 12, No. 2.
- Olin, S., (1999) "Exposure to contaminants in drinking water, estimating uptake through the skin and by inhalation," ILSI Risk Science Institute/ ILSI Press DC.
- Park, D.H., and Zeikus, J.G., (1999), "Utilization of electrically reduced neutral red by *Actinobacillus succinogenes*: physiological function of neutral red in membrane-driven fumarate reduction and energy conservation," *Journal of Bacteriology*, Vol. 181, No. 99, pp. 2403-2410.
- Park, D. H. and Zeikus, J. G., (2003), "Improved fuel cell and electrode designs for producing electricity from microbial degradation," *Biotechnology and Bioengineering*, Vol. 81, No. 3, pp. 348-355.
- Rabaey, K., (2009), *Bioelectrochemical systems: from extracellular electron transfer to biotechnological application*. International Water Association, London, UK.
- Rabaey, K., Boon, N., Siciliano, SD., Verhaege, M., and Verstraete, W. , (2004), "Biofuel cells select for microbial consortia that self-mediate electron transfer," *Applied and Environmental Microbiology*, Vol. 70, No. 9, pp. 5373-5382.

- Renslow, R., et al, (2011), "Oxygen reduction kinetics on graphite cathodes in sediment microbial fuel cells," *Physical Chemistry and Chemical Physics*, Vol. 13, No. 48, pp. 21573-21584
- Seifert, J., Harmon, J., and DeClercq, P., (2006), "Protein added to a sports drink improves fluid retention," *International Journal of Sports Nutrition and Exercise Metabolism*, Vol. 16, pp. 420-429.
- Snider, R.M., Strycharz-Glaven, S.M., Tsoi, S.D., Erickson, J.S., Tender, L.M., (2012), "Long-range electron transport in *Geobacter sulfurreducens* biofilm is redox gradient-driven," *Proceedings of the National Academy of Sciences*, Vol. 109, No. 38, pp. 15467-15472.
- Stams, A. J. *et al*, (2006), "Exocellular electron transfer in anaerobic microbial communities," *Environmental Microbiology*, Vol. 8, No. 3, pp. 371-382.
- Tchobaoglous and Burton (1991) *Wastewater engineering, treatment, disposal and reuse*, 3ed, Metcalf and Eddy, Inc., McGraw-Hill, Inc., NY, pp. 420-428, 430-434, and 835-841
- Tomaszewski, H., Eufinger, K., Poelman, H., Poelman, D., De Gryse, R., Smet, P. F., Marin, G. B., (2007), *International Journal of Photoenergy*, Vol. 8, No. 1.
- Torres, CI., *et al.*, (2009), "Selecting anode-respiring bacteria based on anode potential: phylogenetic, electrochemical and microscopic characterization," *Environmental Science and Technology*, Vol. 43, No. 24, pp. 9519-9524.
- Verostko, C., Carrier, C., and Finger, B., (2004), "Ersatz wastewater formulations for water recovery systems," *Proceedings of the 34th International Conference on Environmental Systems*, Colorado Springs, CO SAE Paper # 2004-01-2448
- Wang, ZK., and Yang, YS., (2013), "Upper gastrointestinal microbiota and digestive disease," *World Journal of Gastroenterology*, Vol. 19, No. 10.
- Water Environment Federation, (1999), "Standard methods for the examination of water and wastewater: Part 9000, Microbiological examination," *American Public Health Association*.
- Wieland, P. O., (1994), "Designing for human presence in space: An introduction to environmental control and life support systems (ECLSS)," *Marshall Space Flight Center*.
- Wiley, P., Linden, H., et al, (2013), "Microalgae cultivation using offshore membrane enclosures for growing algae (OMEGA)," *Journal of Sustainable Bioenergy Systems*, Vol. 3, pp. 18-32
- Wu, J.C.S. and Chen, C.H. (2004), "A visible-light response vanadium-doped titania nanocatalyst by sol-gel method." *Journal of Photochemistry and Photobiology A: Chemistry*, 163, 509-515
- Zhao, J. and Yang, X.D. (2003) Photocatalytic oxidation for indoor air purification: A literature review. *Building and Environment*, 38, 645-654. doi:10.1016/S0360-1323(02)00212-3